Desulfurization of Dibenzothiophene and Thiophene in liquid fuel using Ni-doped carbon beads and a newly isolated bacterial strain

THESIS

SUBMITTED TO

BABASAHEB BHIMRAO AMBEDKAR UNIVERSITY,

LUCKNOW

BABASAHEB BHIMRAO AMBEDKAR UNIVERSITY
LUCKNOW
प्रज्ञा शील करूणा
ESTABLISHED 1996

FOR THE DEGREE OF

Doctor of Philosophy

In

Environmental Microbiology

Submitted By

Rishabh Anand Omar

(Enrolment No. 1385/19)

Under the supervision of

Dr. Pankaj Kumar Arora

(Assistant Professor)

DEPARTMENT OF MICROBIOLOGY

SCHOOL FOR BIOMEDICAL AND PHARMACEUTICAL SCIENCES

BABASAHEB BHIMRAO AMBEDKAR UNIVERSITY

VIDYA VIHAR, RAIBARELI ROAD, LUCKNOW-226025

UTTAR PRADESH, INDIA

JUNE, 2022

Dedicated

to my

beloved

parents and

family

Declaration

I, Rishabh Anand Omar, certify that the work embodied in this Ph.D. thesis is my own bonafide work carried out by me, under the supervision of Dr. Pankaj Kumar Arora at Babasaheb Bhimrao Ambedkar University, Lucknow. The matter embodied in this Ph.D. thesis has not been submitted for the award of any other degree/diploma. I declare that I have faithfully acknowledged, given credit to and referred to the research workers wherever their works have been cited in the text and the body of the thesis. I further certify that I have not lifted up some other's work, para, text, data, results etc., reported in the journals, books, magazines, reports, dissertations, thesis etc., or available at web-sites and included them in this Ph.D. thesis and cited as my own work.

Date:

Place: Lucknow (Rishabh Anand Omar)

BABASAHEB BHIMRAO AMBEDKAR UNIVERSITY
LUCKNOW
प्रज्ञा शील करुणा
ESTABLISHED 1996

Babasaheb Bhimrao Ambedkar University
(A Central University)
Vidya Vihar, Rae Bareli Road, Lucknow - 226 025.
बाबासाहेब भीमराव अम्बेडकर विश्वविद्यालय
विद्या विहार, रायबरेली रोड, लखनऊ - 226 025

Dr. Pankaj Kumar Arora
Assistant Professor
Department of Environmental Microbiology

Letter No: ……..……...
Date:

CERTIFICATE

This is to certify that the thesis entitled "**Desulfurization of Dibenzothiophene and Thiophene in liquid fuel using Ni-doped carbon beads and a newly isolated bacterial strain***"* submitted by Rishabh Anand Omar is an original research work and has not been previously submitted in part of full for the award of any other degree or diploma to this or any other university.

The thesis submitted to Babasaheb Bhimrao Ambedkar University, Lucknow satisfies all the requirement as stipulated in the *Doctor of Philosophy (Ph.D.) Regulations – 1999 as amended in 2008/2010/2013/2016* and it is fit for submission and evaluation for the award of the degree of Doctor of Philosophy of the University

Date:

Dr. Pankaj Kumar Arora

Supervisor

Head of Department

Table of contents

Acknowledgement

I owe my deepest gratitude to Prof. Sanjay Singh, Vice chancellor, Babasaheb Bhimrao Ambedkar University (BBAU) for giving me an opportunity to work in this university and making the facilities available for the pursuance and completion of the study. I am also thankful to Prof. Naveen Kumar Arora, Dean, School of Earth and Environmental Sciences and Prof. Ram Chandra, Head, Department of Environmental Microbiology, BBAU, Lucknow, for his valuable, painstaking and scholarly guidance, constant inspirations, constructive suggestions and encouragement without which this maiden attempt would not be achieved at the desired level of success and provide all necessary facilities for fulfilment of my research at Department Environmental Microbiology, BBAU. I am bereft of words to show my deep sense of gratitude towards my supervisor Dr. Pankaj Kumar Arora, Assistant Professor, Department of Environmental Microbiology, BBAU, Lucknow. I shall remain ever indebted to him for his creative and expert guidance, constructive criticism, valuable suggestions, patience, everlasting moral support and his trust on me. It is my proudest privilege, immense pleasure, deep sense of gratitude to owe my heartfelt thanks to Prof. Nishith Verma, Department of Chemical Engineering and Centre for Environmental Science and Engineering, Indian Institute of Technology, Kanpur, for his unconditional support and providing the necessary facility to carry out my research work without which this maiden attempt would not be achieved at the desired level of success. His advice on both research as well as on my career have been priceless. My great thanks are extended to all the faculty member of Department of Environmental Microbiology, BBAU Lucknow, Prof. Rajesh Kumar, Dr. Ravi Gupta, Dr. Digvijay Verma, Dr. Jay Shankar Singh, Dr. Harish Chandra, Dr. Vinay Singh Baghel, Dr. Ram Naresh Bhargava, and Dr. Suneesh Kumar P. for their scientific advice, many insightful

suggestions in the time of discussion. My acknowledgement will never be complete without the special mention of my colleagues Dr. Ashish Yadav, Dr. Pallab Bairagi, Dr. Arun Kumar, Dr. Govind Sharan Gupta, Dr. Umair Alam, Dr. Aradhana Singh, Mr. Justin K George, Mr. Haider Ali, Ms. Priyanka Gupta, Mr. Mohit, Ms. Komal, Ms, Parul, Ms. Ankita, Mr. Naveen Kumar Gupta, and Mr. Ashish Kumar for all their support and motivation during my stay in the laboratory. My heartfelt thanks to them for always being there and bearing with me the good and bad times during my wonderful days of Ph.D. My heartfelt thanks to my friends Mr. Vinay Kumar, Mr. Abhishek Kumar, Mr. Apoorva Dixit, Ms. Jyoti, Ms. Beema, Ms. Ruchi, Mr. Ajay Prakash for always being there through moments of sorrow, joy, failure or victory and for all the moral support they have given. I am also thankful to Mr. Sarju Singh, Mr. Brijesh Shukla, Mr. Vipin Kumar and Ms. Bhoomika Ranjan, staff members of the Department of Environmental Microbiology for their support during the entire research period. I would like to acknowledge the people who mean world to me, my Family. I extend my respect to my father, Sri Ashok Kumar Omar, my mother, Smt. Geeta Omar, my brother Rishi Anand Omar, my sisters Pranjali Yahsasvi Omar and all other members of my wonderful family who all have been supportive and caring. Finally, I thank the Almighty for giving me the strength and patience to work through all these years so that today I can stand proud with my head held high.

Rishabh Anand Omar

List of Abbreviation

DBT	Dibenzothiophene
TH	Thiophene
HDS	Hydrodesulfurization
EDS	Extractive desulfurization
ODS	Oxidative desulfurization
ADS	Adsorptive desulfurization
BDS	Biodesulfurization
LPG	Liquid petroleum gas
USEPA	United States Environmental Protection Agency
IMO	International Maritime Organization
MO	Metal oxide
MOF	Metal organic framework
MDa	Megadalton
PVA	Poly vinyl alcohol
TEA	Triethylamine
HMTA	Hexamethylenetetramine
CVD	Chemical vapour deposition
CNF	Carbon nanofiber
PSD	Pore size distribution
MR	Methyl red
VP	Voges-Proskaure
CFU	Colony forming unit
$Ni(NO_3)_2$-PhB	Nickel nitrate doped phenolic beads
ACB	Activated carbon beads
NiO-ACB	Nickel oxide doped activated carbon beads
Ni-ACB	Nickel doped activated carbon bead Carbon nanofiber containing nickel doped activated caron beads
DszA	DBT-monooxygenase

DszB	DBTS-monooxygenase
DszC	2'-Hydroxybiphenyl-2-sulfinate desulfinase
DszD	Flavin-reductase
FE-SEM	Field emission scanning electron microscopy
XRD	X-ray diffraction spectroscopy
EDX	Energy dispersive x-ray spectroscopy
AAS	Atomic absorption spectroscopy
TPR	Temperature programmed reduction
TGA	Thermal gravimetric analysis
SCCM	Standard cubic centimetre per minute
GC-MS	Gas chromatography-mass spectroscopy
FT-IR	Fourier transform infrared spectroscopy

List of Figures

List of Tables

Chapter 1

Introduction

Currently, fossil fuels are responsible for more than 80% of the world's energy requirements (Mohr et al. 2015). Unfortunately, the unconventional sources of energy are yet to emerge as a viable option for large scale applications. Thus, the steady increase in the number of automobiles, and aviation and naval sectors continue to exert pressure on the supply of crude oils globally (Huda et al. 2018). The increasing dependence on crude oils as the primary source of energy has a direct impact on the environment, because the combustion or processing of crude oils results in the emission of significant amounts of toxic gases such as sulfur dioxide (SO_2) and hazardous chemicals (Colvile et al. 2001; Koch et al. 1996; Isoda, 1998). Sulfur containing compounds in oils are the primary source of the pollutants (Shiraishi et al. 1998).

Sulfur concentrations in the heavy and light crude oils range from 0.1 to 15% and 0.5 to 4%, respectively (Shang et al. 2013). Distillation or refining of crude oils produces many forms of fuels, including liquefied petroleum gas (LPG), gasoline, jet fuels, diesel, and fuel oil (Fig 1.1). Sulfur concentrations in such fuels range from 10 to 10,000 ppm (Gupta et al. 2022; Lee and Valla, 2019). Sulfur compounds exist mainly in two forms in the liquid fuels: aliphatic/inorganic and aromatic/organic. The inorganic forms include elemental sulfur, sulfides, and disulfides. The organic forms include some aromatic ring-structured compounds such as mercaptans, thiophenes, benzothiophenes, dibenzothiophenes, benzonaphthothiophenes, and dinaphthothiophenes (Shang et al. 2013). Fig 1.1 depicts the detailed molecular structures of the organic compounds.

Sulfur concentrations in the crude and diesel oils vary from region to region across the countries (Hassan et al. 2013; Kulkarni and Afosono, 2010). The average

sulfur concentrations have been measured as 0.18, 1.71 and 2.60% (w/w) in the crude oils of Africa, Middle East, and California, respectively (Krivtsov and Golovko, 2014).

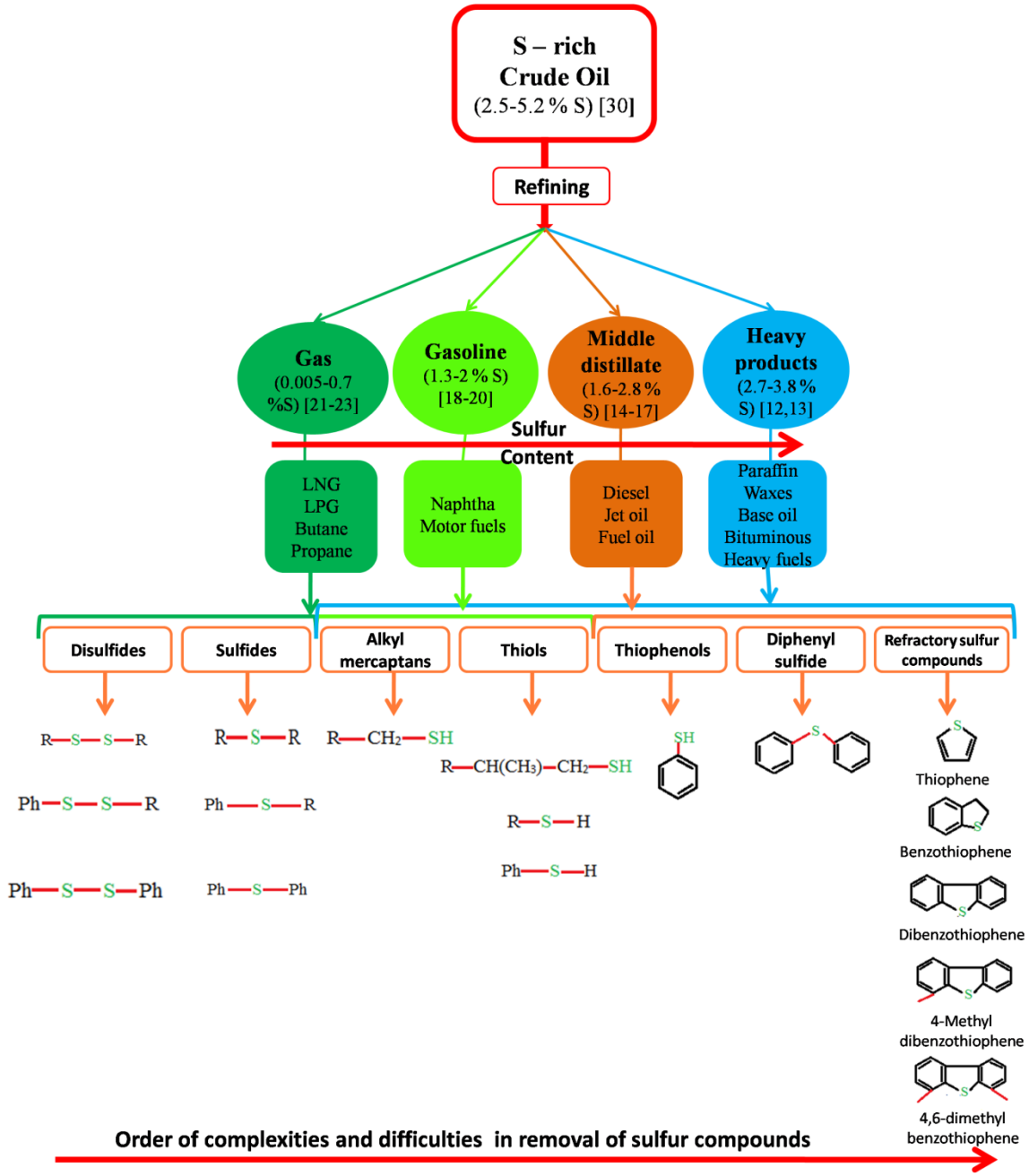

Fig 1.1: Fuel products post-distillation of crude oils and molecular structure of the sulfur containing compounds present in the liquid fuels (Andari et al. 1996; Hua et al. 2003; Fahim et al. 2009)

In 2017, sulfur content in crude oil was measured to be approximately 2.54% (w/w) on a global average (Estephane et al. 2018; Toteva et al. 2009). The average

sulfur content was, however, measured to be 0.08% (w/w) in the refined oils (liquid fuels post-distillation) (Hyrslova et al. 2022; Mello et al. 2009). In 2015, the average sulfur content in the refined oils was found to increase to approximately 0.10% (w/w) (Ogunlaja et al. 2017). Sulfur content in the refined oils ranges between 0.005 and 5.20% (w/w), depending on the types of the oils (Anisimov et al. 2003; Zannikos et al. 1995). In particular, the sulfur concentrations vary between 0.005 and 4% (w/w) in gasoline, and 0.02 and 2.8% (w/w) in diesel (Rafiee et al. 2016; Farshi and Shiralizadeh, 2015; Tang et al. 2013; Prasad et al. 2008).

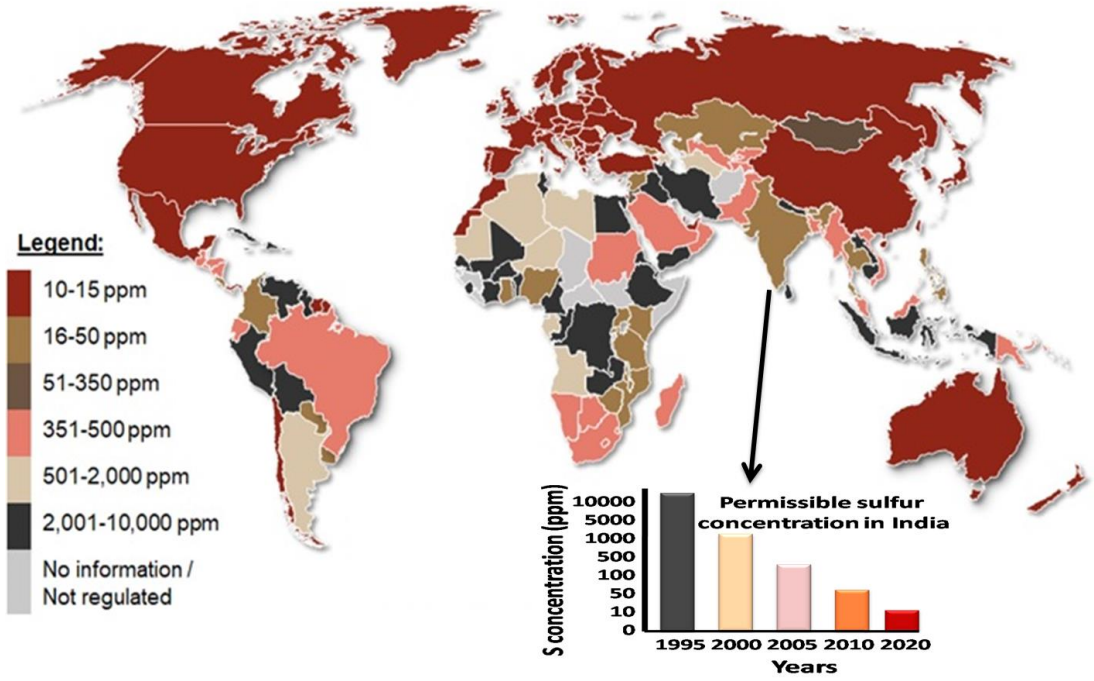

Fig 1.2: Permissible sulfur concentration ranges in the on-road diesels worldwide (Fuel Regulation, 2020; Ogunlaja et al. 2017; Kazakov et al. 2016)

Government agencies have prescribed different maximum (permissible) sulfur concentrations in diesel. Since 2009, the permissible sulfur concentration in diesel in the USA and Japan is specified to be 15 ppm (Nkomzwayo et al. 2022). In the European countries, the limit is 10 ppm (Trakarnpruk and Rujiraworawat, 2009;

Rakhmanov et al. 2016; Shiraishi et al. 2004). In India, the limit is 50 ppm since 2010, which was revised to 10 ppm in 2020 (Fuel Regulations, 2020). Fig 1.2 shows a gradual reduction in the permissible sulfur concentrations in diesel oil, following the periodic revision by the Government of India.

Sulfur concentrations in the on-road diesels varies over the range 10-1000 ppm globally. In some countries, for example, Afghanistan, Central African Republic, South Sudan, Chad, and Somalia, there is no limit or regulation for sulfur emission. Fig 1.2 pictorially presents the permissible sulfur concentration ranges in the on-road diesels worldwide (Stratas, 2020).

In past decades, hydrodesulfurization was commonly used technique for reducing the sulfur level in liquid fuels. However, the process requires harsh conditions (high temperature and pressure) (Otsuki et al. 2000). One another technique which is adsorptive desulfurization (ADS) is studied in last few for the reducing the sulfur level in liquid fuels. The technique was efficient for higher sulfur concentration however, inefficient at low concentrations of sulfur compounds (Pawelec et al. 2005). Therefore, desulfurization using microorganism becomes keen interest of researchers in this field. Some of the bacteria were found to be capable of removing organic sulfur compounds form the liquid fuels and the process was known as biodesulfurization (BDS). The process was efficient for low level (concentration) sulfur removal; however, microorganisms were not able to survive at high concentration of sulfur (Yi et al. 2019; Mei et al. 2003).

Hence, ADS together with BDS can successfully reduce the sulfur content of the liquid fuels. Since, DBT and its derivatives are among the most persistent sulfur heterocyclic compounds present in liquid fuels, therefore DBT and TH is used as a

model compound to study adsorptive and biodesulfurization in this research work. In view of the above, it is of great significance to synthesize and characterize the adsorbent for ADS also isolate and characterize the bacterial species capable of removing sulfur compounds from the liquid fuels so that it could be further used for development of suitable protocol for desulfurization of liquid fuels.

Therefore, the present study is focused on the synthesis and characterization of suitable adsorbent and its activity for adsorption of DBT and TH. For BDS isolation, identification and characterization of desulfurizing bacteria and further optimization of desulfurizing conditions and activity in removal of DBT and TH from liquid fuels. In further ADS and BDS was integrated sequentially for efficient desulfurization of DBT and TH in liquid fuel. In order to achieve these following objectives were set:

1. Synthesis and Characterization of Ni-doped carbon beads

- Synthesis of Ni-doped carbon beads by using the standard suspension polymerization reaction.
- Carbonization, activation and reduction of beads by thermal treatment in appropriate temperature in presence of N_2 and H_2 environment.
- Physico-chemcial characterization of the prepared beads will done by the scanning electron microscopy (SEM), energy dispersive x-ray spectroscopy (EDS), Brunauer-Emmett-Teller (BET) surface area, pore volume and pore size analysis, atomic absorption spectroscopy, thermogravimetric analysis (TGA) and Fourier transform infrared spectroscopy (FT-IR).

2. Adsorption of Dibenzothiophene and Thiophene in liquid fuel by Ni-doped carbon beads

- Prepared beads will be tested for the adsorption of sulfur containing thiol compounds (DBT and TH) in model liquid fuel in a specifically designed reactor in optimized physical parameters.

3. Isolation, identification and characterization of desulfurizing bacteria

- Desulfurizing bacteria will be isolated from soil collected from contaminated fields with liquid fuels, such as near petroleum plants and crude oil refineries.
- The selected bacteria will be characterized at molecular and biochemical levels.

4. Desulfurization test for Dibenzothiophene and Thiophene by bacterial isolates

- The isolates will be tested for their ability to desulfurize thiol compounds (DBT and TH) in various concentrations.
- Desulfurization of DBT and TH will also be performed using the induced/resting cells of the selected bacteria.

5. Complete desulfurization of DBT and TH in liquid fuel using Ni-doped carbon beads followed by an isolated bacterial strain

- In the final experiment, Ni-doped carbon beads will be used in conjunction with isolated bacteria to complete desulfurize thiol compounds.
- Using Ni-doped carbon beads and bacteria sequentially, the complete desulfurization will be achieved in a specially designed reactor.

This study examines the potential of Ni-doped adsorbent material and a few isolated bacterial strains to desulfurize DBT and TH, the most persistent sulfur compounds in liquid fuels. This sulfur removal will help us to better understand the adsorption process and the biodesulfurization of organosulfur compounds. Furthermore, this study could also provide significant benefit in terms of developing an efficient and improved desulfurization technique for complete removal of sulfur compounds which can be applied to the desulfurization of refractory organic sulfur compounds in liquid fuels and sustainable development.

.

Chapter II

Review of literature

2.1 Methods of Desulfurization

In order to meet the regulatory limits, sulfur content or sulfur compounds in liquid fuels must be controlled. Hydrodesulfurization (HDS), oxidative desulfurization (ODS), extractive desulfurization (EDS), adsorptive desulfurization (ADS), and biodesulfurization (BDS) are methods of removing sulfur from liquid fuels (Hyrslova et al. 2022; Crandall et al. 2019; Javadli and De, 2012).

The HDS process use hydrogen (H_2) gas over a catalyst at high temperature and pressure to convert sulfur to hydrogen sulfide (H_2S) (Prajapati and Verma, 2018). Liquid fuelspass through the reactor to a separator where sulfur compounds are separated as H_2S and the rest of the liquid fuel is transferred for distillation, resulting in different fuel products.The ODS process uses an oxidizing agent at high temperatures to covert sulfur to sulfonesor sulfoxides, and their derivatives. Sulfones and sulfoxides are separated using extraction and/or adsorption (Li et al. 2020). However, separation is tedious in ODS process, requiring multi-steps, one for the separation of sulfone and another for the separation of the oxidizing agent. The EDS process uses some liquid solvents, e.g., ionic liquids, or ethanol or acetone or polyethylene glycol which can bind with sulfur compounds in fuels.The spent liquids are then subjected to extraction to produce the treated oils free from sulfur (Lee and Valla, 2019; Ibrahim et al. 2017). However, selection of a suitable ionic liquid and the optimization of the liquid-liquid/liquid-solid extraction conditions is a difficult task in EDS process. The ADS process is approximately similar to EDS. However, instead of using an ionic liquid, ADS uses an adsorbent to remove the sulfur compounds in which a suitable adsorbent is mixed with the sulfur containing liquid fuels at an optimizedtemperature and pressure condition for a certain time.

ADS is an efficient technique, requiring less sever operating conditions (temperature and pressure) than HDS. Therefore, the process is energy-efficient. In addition, this process does not alter the quality (physical properties) of oil. The technique is easy to implement though the process requires an efficient adsorbent, implying that the material should have a large adsorption capacity, and it should also be sustainable (Prajapati and Verma, 2018). Various ADS studies have been performed using several types of adsorbents such as activated carbon, metal oxides (MOs), metal organic frameworks (MOFs), zeolite and its derivatives to achieve the desulfurization (Xu et al. 2022; Nkomzwayo et al. 2022; Shen et al. 2022). Fig. 2.1 presented an overview of various desulfurization processes.

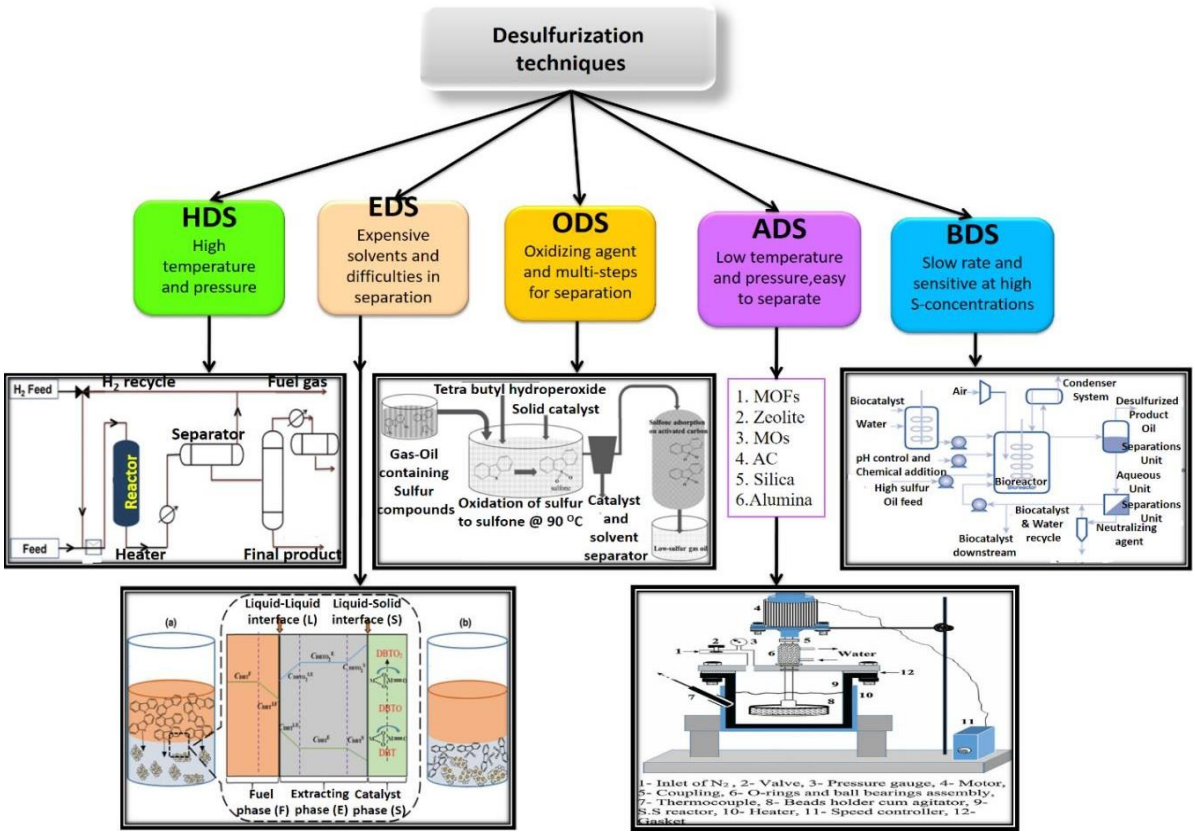

Fig 2.1: An overview of various desulfurization techniques (Prajapati and Verma, 2017; Dizaji et al.2019; Betiha et al. 2018; Badoga et al. 2018; USDE, 2020)

The ADS process is ideal for operation at an industrial scale. The regeneration of the adsorbents is however, challenging. A good adsorbent should be regenerated without loss of its efficiency (i.e., the regenerated materials should be able to adsorb the same amounts of sulfur compounds as adsorbed originally). The ADS adsorbents are often doped with metals with a view to increasing the adsorption capacity of the materials. The metal binds with the sulfur compounds in oil via the covalent bonds (Prajapati and Verma, 2017; Prajapati and Verma, 2018). Denaturation or breakage of such bonds using thermal or chemical methods is challenging.

2.2 Absorbent materials in ADS

The selection of a suitable adsorbent is important for all adsorption processes including ADS. An efficient adsorbent should be porous, physically and chemically stable, environmentally benign, and amenable to regeneration. The ADS adsorbents are microporous activated carbon,zeolites, alumina, mesoporous silica, and MOFs (Ahmed and Jhung, 2016). These adsorbents and the various desulfurization experiments using these adsorbents are described in this section. Additionally, a brief discussion is provided of the various (adsorptive) desulfurization tests and the experimental conditions that were used. During desulfurization tests, the conditions, viz., sulfur concentration, temperature and the time of exposure of the adsorbents to sulfur containing liquid fuels, need to be considered when framing the regeneration strategies.

2.2.1 Alumina-based adsorbents

Activated alumina (aluminum oxide) is a crystalline material and has sufficient porosity to serve as an adsorbent in many adsorption applications including ADS. The material also has the capability of creating oxygen vacancies (defects) in its surface. Thus, it contains both the Lewis and Bronstead acid sites (Rouquerol, 1999). The pores ofthe activated alumina can be modified by chemical treatments using HCL or HF (acid) orsome alkaline substances. A controlled thermal treatment is also used to modify its pore structure. The material shows two phases: an amorphous acidic phase and a nanopowder phase (Etemadi and Yen, 2007). Because of these diverse properties, the activated alumina-based adsorbents are more versatile and efficient than the silica-based adsorbents (Yang, 2003). Zirconia (zirconium oxides), an alternative of alumina (having the same properties as alumina) is also a common adsorbent used for ADS. Some studies have introduced Cu and Zn in the alumina matrix with a view to enhancing the adsorption capacity of the material (Baeza et al. 2008; Kumar et al. 2011). The main disadvantage of using the activated alumina-based adsorbents is its small adsorption capacity for the organic or refractory sulfur compounds because of the presence of amorphous acidic phase in the material and its crystalline nature (Larrubia et al. 2002).

The adsorption tests using alumina-based materials have been performed over the temperature range 25-500 ^{o}C. The adsorbents (without metal) show the maximum sulfur adsorption capacity in the range 2.6-60 mg/g over the initial concentration range 250-1000 ppm. The metal-doped adsorbents show the relatively reduced adsorption capacities (2.17-2.6 mg/g); however, they are effective over the small concentration levels (15-250 ppm) (Neubauer et al. 2019; Qin et al. 2016; Liao et al. 2015; Mansouri et al. 2014).

2.2.2 Silica-based adsorbents

Silica or silica gel has been commonly used for the removal of sulfur from the liquid fuels. Silica modified by the reaction or grafting of a monolayer of organic legends, renders the material even more efficient. The commercially available silica-based adsorbents for ADS are SBA-15 and KIT-6. Park et al. (2008) have studied the adsorption of sulfur compounds over the Ni-doped SBA-15. The adsorption capacity was measured to be approximately 220 ppm in a commercial diesel oil containing sulfur at 240 ppm concentration level in diesel. The silica-based adsorbents are relatively less efficient in adsorbing sulfur at high (>500 ppm) concentrations in liquid fuels (Srivastava, 2012).The adsorption tests in the aforesaid studies were performed at room temperature (30- 35ºC). The adsorbents (with metal) showed the maximum sulfur adsorption capacity in the range 2.60-32.6 mg/g over the initial concentration range 150-1000 ppm (Subhan et al. 2018; Wu et al. 2018; Kong et al. 2017; Ren et al. 2016).

2.2.3 Zeolite-based adsorbents

Zeolites are the naturally occurring aluminosilicate materials. The material is successfully tested as a catalyst and an adsorbent (Přech, 2018; Liang et al. 2017; Burakov et al. 2018; Zanin et al. 2017). The properties and applications of the zeolite aredetermined by its Al/Si ratio that also defines the structure of the material (Nair et al. 2013). The relatively less Al/Si ratio makes the material acidic, and the material is used as an ion-exchanger. Zeolites have also been doped with the metals, making them more efficient in the adsorption applications. Y-zeolite is the commonly used ADS adsorbent. In has a unique three-dimensional structure of faujasite (FAU) framework, with a large surface

area and a large number of acidic sites, making the material suitable for adsorptionof sulfur (Lee and Valla, 2019). However, the material is microporous, which limits the adsorption of the refractory sulfur (Lee et al. 2018). Another drawback is the selectivity of the material. Zeolites show a limited selectivity towards the organosulfur compounds or the sulfur molecules in the presence of aromatic compounds in liquid fuels. The inclusion of a metal in zeolite can mitigate the problem (Kim et al. 2006).

The zeolite-based adsorbents use the relatively high temperature range of 25-500 ^{O}C. The adsorbents (without metal) show the maximum sulfur adsorption capacity in the range 4.72-23.5 mg/g over the initial concentration range 250-700 ppm. The metal- doped adsorbents show the adsorption capacity in the range 0.39-86.4 mg/g sulfur at theinitial concentration of 50-2000 ppm (Lee and Valla, 2019; Han et al. 2019; Bakhtiari et al. 2019).

2.2.4 Carbon-based adsorbents

Activated carbon is probably the oldest material used as an adsorbent for pollution control, both in the gaseous as well as aqueous phases. The material is microporous with a significantly large BET surface area (1500-3000 m^2/g) and pore volumes, amenable to surface functionalization, and stability in acidic medium (Bandosz, 2006). Most of the commercially available granular and powdery carbons are bioresourced, e.g., synthesized from coconut shells and woods. Synthetic carbon is prepared by carbonizing a polymer and then activating the carbonized mass using some chemical reagents. The activation step creates a porous structure in the material (Yang et al. 2011). Considering a large internal surface area of the material, activated carbon expectedly shows higher

physisorption than its counterparts, namely: silica and alumina (Prajapati and Verma 2017; Yu et al. 2008; Moreira et al. 2017). However, the selectivity for aromatic hydrocarbons is inferior (Lee et al. 2019). Thus, introduction of some transition metals such as Ag (Ai etal. 2012), Cu, Co (Seredych et al. 2012), Ni (Saleh, 2018), and Mn (Liu et al. 2019) renders the carbon materials more efficient, and capable of removing the aromatic hydrocarbons. The metal-doped carbon-based adsorbents can remove sulfur from the liquid fuels by forming π-π complexation (between carbon and sulfur compounds) or metal-sulfide interaction (between metal nanoparticles and sulfur compounds) (Jung and Jhung, 2015; Nunthaprechachan et al. 2013). The activated carbon-based adsorbents are alsothermally stable.

The adsorption tests using carbon have been performed over the temperature range 23- 20 ^{o}C. The adsorbents (without metal) show the maximum sulfur adsorption capacity in the range 2.0-18 mg/g over the initial concentration range 100-600 ppm. The metal-doped adsorbents show the relatively larger adsorption capacity in the range 2.0-62.0 mg/g sulfur at the initial concentration of 20-1000 ppm (Jha et al. 2020; Jha et al. 2019, Li et al. 2018; Zhao et al. 2018).

2.2.5 MOF adsorbents

MOFs are the relatively newer materials tested an ADS adsorbent, although with limited success. The materials are the hybrid organic-inorganic frameworks consisting of mainly two components: a metal ion or cluster of metal ions and an organic linker that connects the metal ions or clusters to build up the framework. The linker molecule connects the metal ion by di, tri, or tetra dentate chelating sites. Some commonly-used linkers are imidazole, benzene dicarboxlic acid and benzene tricarboxlic acid (Yang et al.

2013; Decoste and Peterson, 2014; Wu et al. 2012). These materials contain pores of different sizes and shapes, which make them characteristically unique (Khan et al. 2017). The common MOFs discussed in the literature for ADS are MIL 101, HKUST-1, NENU-511,and UMCM (Cychosz et al. 2008; Schnobrich et al. 2010; Shah et al. 2017). The adsorption capacity and selectivity of an MOF depend on the types of metal ion and organic linker. The salient feature of the MOFs is the flexibility of the materials to bind most of the metals with an appropriate linker, thus exhibiting a wide range of physicochemical properties. The main disadvantage of the material is that the linker molecules often collapse at high temperatures or under severe hydrothermal conditions. Also, in most of the MOFs, porosity in the material is too small to allow for the large adsorption of the sulfur compounds in liquid fuels (Mcnamara et al. 2013).

The MOF-based desulfurization studies have used the temperature range of 25-220 ^{O}C. The adsorbents show the maximum sulfur adsorption capacity in the range 2.0-227 mg/g over the concentration range 14-1000 ppm (Mahmoudian et al. 2020; Song et al. 2019; Aslam et al. 2017; Khan et al. 2016).

2.2.6 Metal oxides

The oxides of several transition metals, viz. Fe, Ni, and Co have been used for ADS (Kharisov et al. 2017). Titania (TiO_2)-supported metal oxides have also been found to be efficient in removing DBT and TH from the liquid fuels (Tran et al. 2018). Menzel et al. (2016) have studied the mixed metal oxides supported on graphene oxide for ADS. Such adsorbents are relatively less expensive to prepare. However, the adsorption capacities of the oxides for the refractory sulfur compounds are small. The metal oxides also require

a support for their stability, which makes them cost-ineffective (Zhang et al. 2005). Desulfurization tests using metal oxides and metal nanoparticles have been performed over the temperature range 25-60^{o}C. The adsorbents show the maximum sulfur adsorption capacity in the range ~1.5-35 mg/g over the initial concentration range 100-1390 ppm (Xiong et al. 2020; Yang et al. 2018; Li et al. 2015; Xu et al. 2016).

Table 2.1 summaries the operating conditions used in various adsorptive desulfurization studies in different thiol compounds, and sulfur loading on various adsorbents at different initial concentrations.

Table 2.1: An overview of adsorptive desulfurization studies

S. No.	Adsorbents	Sulfur Compound	Initial Sulfur concentration (ppm)	Sulfur loading	Temperature (^{o}C)	References
1	Alumina	DBT	700	3.5 mg/g	200	Etemadi and Yen, 2007
2	Cu-Zirconia	TH	2000	0.49 mM/l	30	Baeza et al. 2008
3	Zirconia	DBT	1000	55 mg/g	50	Kumar et al. 2011
4	Alumina	DBT	1000	16.6 mg/g	30	Srivastav and Srivastava, 2009
5	γ-Al_2O_3	DBT	1000	59.7 mg/g	30	Qin et al. 2016
6	γ-Al_2O_3	DBT	900	2.6 mg/g	30	Neubauer et al. 2019
7	Ni-Cu-Y	DBT	250	3.6 mg/g	150	Mansouri et al. 2014
8	Zn-Al_2O_3	TH	20	2.8 mg/g	500	Yang et al. 2007
9	Y-Al_2O_3	TH	250	2.2 mg/g	30	Liao et al. 2015
10	Ni-SBA15	DBT	10	1.7 mg/g	100	Park et al. 2008
11	Ag-SBA15	BT	150	2.6 mg/g	30	Wu et al. 2018
12	Ti-SBA15	TH	300	12.7 mg/g	35	Ren et al. 2016
13	Ni-KIT6	TH, DMTH	517	0.2 mmol/l	30	Aslam et al. 2016
14	Cu -SBA15	TH	1000	28.94 mg/g	30	Kong et al. 2017
15	Ce/KIT-6	TH	510	0.1 mmol/l	30	Subhan et al. 2018

16	CuCe-Y	DBT	100	99%	30	Lee et al. 2018
17	Zeolite	BT	250	5 mg/g	25	Sotelo et al. 2007
18	Zeolite	BT	500	4.7 mg/g	25	Nuntang et al. 2008
19	Na-Y	TH, DBT	500 -700	23.5 mg/g	80	Zhang et al. 2008
20	CuCe-Y	DMDBT	100	6.8 mg/g	500	Lee et al. 2019
21	Cr-Mil	DBT	2000	86.4 mg/g	25	Han et al. 2019
22	Ag-zeolite	TH	400	1.1 mmol/g	75	Bakhtiari et al. 2019
23	Cu-zeolite	MBT	750	36 mg/g	180	Dias et al. 2019
24	Na- zeolite	Diesel	50	0.4 mg/g	400	Dasgupta et al. 2015
25	Cu-zeolite	DBT	15 mmol/g	0.5 mmol/g	30	Li et al. 2005
26	Ag-zeolite	DBT	8 mmol/g	0.3 mmol/g	30	Li et al. 2009
27	Ni-Y	Diesel	450	50 mg/g	30	Dasgupta et al. 2013
28	Ni-C	DBT, TH	1200	40 mg/g	120	Prajapati and Verma, 2018
29	P on carbon	DBT	20	0.2 mmol/g	400	Seredych et al. 2012
30	Cu-CO-AC	TH, DBT	50	3.6 mg/g	25	Saleh et al. 2018
31	AC	DBT	500	2.012 mg/g	23	Alhamed and Bamufleh, 2009
32	AC	BT	100	67 mg/g	25	Jung and Jhung, 2015
33	AC	DBT	100	55 mg/g	30	Nunthaprechachan etal. 2013
34	Graphene	DBT	600	117.2 mg/g	30	Jha et al. 2020
35	AC	DBT	500	84.4 mg/g	30	Jha et al. 2019
36	AC	DBT	300	41.5 mg/g	30	Shi et al. 2015
37	C-spheres	DBT	200	33.2 mg/g	30	Li et al. 2018
38	N-S-AC	DBT	500	83.3 mg/g	30	Zhao et al. 2018
39	Polymer-GO	DBT	500	181 mg/g	25	Duan et al. 2014
40	CNT, CNF	DBT	250	25 and 20 mg/g	30	Jha et al. 2019
41	AC	DMDBT	150	20 mg/g	25	Triantafyllidis and Deliyanni, 2014

42	AC	DBT	100	18.3 mg/g	25	Shi et al. 2015
43	AC	BT, DBT	400	11.6 mg/g	60	Zhou et al. 2009
44	Waste tyres	P-thiol	50	9.6 mg/g	25	Chao et al. 2019
45	Br-C	DMBT	300	4.8 mg/g	30	Ganiyu et al. 2017
46	Zn-AC	DBT	15.6 mmol/g	0.4 mmol/g	30	Thaligari et al. 2016
47	Ag-Ac	DBT	600	26.9 mg/g	25	Olajire et al. 2017
48	Ag-C-Si	DBT	206	6.8 mg/g	30	Liu et al. 2019
49	Zn-C	TH	250	12.5 mg/g	25	De et al. 2018
50	MnO2-AC	TH, DBT	50	11.4 mg/g	25	Saleh et al. 2017
51	Ni-Fe-rGO	BT, DBT	100	1 mmol/g	40	Zhao et al. 2019
52	CO-MO-AC	TH, DBT	300	3.7 mg/g	30	Saleh, 2018
53	Zn-Co-C	DBT	500	40.6 mg/g	100	Huo et al. 2019
54	Ce-Fe-AC	TH, DBT	150	16.5 mg/g	30	Danmaliki and Saleh, 2017
55	Cu-Zn-C	DBT	500	60 mg/g	30	Huo et al. 2019
56	Zn-MOF-C	TH, DBT	100	11.3 mg/g	25	Zhu et al. 2018
57	Zr on rGO	DBT	500	46.6 mg/g	30	Safari et al. 2016
58	Ni-AC	DBT	20	2.8 mg/g	30	Selvavathi et al. 2009
59	Ni-C	DBT	1000	62.8 mg/g	40	Nejad et al. 2013
60	Ni-C	TH	35	0.6 mg/g	30	Prajapati and Verma, 2018
61	Ni-AC	DBT	59	96%	30	Danmaliki et al. 2017
62	CuCe-MIL	BT	1000	87 mg/g	25	Khan et al. 2017
63	MCM-150	BT, DMDBT	1500	41 mg/g	25	Cychosz et al. 2008
64	Cu-MOF	DBT	1000	90 mg/g	25	Mahmoudian et al. 2020
65	Eu-MOF	TH	100	24.6 mg/g	30	Habimana et al. 2016
66	Cu-MOF	DBT	100	4.7 mg/g	30	Song et al. 2019
67	Cu-MOF	BT, DBT	1000	80 mg/g	30	Hasan and Jhung, 2015
68	Pd-MCM	MDBT	300	2.2 mg/g	200	Teymouri et al. 2013

69	Ni-MCM	DMDBT	14.4	2.1 mg/g	220	Sentorun et al. 2011
70	Cu-MOF	BT	1000	77.5 mg/g	25	Khan and Jhung, 2012
71	Ni-MOF	TH	700	25 mg/g	25	Aslam et al. 2017
72	MIL-AC	TH, DBT	1000	277 mg/g	25	Khan et al. 2016
73	Cr,Al-MIL	BT	1000	80 mg/g	25	Khan et al. 2011
74	Cr -MOF	BT, DMDBT	550	1.3 mmol/g	30	Li et al. 2015
75	Mixed MOs	TH	1500	70 mM/l	60	Menzel et al. 2016
76	Metal-PMB	DBT	462	20.37 mg/g	25	Xia et al. 2016
77	AgCl NPs	TH	550	0.5 mM/l	25	Li et al. 2015
78	Ni,Cu-CLP	DBT	500	28.1 mg/g	25	Moradi et al. 2018
79	TiO2–CeO2	BT, DBT	100	1.45 mg/g	25	Xiao et al. 2013
80	BN	DBT, MDBT	500	45.2 mg/g	25	Xiong et al. 2020
81	$AgTiO_2SiO_2$	DMDBT	953	5.4 mg/g	60	Xu et al. 2016
82	Cu-BTC/HG	TH	550	35.6 mg/g	25	Yang et al. 2018

2.3 Biodesulfurization

BDS is an alternative technique based on microorganism, biological activities and enzymes (Caro et al. 2007). It is a cost and energy efficient process in comparative to other desulfurization techniques. In this process, several different types of microbes such as bacteria and fungi remove sulfur from the liquid fuels at moderate temperature and pressure, without breaking the carbon skeleton. (Monticello, 2000).

In BDS, microorganism uses sulfur for their growth and important element for physiological and metabolic activity (Prasoulas et al. 2021). Because for metabolic activity, microorganism produces some enzymes, and cofactors (such ads thiamine, biotin, cystine, and methionine) contains sulfur in their structure (Gray et al. 2003; Guobin et al. 2006; Kertesz, 2000). To fulfill the requirement of sulfur, microorganisms

intake the sulfur from different sources, depending on the metabolic activities and enzymes produces by microorganisms (Maghsoudi et al. 2001). In these variation in sulfur sources, some microorganisms uptake the sulfur form thiol compounds namely BT, DBT, DMDBT, and TH, and reduces the sulfur amount in liquid fuels (Alves et al. 2005; Tanaka et al. 2002; Furuya et al. 2001; Li et al. 2005). Additionally, the BDS process uses moderate temperature and pressure. This property makes the process superior than HDS process. Also, BDS process uses enzymes, due to which the desulfurization is highly selective. This property of BDS make it superior than the EDS because it is difficult to find a suitable ionic liquid for desulfurization. In the following section, various metabolic pathways of BDS are discussed.

2.3.1 Metabolic pathways of Biodesulfurization

Mainly three different pathways have been categories for biodeuslfurization. The pathways are as follow

2.3.1.1 Biodesulfurization via disruptive pathway

Few bacteria having capability to use DBT as their energy source were isolated form natural habitat contaminated with oil/sulfur containing compounds (Castorena et al. 2002; Malik and Ka, 1978; Laborde and Gibson, 1977). Some of the isolated bacteria were not capable for specific removal of sulfur from the DBT. Few of them used thiophenic compound as their sulfur and carbon source (Monticello et al. 1985; Kodama et al. 1970; Yamada et al. 1968). However, some other bacteria used DBT as their energy source and via a series of oxidizing reactions and convert them into some water-soluble

compounds. In spent solution, these water-soluble compounds started to accumulate and cause inhibition of microbial growth and the DBT degradation (Peh et al. 2022). In this pathway the microbial enzymes attack on phenyl ring cause breakage of one or more bond or a fragment form the phenyl ring. However, due to non-specific sulfur removal from compound, this microbial treatment was not considered under biodesulfurization approach. Pathway is not limited to DBT only, other aromatic compounds not having sulfur in their structure was also targeted through this pathway for the breakage of aromatic bonds. Due to non-specific cleavage of carbon-carbon bond in benzene ring, this pathway named as disruptive biodesulfurization pathway (Soleimani et al. 2007).

The carbon disruptive and oxidative series of enzymatic reactions attacks carbon atoms of phenyl ring of DBT is also known as Kodama pathway of biodesulfurization (Mcfarland et al. 1998). The pathway consists of mainly three steps. The first one is hydroxylation, then ring cleavage and in last hydrolysis (González et al. 2021; Gupta et al. 2005). Fig 2.2 describes the Kodama pathway structurally.

Diverse groups of bacteria have been reported for desulfurization of DBT through carbon disruptive pathway. However, *Pseudomonas* was reported as a dominant species for disruptive desulfurization (Hartdegen et al. 1984). Monticello et al. (1985) also studied the microbial degradation of DBT through Kodama pathway of desulfurization. They used two different *Pseudomonas* cultures namely *Pseudomonas alcaligenes* and *Pseudomonas putida*. Their studies demonstrated that the desulfurization in two *Pseudomonas* species were plasmid-mediated. Therefore, plasmids were responsible for degradation of DBT through Kodama pathway in *Pseudomonas* spp. (Monticello et al. 1985).

2.3.1.2 Biodesulfurizarization in anaerobic environment

Few bacterial strains are capable to remove organic sulfur such as DBT from the liquid fuels under anaerobic environment. Yeong et al. (1990) have studied the anaerobic desulfurization by *Desulfovibrio desulfuricanse* M6. This bacterium degraded approximately 96% and 42% of benzothiophene (BT) and dibenzothiophene (DBT), respectively under anaerobic conditions. Additionally, they analyzed the metabolic product of desulfurization. Anaerobic degradation of DBT produced biphenyl and hydrogen sulfide (H_2S), which is indicative of anaerobic degradation. Anaerobic bacteria such as *Desulfomicrobium scambium* and *Desulfovibrio longreachii* have also been reported to be capable of anaerobic desulfurization (Sousa et al. 2020; Onodera et al. 2001). In an anaerobic environment, these bacteria showed approximately 10% degradation of DBT in kerosine.

The GC analysis of spent solution showed unknown metabolites, which is conforming that the bacteria were followed some other pathway for DBT degradation, that common anaerobic pathway of degradation.

The main advantage of anaerobic desulfurization is that reaction occurs in reducing environment, due to which oxidation of hydrocarbons to undesirable products such as colouring compound and/or gum forming product is minimal (Mcfarland, 1999). This advantage could be considered as an initiative to continue research in anaerobic desulfurization or reductive desulfurization. However, maintaining the anaerobic environment for anaerobic activity is extreme difficult. During anaerobic conditions, the mechanisms of microbial desulfurization is still not well-understood (Mcfarland et al. 1998).

2.3.1.3 Biodesulfurization via specific oxidative pathway

The process of desulfurization through Kodama pathway was non-specific for removing sulfur form DBT/TH rings and destructive in nature due to cleavage of carbon-carbon bond of benzene ring. There was a need to overcome this problem. Therefore, some attempts were made to isolate some microorganisms capable of removing sulfur from the organosulfur compounds in non-destructive manner in aerobic or anaerobic environment. In that time most of the attempts were insignificant because it gave rise for the isolation of more bacteria following carbon destructive pathway (Soleimani et al. 2007; Stevens and Burgess 1987).

Kilbane (1989) have proposed a hypothetical specific oxidative biodesulfurization pathway with the assumption that if any specific oxidative biodesulfurization activity will occur in future, will follow this pathway only. The proposed pathway was known as 4S pathway due to four consecutive oxidations of DBT to sulfoxide (DBTO) then sulfone ($DBTO_2$) then sulfinate (HPBS) and finally hydroxybiphenyle (HBP) (Kilbane, 1989). Fig 2.2 describes the 4S pathway of biodesulfurizion. After the discovery of Kilbane's hypothetical pathway (Kilbane, 1989), isolation of non-destructive sulfur removing bacteria becomes key of interest.

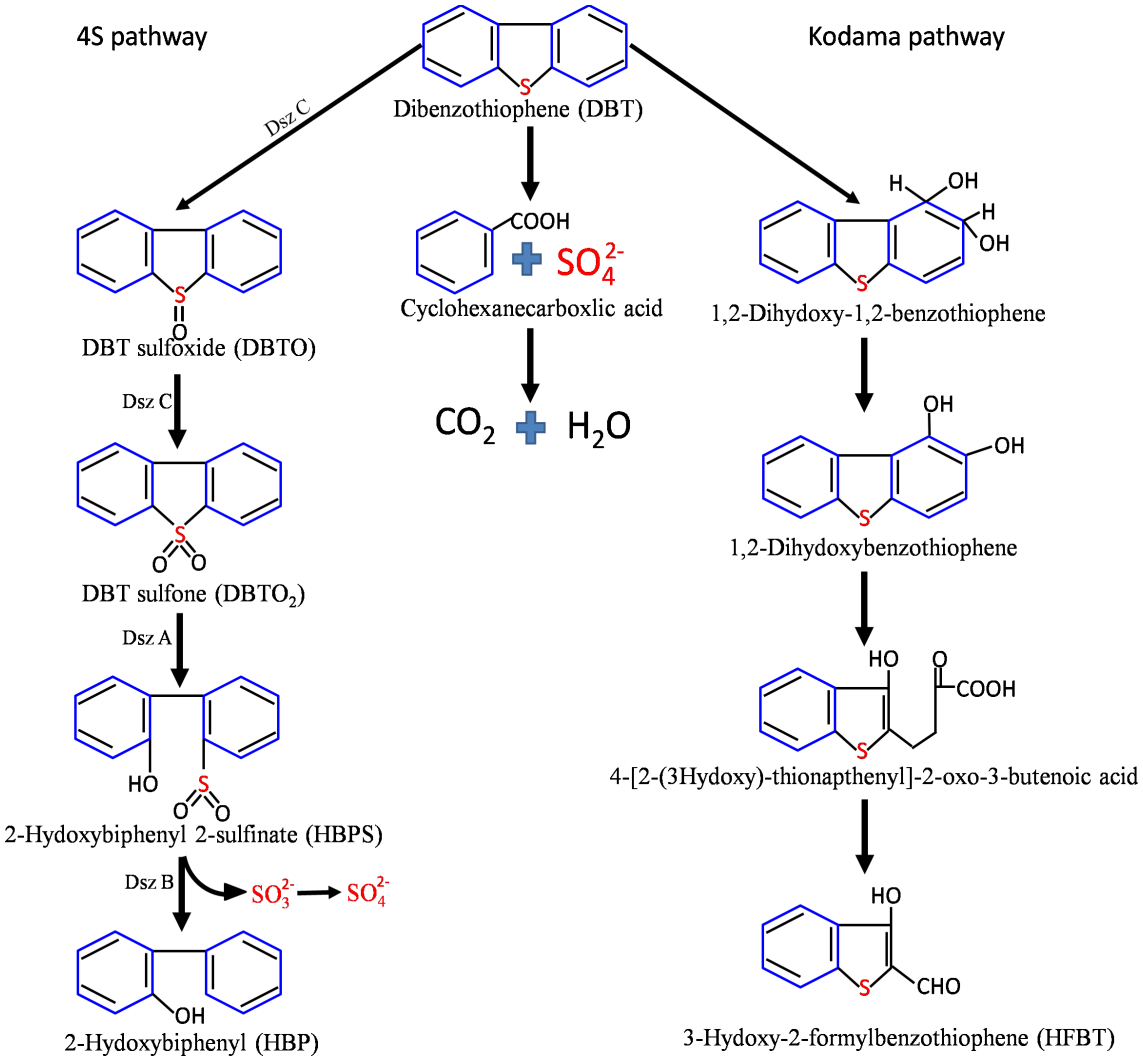

Fig 2.2: Bacterial metabolic pathways of DBT removal (Li et al. 2009; Alves et al. 2008)

Van et al. (1990) have isolated *Brevibacterium* sp. DO bacterium. This bacterium was capable to grow in sulfur environment and consumed DBT as their sulfur and carbon source. The DBT degradation pathway in this bacterium was different from the Kodama pathway and somewhat similar to 4S pathway. The bacterial strain firstly transforms DBT to DBTO and the into $DBTO_2$. The $DBTO_2$ sulfur was removed to form SO^{2-} and SO^{2-} consecutively. After the removal of sulfur $DBTO_2$ converted to benzoate and further mineralized to water and carbon dioxide. However, the pathway of desulfurization was

somewhat similar to 4S pathway, but still it was considered as carbon destructive pathway because some aromatic compounds was deteriorated during desulfurization process (Van et al. 1990). Similar to *Brevibacterium* sp. DO, other bacterium, *Arthrobacter* sp. K3b was also isolated from oil contaminated field. This bacterium was capable to transform the $DBTO_2$ (not DBT) to benzoate and sulfate. The benzoate was further used in the energy cycle (tricarboxylic acid cycle) (Malani et al. 2021; Dahlberg et al. 1993; Nojiri et al. 2001). Desulfurization by this bacterium was also considered in disruptive desulfurization due to the similar reason mentioned above for *Brevibacterium* sp. DO.

Apart from bacteria, a species of fungi named *Cunnighamella elegans* have also been studied for desulfurization of DBT. The fungi sowed transformation of DBT to DBTO and finally in $DBTO_2$. However, no further studies were reported for desulfurization using these fungal strains (Holland et al. 1986; Crawford and Gupta, 1990). Inanother study, Stevens and Burgess (1989) have used mixed culture of cells of *Hansenula*sp. for non-specific oxidative desulfurization of DBT. The mixed culture secretes surfactant like matrix, leads to enhance the desulfurization activity. However, due to non-specific desulfurization, the study was not found useful in this field (Stevens and Burgess, 1989). These all the studies concluded that the specific oxidation of C-S bond is not possible naturally. In 1990, the Institute of Gas Technology (IGT), Chicago have attempted to develop a new bacterial strain by modifying its genetic structure through unnatural selective mutation (Soleimani et al. 2007). They have used a mixed culture soil sample of an oil contaminated field. The sample was incubated in a bioreactor containing mutagens NTG (1-methyl-3-nitro-1-nitrosoguanidine) act as a chemical mutagen. After incubation, it was noticed that certain group of bacterial species surviving

in the bioreactor. After further experiments, it confirmed that those bacterial species are capable to degrade DBT through specific C-S breakage pathway. They removed approximately 90% of organic sulfur from the coal sample through specific oxidation activity. At that time this microbial consortium was named as IGTS7, comprising of seven different types of bacteria (Kilbane and Bielaga, 1990; Kilbane, 1992). Among them two previously known desulfurizing bacteria namely, *Rhodochrous rhodochrous* and *Bacillus sphaericus* were also present in least abundance. These bacterial strains were confirmed the desulfurization capability. They had a small population and a slow growth rate. In this case, these two species were *Rhodococcus rhodochrous* and *Bacillus sphaericus*. Therefore, these two mutant strains were referred to as *R. rhodochrous* IGTS8 and *B. sphaericus* IGTS9 (Ohshiro et al. 1994).

The mutated strain IGTS8 was further tested with other Gram-negative desulfurizing bacteria such as *Enterobacter cloacae*. At the initial time IGTS8 showed fast growth. However, after sometime of incubation, the *Enterobacter* species grew faster and becomes dominant and formsulfate ion during desulfurization. The test concluded that sulfate ion forms in 4S pathway and releases into the medium. This sulfate ion could be assimilated by another bacterium(Kilbane, 1996; Monticello and Kilbane, 1994). The mixture of two bacteria did not enhance the desulfurization activity. Highest desulfurization was observed in IGTS8 strain alone.

In 1992, further study on IGTS8 strain was done by Kilbane and Jackowski (1992). They cultivate the bacterium into water soluble coal–derived compound. Approximately 30-40% reduction in the concentration of organic sulfur was observed after 24 h of incubation. Carbon to sulfur ration confirms that the sulfur only removes from DBT

without losing its calorific value.

2.3.2 Enzymes involve in 4S pathway

At the initial time the genes involve in desulfurization activity and product (enzymes) of these genes called *sox* (sulfur oxidation). Later on, the name *sox* were replaced by *dsz* (desulfurization) (Denome et al. 1994). These *dsz* genes are present in a 4 Kb fragment of DNA. The fragment is present on a mega plasmid named as pSOX. Size of this plasmid was 150 Kb. This plasmid was observed in *Rhodochrous erythropolis* IGTS8 bacterial strain (Denis-Larose et al. 1997). The fragment of these genes contains three genes, which were regulated by a single operon called *dsz*ABC (Alves et al. 2005). In existence of sulfur containing compound namely methionine, sulfate, and cystine, this operon undergoes in a negative regulation (Styliano et al. 2021, Del et al. 2005).

Piddington et al. (1995) had compared the *dsz* genes and also their encoding proteins with the sequence of other genes and enzymes deposited in biological databases such as the GenBank and the Swiss-Prot etc. However, no significant match was found with *dsz* gene and encoding protein. The study concluding the desulfurization enzymes DszC, DszA, and DszB are encoded by specific genes.

In 4S pathway, this multienzyme complex (DszABC) revealed three different activities. In first step DszC (DBT monooxygenase) catalyzed the DBT transformation via successive oxidations, where DBToxidized to DBT sulfone that was further converted to 2-hydroxybiphenyl 2-sulfonate (HPBS) by DszA (DBT-sulfone monooxygenase) (Gray et al. 1996). In further, DszB (HPBS desulfinase) transforms the HBP-sulfate to HBP. These enzymes and their co factors such as NADH and $FMNH_2$ are key elements of 4S pathway to perform oxidation steps (Monticello, 1998). Apart from these enzymes, one

another protein named DszD also involved in 4S pathway. This protein is a flavin mononucleotide (FMN). Activity of DszD depends on reduced nicotinamide adenine dinucleotide (NADH). This protein is encoded by *dsz*D gene (Santos et al. 2006). DszC and DszA require enzyme DszD for their activity.

2.3.3 Recent studies on Biodesulfurization

In past 20 years, many studies have done on the BDS process. In most of the studies the bacteria were isolated form the oil contaminated fields in different countries. Table 2.2 summaries the BDS studies in past 20 years. Most of the researches have been made for the removal of DBT. However, in some studies, BT, TH, 4, 6-DMDBT were also removed from the liquid fuels (Gupta et al. 2022; Nassar et al. 2021). The isolated bacteria were capable to remove approximately 11 to 100% (v/v) DBT of its initial concentration in 8 to 72 h at the temperature range of 25 to 37 ^{O}C. However, some studies have been performed for 5 to 15 days of incubation. In some studied micro thermophilic bacteria such as *Mycobacterium phlei* WU-F1, *Bacillus subtilis* WU-S2B, *Mycobacterium* sp. X7B, *Mycobacterium phlei* GTIS10, and *Mycobacterium goodii* X7B were isolated (Furuya etal. 2001; Kirimura et al. 2001; Li et al. 2003; Kayser et al. 2002; Li et al. 2007). These bacteria were capable to tolerate high temperature. The desulfurization studies with these bacteria were performed in the temperature range of 40 to 57 ^{O}C. Approximately, 95 to 100% (w/v) DBT of its initial concentration were removed within 8 to 24 h of incubation. Alves et al. (2007) have used a genetically modified strain and showed approximately 11.4% removal of DBTS in 60 h. Awadh et al. (2020) used bacterial consortium of *Klebsiella*, *Pseudomonas*, *Rhodococcus* and *Sphingomonas* species for the removal of DBT. The consortium was not seeming efficient, showed

approximately 25% removal at the inceptive concentration of 0.1mM/l, after the incubation of 24 h at 30 ^{O}C. Similarly, Boshagh et al. (2014) have used a consortium of two bacterial strains namely, *Rhodococcus erythropolis* PTCC1767 and *Bacillus subtilis* DSMZ 3256. This study showed approximately 66% of DBT removal at the inceptive concentration of 100 nM/l, in incubation of 120 h at 30 ^{O}C. The results from both of the studies concluding that, bacterial consortium is less efficient than single bacterium which might be due to the antagonistic nature of the bacterium, which was not tested in both of the studies. Approximately, all the studies confirming the thiol compound removal via 4S pathway, confirmed by GC-MS analysis of the spent samples. Result of all these studies summarized the desulfurization capabilities of different bacteria, their incubation temperature and time and indicating that the BDS technique could be an energy and cost-efficient alternative of HDS process in oil refineries (Martinez et al. 2016).

2.3.4 Microorganisms involve in BDS process

To date many bacteria species have reported for desulfurization (Peighami et al. 2022). Some of them are *Bravibacterium*, *Pseudomonas*, *Anthrobactor*, *Gordona*, and *Rhodococcous* and their related species are capable in transformation of DBT for their metabolism (Chen et al. 2019; Grossman et al. 1999; Konishi et al. 1999). These bacteria transform the organosulfur compounds mainly in three ways as follow: The first one is C-S bond braking (reductive), then C-C bond braking (oxidative), and finally C-S bond breaking (oxidative). In most of the studies DBT serves as an imitation compound for biodesulfurization studies. Some of the bacterial strains such as *Pesudomonas* showed approximately up to 90 % removal of sulfur in 24 h by C-S bond braking pathway (Kim et al. 1990; Borole et al. 2002; Nehlsen, 2006).

Some of the fungal species such as *Cunnighamella elegans* have also been used

for desulfurization studies. However, the research on fungal desulfurization was discontinued due to loss of desulfurization activity in fungus species (Holland et al. 1986; Crawford and Gupta, 1990).

Apart from these a mixture of yeast cells of *Hansenula* species have also used by Stevens and Burgess in 1989. Yeast cells enhances the desulfurization efficiency by secretion of surfactant like matrix. However, due to focusing on specific sulfur removal studies, further research on yeast cells was also discontinued (Stevens and Burgess 1989).

The reported literature concluded that present desulfurization technologies are efficient for desulfurization. However, every technique has their own drawback such as, HDS process requires harsh conditions (high temperature and pressure); ODS is a multistep technique of desulfurization which makes the process cost inefficient; extraction of ionic liquid in EDS is a difficult process. ADS is efficient in high concentration of refractory sulfur compounds however, inefficient in lower concentrations.

BDS is efficient in low concentration of sulfur compounds but requires alot of time for desulfurization. A sequential integration of ADS and BDS is the focus and nobility of the present study and could be an efficient alternative for the present desulfurization technologies. Which can remove the sulfur from the liquid fuels in efficient manner with minimal cost.

Table 2.2: An overview of biodesulfurization studies

S. No.	Bacterial strain	Sulfur Compound	Initial concentration (ppm/mM/L)	Desulfurization %	Bacterial cells form	Temperature (^{O}C)	time (h)	References
1	*Pseudomonas putida* CECT 5279	DBT	200	75	Resting	30	24	Caro et al. 2007
2	*P. delafieldii* R-8	DBT	591	47.1	Growing	30	24	Guobin et al. 2006
3	*Rhodococcus* sp. P32C1	DBT	24	25	Growing	30	24	Maghsoudi et al. 2001
4	*Gordonia alkanivorans* Strain 1B	BT, DBT, TH, DBTS	1	90	Resting	30	192	Alves et al. 2005
5	*Rhodococcus* strain	DBT	0.1	60	Resting	28	100	Tanaka et al. 2002
6	*Mycobacterium phlei* WU-F1	DBT, 4,6-DMDBT	0.81	100	Resting	50	8	Furuya et al. 2001
7	*Microbacterium* strain ZD-M2	DT, TH	0.2	100	Growing	30	72	Li et al. 2005
8	*Rhodococcus* sp. Strains	DBT	500	60	Resting	30	168	Castorena et al. 2002
9	*Gordonia alkanivorans* strain 1B	DBTS	0.2	11.4	Resting	30	60	Alves et al. 2007
10	*Rhodococcus erythropolis* IGTS8	DBT	0.025	70	Growing	30	30	Del et al. 2005
11	*Gordonia* sp. strain F.5.25.8	DBT	1.1	70	Resting	37	360	Santos et al. 2006
12	*P. delafieldii* R-8	DBT	261	72	Resting	30	24	Luo et al. 2003
13	*Rhodococcus globerulus* DAQ3	DBT	1580	65	Resting	30	48	Yang and Marison, 2005
14	*Pantoea agglomerans* D23W3	DBT	100	93	Growing	30	24	Bhatia and Sharma, 2010

15	*Corynebacterium* sp. strain P32C1	DBT	0.25	100	Resting	30	27	Maghsoudi et al. 2000
16	*Pseudomonas stutzeri* UP-1	DBT	2.7	74	Resting	31	100	Hou et al. 2005
17	*Rhodococcus* sp.	DBT	0.5	78	Growing	30	42	Ma et al. 2006
18	*Gordonia alkanivorans* strain 1B	DBT	0.23	63	Growing	30	168	Alves et al. 2008
19	*Rhodococcus erythropolis* IGTS8	DBT	50	95	Resting	30	96	Abbad et al. 2003
20	*Mycobacterium* sp. ZD-19	DBT, TH	0.5	100	Resting	30	56	Chen et al. 2008
21	*Gordonia alkanivorans* RIPI90A	DBT	0.5	83	Resting	37	72	Shavandi et al. 2009
22	*Rhodococcus erythropolis* strain	DBT, TH	100	100	Resting	30	10	Davoodi et al. 2010
23	*Lysinibacillus sphaericus* DMT-7	DBT	0.2	60	Growing	30	24	Bahuguna et al. 2011
24	*Bacillus subtilis* WU-S2B	DBT, 4,6-DMDBT	0.8	100	Resting	50	20	Kirimura et al. 2001
25	*Mycobacterium* sp. X7B	DBT	0.5	86	Resting	45	24	Li et al. 2003
26	*Mycobacterium phlei* GTIS10	DBT	0.1	95	Growing and resting	57	24	Kayser et al. 2002
27	*Gordonia* sp.	DBT	2.8	70	Resting	30	192	Li et al. 2006
28	*Bacillus subtilis*	DBT	0.5	75	Resting	37	72	Ma et al. 2006
29	*Rhodococcus erythropolis*	DBT	0.5	97	Growing	30	72	Zhang et al. 2007
30	*Mycobacterium* sp.	DBT	0.4	100	Resting	30	50	Chen et al. 2009
31	*R. globerulus* DAQ3	DBT	1500	100	Growing	30	120	Yang et al. 2007
32	*Rhodococcus erythropolis* IGTS8	DBT	0.025	100	Growing	30	20	Gomez et al. 2015

33	*Gordonia* sp. SC-10	DBT	167.7	88.3	Growing	30	120	Chen et al. 2021
34	*Klebsiella, Pseudomonas, Rhodococcus* and *Sphingomonas* consortium	DBT	0.1	25	Growing	30	25	Awadh et al. 2020
35	*Rhodococcus erythropolis* IGTS8	DBT	50	50	Growing	30	24	Caro et al. 2007
36	*Mycobacterium goodii* X7B	DBT	200	99	Resting	40	24	Li et al. 2007
37	*Rhodococcus erythropolis* IGTS8	DBT	0.025	70	Growing	30	40	Del et al. 2005
38	*Gordonia alkanivorans* RIPI90A	DBT	0.5	50	Growing	30	240	Mohebali et al. 2007
39	*Rhodococcus erythropolis* and *Bacillussubtilis* DSMZ 3256	DBT	100	66	Growing	30	120	Boshagh et al. 2014
40	*Gordonia* sp. IITR100	DBT	0.3	100	Growing	30	360	Chauhan et al. 2015
41	*Gordonia* sp.	DBT	0.3	95	Growing	30	60	Feng et al. 2016
42	*Gordonia alkanivorans* strain 1B	DBT	0.25	100	Growing	30	124	Pacheco et al. 2019
43	*Pseudomonas putida* CECT5282	DBT	0.025	100	Resting	30	30	Calzada et al. 2009

Chapter III

Objective 1: Synthesis and characterization of Ni doped carbon beads

3.1 Introduction

Desulfurization of sulfur containing liquid fuels is an essential step to reduce the environmental pollution. Adsorptive desulfurization is an efficient technique for desulfurization of these liquid fuels. Adsorption desulfurization relies on the selection of an appropriate adsorbent. Although selecting an adsorbent for adsorptive desulfurization is still difficult (Ai et al. 2012).

An ideal adsorbent should have some unique physicochemical properties such as high surface area, thermostable and non-reactive nature and amenity to surface functionalization (Prajapati and Verma, 2017).

Carbon based materials such as activated carbon, carbon nano tubes, activated carbon fibers, and carbon nanofibers were containing high surface area and stable in acidic as well as basic medium. Also, these materials are amenable to surface modification (Prajapati and Verma, 2018). These properties make them a potential candidate in adsorption and other application. The literatures reported that carbon-based materials were found more efficient than other adsorbent materials in adsorptive desulfurization application (Jung and Jhung, 2015). In addition, a composite of carbon-based material with some transition metal such as Cu, Ni, Ag, Fe etc. was found efficient in many studies (Kharisov et al. 2017). In a study it was reported that the transition metals are able to interact with the sulfur compound in the following order: Zn < Cu < Ni < Ag (Ma et al. 2006). However, these transition metal requires some support to become stable. Therefore, on the basis of nontoxic behaviour, Ni-doped activated carbon-based material could be an efficient adsorbent for adsorptive desulfurization applications (Omar et al. 2020).

Metal-doped carbon-based beads were found efficient in adsorption and adsorptive desulfurization applications, because round shape of beads having more surface to volume ratio, gain more exposure to sulfur compounds in oil (Omar et al. 2022). Therefore, Ni-doped activated carbon-based beads were found efficient for adsorptive desulfurization application and used in this study. Additionally, growth of carbon nanofiber onto Ni-doped activated carbon beads makes them more efficient due to enhancement in the graphitic content of the material. This graphitic content enhances the π-π complexation between sulfur compound and adsorbent material, results in increased adsorption capacity of the adsorbent material (Yadav et al. 2017).

In this objective, the Ni-doped activated carbon beads were synthesized. The synthesized beads were characterized by several physicochemically characterization techniques including SEM, EDX, XRD, TPR, TGA, FT-IR and BET analysis.

3.2 Materials and Methods

3.2.1 Materials.

Polyvinyl alcohol (PVA) (M.W. = 95000), phenol (> 99.5%), formaldehyde (37 – 38%), hexamethylenetetramine (HMTA, 99%), triethylamine (TEA, 99%), nickel nitrate hexahydrate (> 98%) and n-octane (> 99%) were purchased from Merck, Germany. The sulfur containing compounds, namely, TH (99%) and DBT (98%) were purchased from Alfa Aesar and Spectrochem Pvt. Ltd, India. All gases used in the study were zero grade and purchased from Sigma Gases, India. Milli Q water was used from the Elix Mili Q system, USA.

3.2.2 Methods

3.2.2.1 Ni-doped beads preparation

Ni-doped carbon beads (Ni-ACB) and Ni-doped phenolic beads were synthesized via suspension polymerization reaction with some modifications. The modifications were made in the synthesis conditions, viz., the amount of precursor, mixing time, temperature, stirring speed, heating time, and the metal-salt amount, with a view to increasing the bead size and yield. Briefly, approximately 50 mL of molten phenol (> 99.5%) was mixed with 63 mL of formaldehyde (37–38%) and 2 mL of TEA in a round bottom flask at room temperature (~30 °C). The mixture was stirred at 150 rpm for 5 h to prepare the homogenous solution. Approximately 200 mL of distilled water was added to the solution, and stirring speed was increased to 330 rpm. The solution became transparent from milky white in ~ 30 min. Approximately 3.5 g of HMTA, used as a cross-linking agent, was mixed in the solution and the solution was heated to 90 °C at the heating rate of 3 °C per min. The colour of the solution changed to pale yellow. Next, approximately 3 g of PVA, used as a suspension stabilizing agent, was added to the solution. After ~ 20 min of adding PVA, a soft gel-like material was formed. At this instance, 5 g of $Ni(NO_3)_2$ was mixed in the solution. After ~ 30 min of mixing the metal salt, spherical beads of ~ 1.2 mm average size were formed in the flask. Heating was switched off and the reactor was cooled to room temperature. Solid beads formed in the reactor were collected and washed 2–3 times with deionized water. The synthesized metal salt-doped polymeric beads were termed as Ni $(NO_3)_2$-PhB for reference. The polymeric beads were then carbonized and activated to prepare the Ni-doped activated carbon beads (Ni-ACB). Some samples of Ni-ACB were decorated with CNFs by subjecting the activated beads to chemical vapor deposition (CVD) for preparing Ni-CNF-ACB.

3.2.2.2 Carbonization and activation of $Ni(NO_3)_2$-doped phenolic beads

The prepared Ni-salt containing polymeric beads was carbonized at 900 °C under the nitrogen flow at 150 standard cubic centimetre per minute (sccm) for 1 h in a horizontal stainless steel (SS) tubular reactor mounted in a tubular furnace. The carbonized beads were activated at the same temperature using the mixture of nitrogen (150 sccm) and steam (0.3 g per min) for 1 h. The calcined beads were subjected to the H_2-reduction (flowrate = 150 sccm) at 600 °C for 2 h to convert NiO to Ni^0. After carbonization, average size of thus prepared beads was ~0.8 mm, and these samples were termed as Ni-ACB. Some samples without Ni were also prepared for comparison and termed as ACB.

3.2.2.3 Ni-doped CNFs grown ACB (Ni-CNF-ACB)

Ni-CNF-ACBs were prepared by growing the CNFs over Ni-ACB by CVD technique using acetylene as the carbon source. The CVD was carried out at 600 °C for 0.5 h under the acetylene flow (30 sccm).

3.2.2.4 Characterization of Ni-doped activated carbon beads

Surface area, the BET isotherms, pore volume and pore size distribution (PSD) of the materials were determined using the Autosorb-1C (Quantachrome, USA) instrument. N_2 gas was used as the adsorption probe molecule at 77 K. Before the analysis, samples were kept for outgassing at 150 °C for 12 h to remove moisture and other gaseous impurities from the samples. Total pore volume was calculated at the relative pressure P/Po = 0.9994. Micropore volume was calculated by the t-plot method and *meso*-macro pore volume was calculated by subtracting micropore

volume from total pore volume (Passe-Coutrin et al. 2008). The H_2-reduction temperature of the calcined sample was determined from the temperature programmed reduction (TPR) analysis using the Autosorb-1C instrument. Approximately 100 mg of the dried sample was purged with helium gas (flowrate =10 sccm) for 30 min at room temperature to remove moisture. Temperature of the sample was increased 10 °C per min to 900 °C. Ni-loadings in the metal-doped beads were determined using the atomic absorption spectroscopy (AAS) (Varian AA-420, USA) with a radiation source of hollow cathode lamp and the deuterium background corrector. Before the analysis, the samples were digested in a concentrated HNO_3 solution at 80 °C for 3 days to prepare the leachate of the metal. Metal digestion was considered to be complete when the solution turned colourless. Surface morphology of the samples was observed using the high-resolution field emission scanning electron microscope (FE-SEM) (MIRA-3 TESCAN, Brno, Czech Republic) by capturing the electronic images. Metal dispersion and surface elemental compositions were determined using the energy dispersive X-ray spectroscopy (EDX) (JSM-7100F, JEOL, USA). Broad angle X-ray diffraction (XRD) spectra were recorded using the PAN analytical X'Prert - Pro diffractometer and a Cu Kα radiation (k = 1.54178 A°) source. The spectra were recorded over the 2θ range 3 − 80° using the ramp rate of 3° per min. Thermal stability of the prepared materials was determined using the thermogravimetric analysis (TGA) (Toledo – Mettler, United States). Surface functional groups in the materials were determined using Fourier – transform infrared (FT-IR) spectroscopy (Bruker Tensor 27, Germany). The FT-IR spectra were recorded using an attenuated total reference (ATR) and a germanium crystal.

3.3 Results

3.3.1 Physical appearance of beads

Approximately 0.8 to 1.2 mm diameter sized, green colored beads were prepared using suspension polymerization reaction (Fig 3.1a). On carbonization and activation, polymer of the bead turns to carbon and color of the beads turns to black (Fig 3.1b). After reduction Ni salt converts to nascent nickel (i.e., zerovalent form of the nickel) (Fig 3.1c). In final after CVD fibrous structure appeared on the surface of the beads (Fig 3.1d), which was due to growth of carbon nanofibers.

3.3.2 Ni loading

Metal content in $NiNO_3$-PhB was determined to be approximately 5.37 mg/g. Metal loading significantly increased to 33.4 mg/g in the activated beads, viz. Ni-ACB (Table 3.1). Post carbonization and activation, material weight loss decreased by ~ 55% because of decomposition of the surface functional groups such as –OH and –COOH. However, metal loading decreased to 16.43 mg/g in Ni-CNF-ACB, attributed to increase in weight of the sample because of the CNF-growth.

Table 3.1: Metal loading in the adsorbent materials

S. No.	Material	Metal loading (mg/g)
1	Ni-ACB	33.40
2	Ni-CNF-ACB	16.43

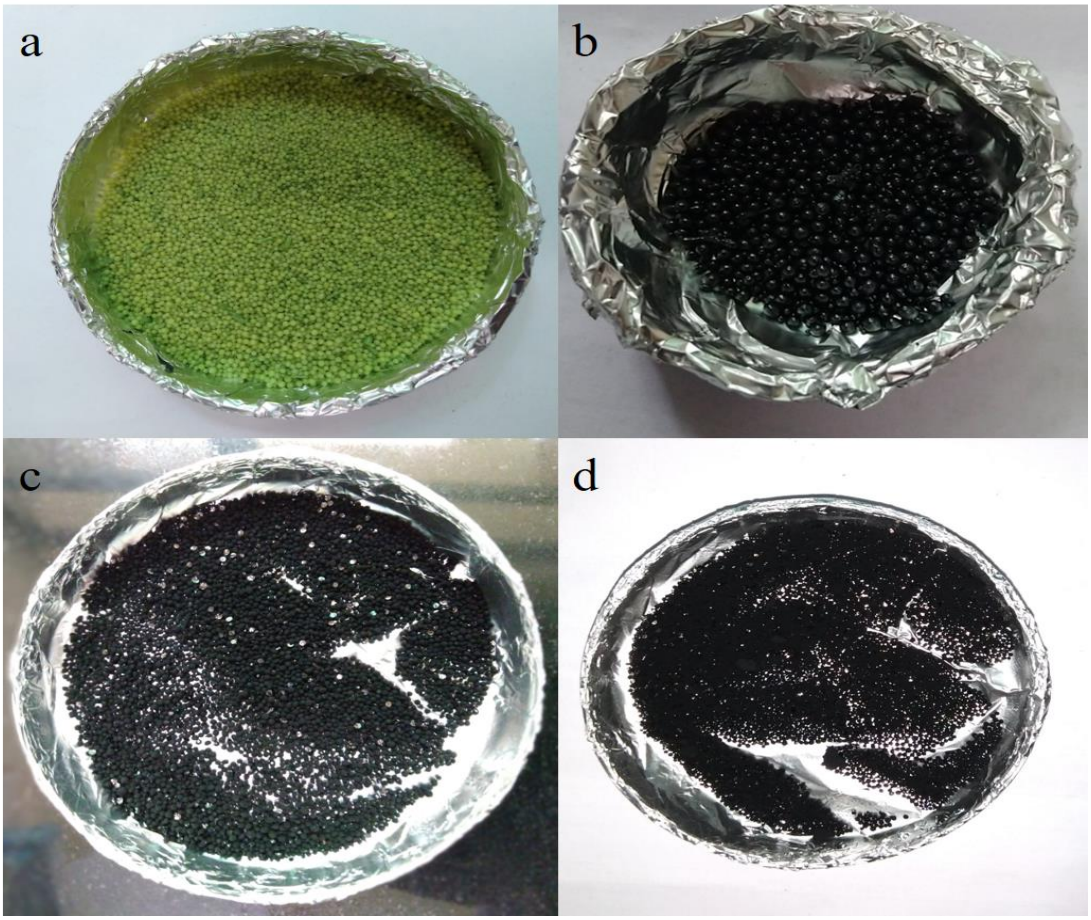

Fig 3.1: Physical appearance of prepared beads **(a)** $Ni(NO_3)_2$-doped phenolic beads ($Ni(NO_3)_2$-PhB), **(b)** NiO-activated carbon beads (NiO-ACB), **(c)** Ni-doped activated carbon beads (Ni-ACB), and **(d)** Ni doped carbon nano fiber grown activated carbon beads (Ni-CNF-ACB)

3.3.4 SEM and EDX analysis

Fig 3.2 showing the SEM image of activated carbon beads. Development of pores through the activation process can be observed in SEM image of ACB. Fig 3.3 (a-b) shows the SEM images at low and high magnifications of the fresh absorbent samples. Pores occupied with shiny nanoparticles can be seen in the image of Ni-ACB (Fig 3.3a-a'). The SEM images of the CNFs-containing beads are shown in Fig 3.3(b-b'). A fiber like structure confirmed the CNF-growth, with the shiny metal particles

clearly seen in the images. Fig 3.3(c-d) shows the EDX spectra of Ni-ACB and Ni-CNF-ACB. The nanoparticles observed in the SEM images were confirmed to be a Ni by the EDX analysis. Elemental analysis showed 19% and 15% (w/w) Ni in Ni-ACB and Ni-CNF-ACB, respectively.

3.3.5 TPR analysis

Fig 3.4a shows the TPR spectra of NiO-ACB. Only one peak was observed at ~ 650 °C over the temperature range 491–865 ^{O}C, attributed to reduction of NiO to Ni.

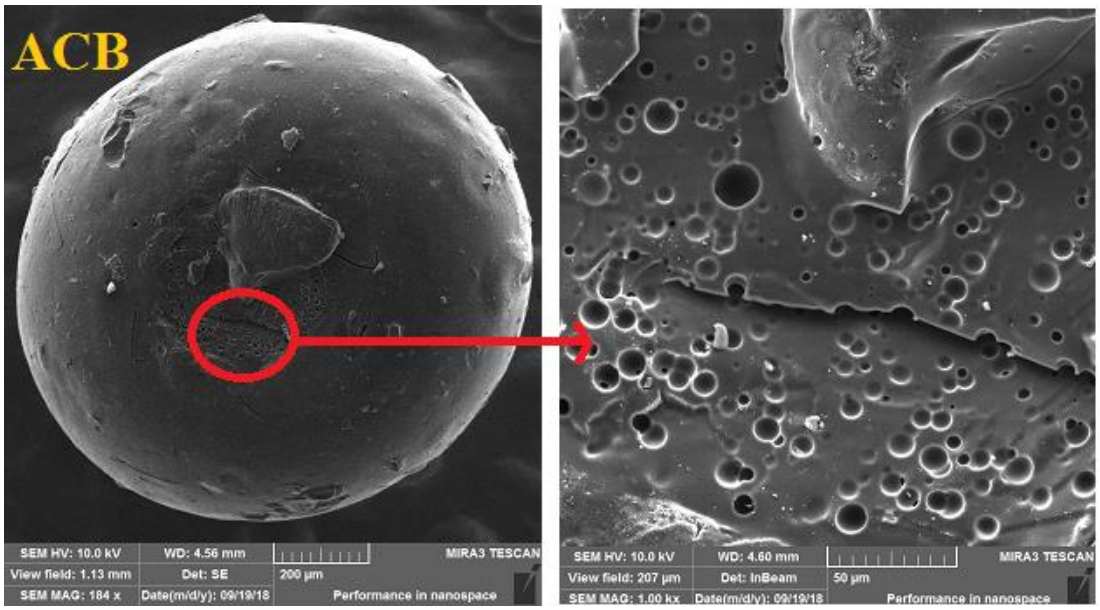

Fig 3.2: SEM images of activated carbon beads

3.3.6 XRD analysis

XRD spectra of the materials (ACB, Ni-ACB, and Ni-CNF-ACB) are shown in Fig 3.4b. A wide peak at the 2Θ angle of ~ 22.5° corresponds to amorphous carbon having the crystal plane (0 0 2). The characteristic peaks observed at 2Θ angle of ~ 38.3 and 46.4° correspond to the crystalline metallic planes of (1 1 1) and (2 0 0),

respectively in the Ni containing samples. These peaks were absent in the ACB samples. The peaks and planes of Ni were confirmed from JCPDS#70–0989.

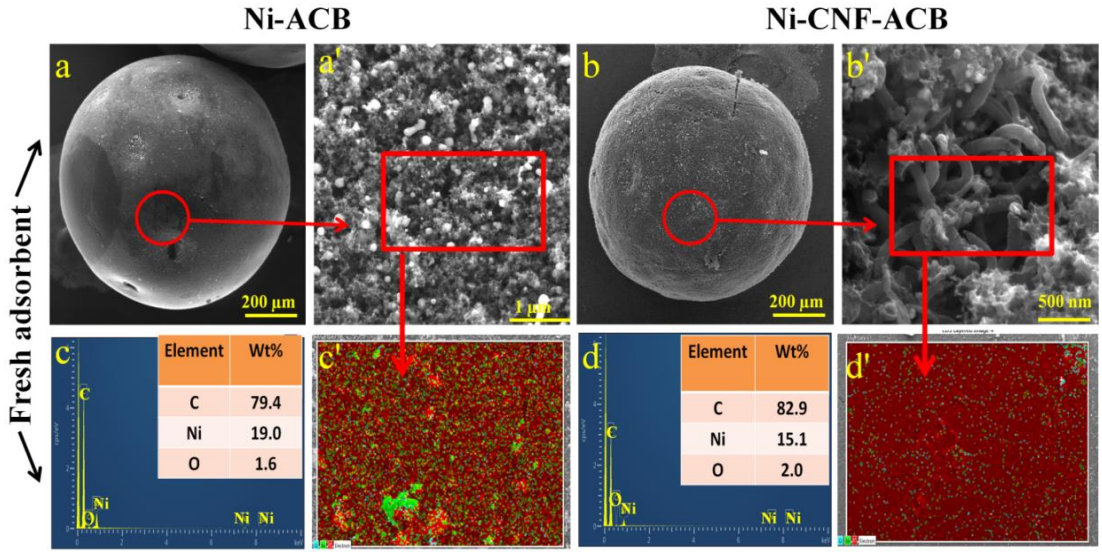

Fig 3.3: (a-b') SEM images of fresh adsorbent, (c-d') EDX analysis of the fresh absorbents (spectra and mapping)

3.3.7 TGA analysis

Fig 3.4c shows the TGA spectra of the materials over the temperature range 30–800 °C. The weight of the materials gradually decreased to ~ 46% in PhB. However, weight-loss was much lower in the activated beads, i.e., ~19 and 21% in Ni-ACB and Ni-CNF-ACB, respectively, indicating the materials to be thermally stable over the temperature range. The weight loss in Ni-CNF-ACB is higher than that in Ni-ACB because of gasification of the CNFs at temperatures above 650 °C.

3.3.8 FT-IR analysis

Fig 3.4d shows the FT-IR spectra of prepared materials. A single peak was observed in Ni $(NO_3)_2$-ACB at the approximate wavelength of 1100 cm^{-1}, attributed

to C-C interaction. There other major peaks were observed in other materials confirming the complete carbonization of the material. All the functional groups were lost during the carbonization step of the material. However, some functional groups were determined in spent adsorbent, which will be discussed in later part.

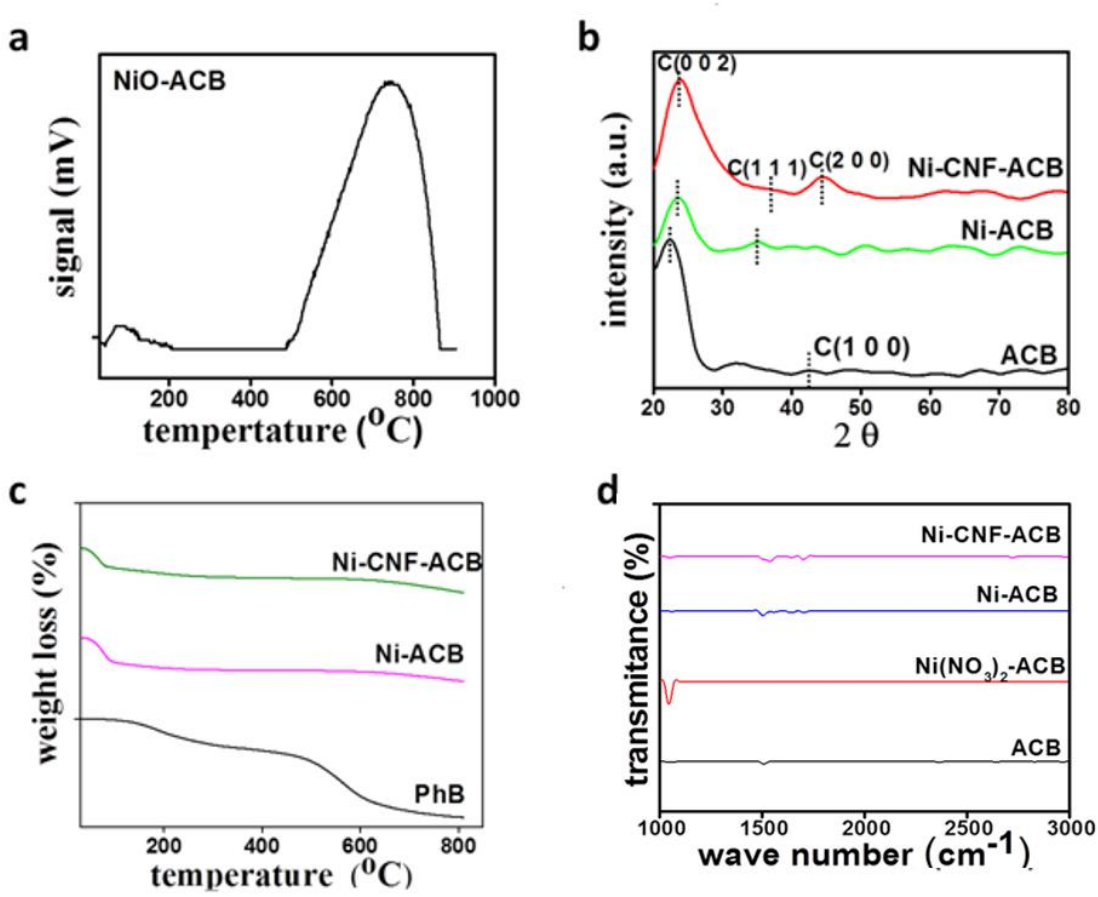

Fig 3.4: (a) TPR, (b) XRD, (c) TGA, and (d) FT-IR analysis of prepared beads

3.3.9 BET analysis

Fig 3.5a shows the adsorption–desorption isotherms of the materials. Adsorption of N_2 rapidly increased up to the relative pressure of ~0.4 mm Hg in ACB. Thereafter, the N_2 uptake was virtually constant, indicating that the isotherm was type – 1. Ni-ACB showed mixed isotherms: type 1 at low relative pressure and type 4 at

high relative pressure. The CNFs-containing material showed a H4 type hysteresis loop in the material. Such loop is the characteristics of a significant amount of slit-shaped mesopores present in the material. Fig 3.5b shows the S_{BET} surface area, total, micro and mesopore volumes in the materials. The highest surface area (~1252 m^2/g) was determined in ACB. The area decreased to ~1090 m^2/g in Ni-ACB because of inclusion of the metal in the pores of the material. The Ni-CNF-ACB has the smallest surface area because of growth of the CNFs in the pores. The micropore volumes in the materials followed the similar trend as that of the BET areas.

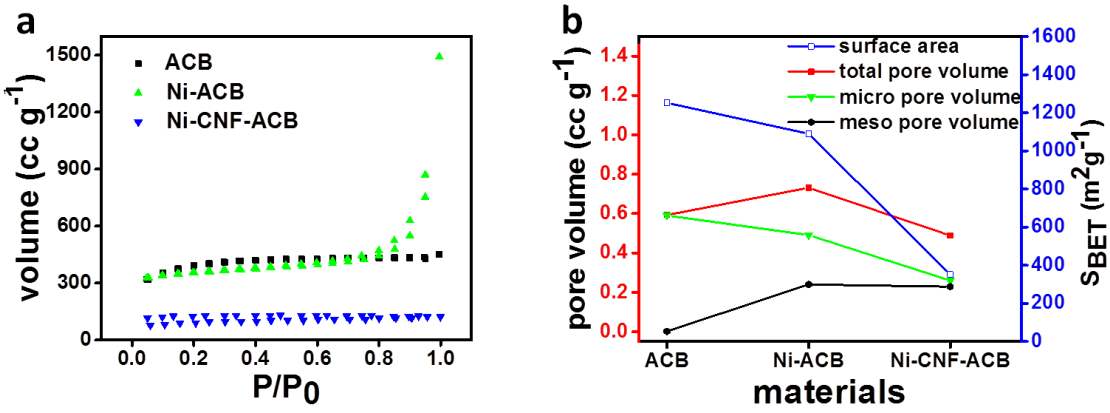

Fig 3.5: (a) BET isotherm, and (b) pore volume and surface area of beads

3.4 Discussion

In this study, Ni-doped activated carbon beads were synthesized for the adsorption of DBT and TH. In literature, researchers have synthesized the same adsorbent (Prajapati and Verma, 2017; Prajapati and Verma, 2018; Yadav et al. 2017). In contrast, the previously reported beads were smaller in size than those synthesized in the present study. In this study, the size of the beads was slightly larger, which was around 1.2 mm. Furthermore, 0.8 mm is the maximum size of beads reported in the literature. Round beads are indicative of a proper synthesis. Green colour of the beads confirming doping of Ni $(NO_3)_2$ nanoparticles into beads, because,

physical appearance (colour) of Ni $(NO_3)_2$ salt was green in colour. Presence of Ni onto beads was also confirmed by AAS and EDX analysis. After carbonization, colour of beads turns to black confirming conversion of all the polymeric material into carbon material (Kumar and Verma, 2020). After carbonization, micro and meso pores were developed by purging of steam under inert atmosphere at high temperature and the process were known as steam activation (Prajapati and Verma, 2017). Development of pores and size of the pores were confirmed by SEM and BET analysis, respectively. After the process of activation, activated beads were subjected to calcination and reduction process, because metal nanoparticles present in the beads were in nitrate form, which needs to be converted in zerovalent/nascent form of Ni. During the calcination process nitrate of nickel was replaced by oxygen and forms nickel oxide (NiO) (Bairagi and Verma, 2018). In further, reduction was performed at high temperature (650 ^{O}C) under the hydrogen flow. In reduction, H_2 bind with oxygen of NiO, and forms water (H_2O). The NiO gets converted to Ni (Yadav et al. 2017). In next part, the CNF were grown on the surface of Ni-ACB by CVD process. Here, acetylene (C_2H_6) was used as carbon source and Ni act as catalyst for CVD process. After the growth of CNF, colour of beads turns to dark grey confirming presence of CNF onto the surface of beads (Prajapati and Verma, 2018). Presence and structure of CNF was also determined by SEM analysis in the study.

Presence and amount of Ni in beads at different stages were determined by AAS analysis. The approximate loading of Ni was determined 3.5 and 1.6% of the carbon material which was approximately similar to reported studies (Prajapati and Verma, 2017). The Ni content was reduced in CNF containing beads, which was due to increment in amount of caron in the form of CNF (Prajapati and Verma, 2018).

Morphology of the beads was observed by SEM analysis. At lower magnification round shaped spherical beads were observed confirming successful synthesis of beads (Kumar et al. 2018). At higher magnification the pores can be visualize onto the surface of beads confirming activation of beads (Kumar and Verma, 2020). The SEM image of Ni nanoparticle containing beads were also observed round shaped. At its higher magnification shiny dots on the surface of the beads were confirming presence of metal nanoparticle in the beads. After CVD, a feather like structure was observed in physical appearance of CNF containing beads. However, at its higher magnification fibre like structure were clearly visible confirming the presence of CNF onto the surface of beads. Some of the tips of the CNF's showing shiny dots, confirming presence of metal nanoparticles on the tip of CNF, in CNF containing beads.

Presence of Ni and ratio of carbon and Ni on the surface of the prepared adsorbent material was determined EDX analysis. The results indicated that the percentage of Ni was higher in Ni-ACB (i.e., without CNF containing beads). However, it was slightly reduced in Ni-CNF-ACB (i.e., CNF containing beads) which was due to increment in percentage of carbon by the growth of CNF (Prajapati and Verma, 2017). The increased carbon percentage can be clearly seen on the EDX spectra of Ni-CNF-ACB.

The TPR analysis was performed to determine reduction temperature of the NiO-ACB beads. The spectra showing a temperature range in between 491–865 ^{O}C for the reduction of NiO. This range was determined approximately similar to the reported literature (Bairagi and Verma, 2019). Therefore, mediate temperature of this

range (i.e., 650 ^{O}C) was used to convert NiO to Ni through reduction at high temperature and hydrogen atmosphere.

The crystalline structure of Ni and carbon was determined by XRD analysis. Peak values of Ni and carbon in all the planes were determined at the same angels as reported in literature confirming presence of carbon and zerovalent form of Ni in prepared adsorbent material (George et al. 2021).

Thermal stability of the prepared material was determined by TGA analysis. Spectrum showing that before carbonization approximately 60% weight loss was determined in the material. However, after carbonization and activation, prepared material was becoming thermally stable. TGA analysis conforming that, prepared materials were thermally stable and can be also used at high temperature (Prajapati and Verma, 2018).

The FT-IR analysis was performed to determine the surface functional groups of the materials. The spectra indicating that all the material have been complete carbonized and no functional groups were observed in the FT-IR spectrum, which was due to loss of function groups during the carbonization process (Gupta et al. 2022).

The isotherm pattern and surface area of material was determined by BET analysis. Prajapati and Verma (2017) showed that ACB and Ni-ACB followed type I isotherms. However, Ni-CNF-ACB was showing a mixed type isotherm combining type I and type IV, which was due might be due to presence of meso/micropores in the material (Passe-Coutrin et al. 2008). The maximum surface area was determined in the ACB, which was slightly reduced in Ni-ACB, due to incorporation of metal nanoparticles into to pores of ACB (Kumar and Verma, 2020). In CNF containing

beads the area was highly reduced due to the growth of CNF on the pores of the material (Prajapati and Verma, 2017). The ACB was determined enriched with mesopores. In Ni-ACB the mesopores converted to micropores due to incorporation of metal nanoparticles into the pores of the material (Ai et al. 2012). The CNFs containing beads showing both meso and micro pores in the material, therefore the isotherm was mixed type isotherm (Passe-Coutrin et al. 2008).

The synthesized beads were determined spherical in shape containing metal nanoparticles and carbon nanofibers. The synthesis of beads, their structure, surface texture, thermal stability, and surface characteristics were determined using several physicochemical characterizations, showing conventional synthesis of beads.

3.5 Conclusion

Ni-doped active carbon beads (with and without CNF) were synthesized successfully. The accurate synthesis was confirmed by determining the physical appearance of beads and characterizing them by several physicochemical characterization techniques such as SEM, XRD, TPR, FT-IR, TGA, EDX and BET analysis. All the characterization were found accurate confirming appropriate synthesis of beads.

Chapter IV

Objective 2: Adsorption of Dibenzothiophene and Thiophene in liquid fuel by Ni-doped carbon beads

4.1 Introduction

On burning, liquid fuels release sulfur compounds into the environment that cause a variety of problems for living organisms. These compounds should be removed. Fortunately, adsorption is an efficient method of removing sulfur compounds from the environment (Chao et al. 2019).

Adsorption is a mass transfer process which is a process that involves sorption of solutes or gasses by solid or liquid surfaces. When a solid molecule adheres to solid surface it creates some unbalance force. Due to this force the adherent solid molecule stays on that solid surface.

Among the different desulfurization techniques, adsorptive desulfurization (ADS) is an efficient technique requiring relatively less severe conditions. The technique was found efficient in room temperature and pressure. Also, it does not alter or modify physical properties of liquid fuels. In addition, separation of spent adsorbent from the desulfurized liquid fuel is also easier than the other desulfurization technique. Activated carbon supported-transition metals including Cu, Zn, Ag, and Ni have been extensively studied for ADS (Malani et al. 2021). Besides the metal–carbon composite adsorbents possessing a large surface area, the materials are capable of desulfurizing the liquid fuels via formation of metal-sulfur complexation. Also, such materials contain abundant surface functional groups. Therefore, the materials are amenable to surface modifications for an enhanced species-specific adsorption (Omar et al 2020, Omar et al. 2022). The following order of activity has been indicated in the literature for desulfurization using the transition metals: Ag > Ni > Cu > Zn. Based on the combined activity and cost-effectiveness considerations, Ni is recommended for treating thiol compounds (Prajapati and Verma, 2017).

In this objective, the desulfurization of DBT and TH using the prepared Ni-doped activated carbon beads was performed. The test was done in a specially designed reactor at 30 ^{O}C and 100 rpm.

4.2 Materials and methods

4.2.1 Materials

n-octane (> 99%) was purchased from Merck, Germany. The sulfur containing compounds, namely, TH (99%) and DBT (98%) were purchased from Alfa Aesar and Spectrochem Pvt. Ltd, India. All gases used in the study were zero grade and purchased from Sigma Gases, India.

4.2.2 Desulfurization test

A high-pressure vessel (I.D. = 45 mm, O.D. = 80 mm, height = 60 mm) was used for performing the tests. The vessel was equipped with an electric heater with a PID temperature controller. An especially fabricated agitator cum sample holder (basket) was fabricated from SS. The cylindrical sample holder (diameter = 40 mm, height = 15 mm) was fitted to the bottom end of the vertical shaft of an electrical motor. The sidewalls and base of the holder were perforated with 0.5 mm diameter holes. The suitably chosen perforation size prevented escaping of beads from the sample holder during stirring, but allowed the liquid to pass through the beads packed in the holder. Fig 4.1 describes the schematic representation of reactor.

All tests were performed at 30 ºC. Approximately 0.1 g of the prepared beads (Ni-ACB, Ni-CNF-ACB) were packed in the sample holder. Approximately 20 mL of the test oil (n-octane containing DBT/TH) was used in the vessel. The mixture was stirred at 200 rpm for 4 h. The DBT/TH concentrations were measured every 30 min,

using a gas chromatography equipped with the flame ionization detector (Nucleon-5700, India).

4.2.3 Gas chromatography

The concentration of DBT and TH in oil before and after desulfurization was determined using gas chromatography (Nucleon-5700, India). The chromatography was equipped with flame ionization detector and Ch. W. hp column. Nitrogen at the frow rate of 200 sccm was used as carrier gas. However, hydrogen in combination with air was used for flame ionization. Approximately 2 µl of each sample was taken for GC analysis.

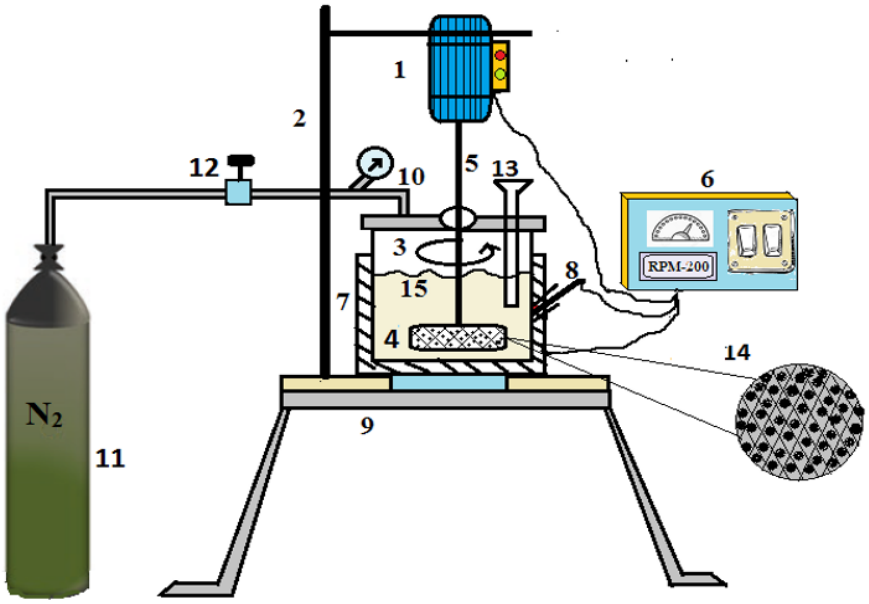

1 – Motor, 2 – Motor holder, 3 – Reactor, 4 – Beads holder cum agitator, 5 – Motor shaft, 6 – Motor – heater control unit, 7 – Heating jacket, 8 – Thermocouple, 9 – Reactor stand, 10 – N_2 gas line and pressure gauge, 11 – N_2 gas cylinder, 12 – gas valve, 13 – bacterial culture inoculation tube, 14 – Base of bead holder, 15 – DBT/TH solution in n-octane.

Fig 4.1: Schematic representation of desulfurization reactor setup

4.2.3 Physicochemical characterization of spent adsorbent (post adsorption)

Spent adsorbent was physicochemically characterized by FE-SEM, FT-IR and BET analysis to confirm the adsorptions of sulfur compound onto the surface of the adsorbent.

4.3 Results

4.3.1 Adsorptive desulfurization test

Adsorptive desulfurization tests were performed at four different initial concentrations (300, 600, 900, and 1200) of DBT and TH. The concentrations rapidly decreased initially, before gradually reaching the approximately constant equilibrium levels (Fig 4.2). The lowest concentration levels measured in the tests were approximately 47 and 53 mg L^{-1} for DBT and TH, respectively, corresponding to 300 mg L^{-1} of the initial concentration, indicating approximately 80% desulfurization efficiency of the adsorbents for DBT/TH. Mechanistically, adsorption of such sulfur containing organic compounds on Ni-ACB has been attributed to the Ni-S interactions and that on Ni-CNF-ACB has been attributed to the π-π interactions between the CNFs and aromatic rings of TH. With a gradual saturation of the active sites for adsorption in the adsorbents, sulfur concentrations expectedly reached the equilibrium values. Adsorption of DBT/TH was confirmed by the SEM images and FT-IR spectra of the fresh and spent adsorbents. Final concentrations of DBT/TH measured for the other conditions used in the study are mentioned in Table 4.1. The data indicate more than 80% S-removal by adsorption. Thus, the results indicate adsorption to be an efficient route to desulfurizing liquid fuels at high sulfur concentration levels (> 400 mg L^{-1}). Alternatively, the data indicate the adsorption process to be ineffective in treating liquid fuels at low concentration levels (< 50 mg L^{-1}).

Table 4.1: Initial/Final concentration in adsorption test

S. No.	Initial concentration of DBT/TH (mg L^{-1})	Final concentration of DBT (mg L^{-1})	Final concentration of TH (mg L^{-1})
1	1200	237.62	107.37
2	900	147.79	81.48
3	600	82.51	75.96
4	300	47.33	53.5

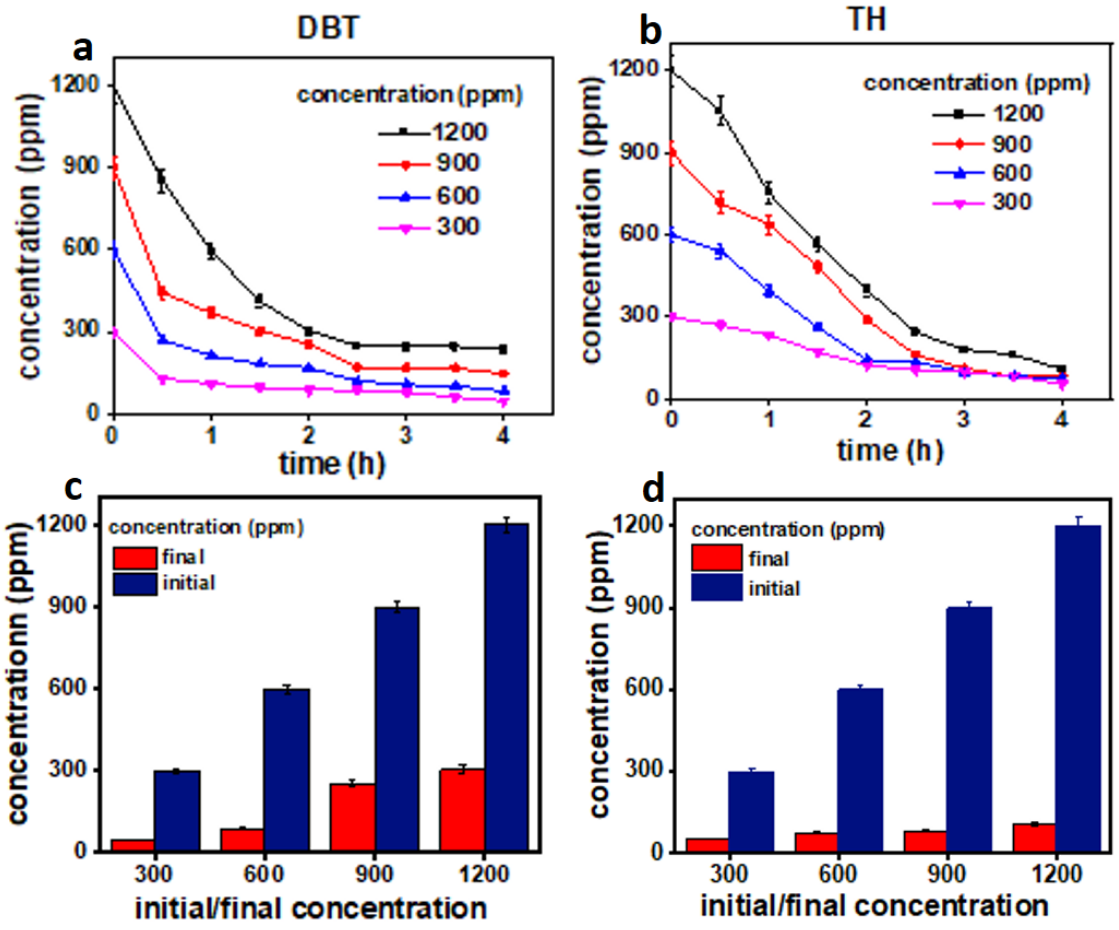

Fig 4.2: adsorption of (a) DBT, and (b) TH on Ni-ACB in respect of time, Initial/final concentration of (c) DBT, and (d) TH after the 4 h of adsorption test

4.3.2 Spent material characterization

4.3.2.1 FE-SEM analysis

Fig 4.3(a-b') shows the SEM images of the spent beads (post-adsorption of DBT and TH in Ni-ACB and Ni-CNF-ACB, respectively). Shape of the beads remains spherical however, texture of the spent materials changed post treatment (adsorption). DBT/TH partly covered the surface; some metal nanoparticles and uncovered CNFs could be seen in the images.

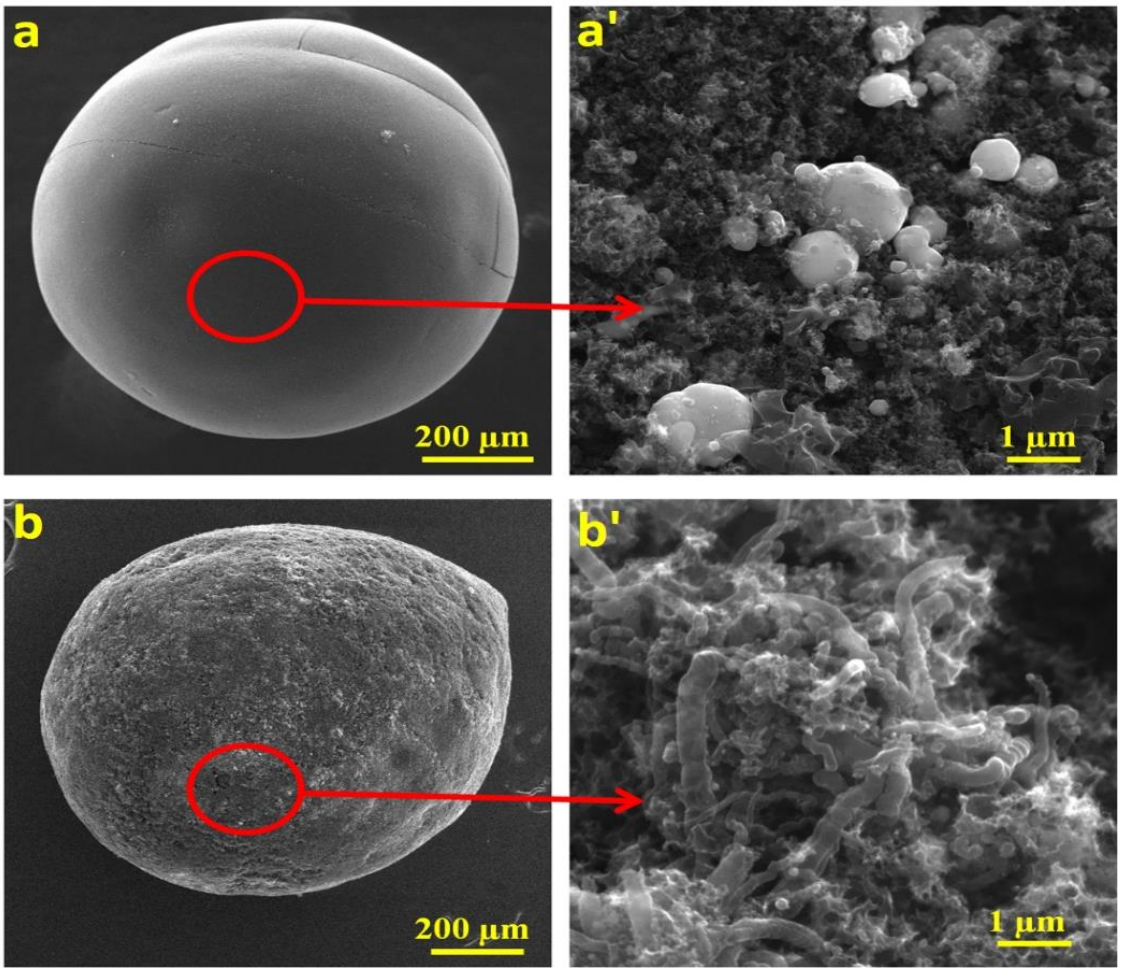

Fig 4.3: (a-a') SEM image of post adsorption (spent) of DBT on Ni-ACB, (b-b') SEM image of post adsorption (spent) of TH on Ni-CNF-ACB

4.3.2.2 BET analysis

Fig 4.4a and 4.4b shows the adsorption desorption isotherm of Ni-ACB and Ni-CNF-ACB respectively. The N_2 adsorption was rapidly increased up to 0.2 relative pressures then becomes constant in fresh adsorbents (Ni-ACB and Ni-CNF-ACB), however in the N_2 adsorption was slightly increased in Ni-ACB and constant in Ni-CNF-ACB spent adsorbents, indicating the type 1 isotherm. The decrement of N_2 adsorption in spent adsorbent indicating the saturation of adsorption capacity of adsorbent. Fig 4.4c shows the S_{BET} surface area of the adsorbent at different stages. The maximum surface area (1090.6 m^2/g) was determined in Ni-ACB (Fig 4.4c, Table 4.2) due to formation of pore onto the surface of the material during the steam activation process. The surface area was decrease (140.4 m^2/g) in spent adsorbent confirming the adsorption of the sulfur compounds or blocking the mouths of pores of the material by sulfur compounds. After desulfurization tests (in spent adsorbent) the surface area of Ni-CNF-ACB was decreased from ~284.1 m^2/g to 24.5 m^2/g) confirming the successful adsorption of TH on the adsorbent surface. The adsorption was also further confirmed by FT-IR analysis.

4.3.2.3 FT-IR analysis

The FT-IR analysis was performed for the fresh, spent adsorbent (Fig 4.4d). In fresh adsorbents (Ni-ACB and Ni-CNF-ACB) none of the vibrational peak was observed. It might be due to the loss of all the surface functional groups at the during the carbonization process, in which the material was converted to carbon. In spent adsorbent at ~782, 993, 1450, and 1750 cm^{-1} wavelengths represents the sulfone group, benzene ring of DBT and TH, organic sulfates and aromatic carbons respectively, confirming the successful adsorption of sulfur compounds on the surface

of the material. A vibration broad range after 3000 cm^{-1} wavenumber was observed in all the materials, attributed to moisture or –OH groups in the material.

Table 4.2: S_{BET} surface area of adsorbents

Adsorbent stages	Ni-ACB (Area in m^2/g)	Ni-CNF-ACB (Area in m^2/g)
Fresh	1090.6	284.1
Spent	140.4	24.59

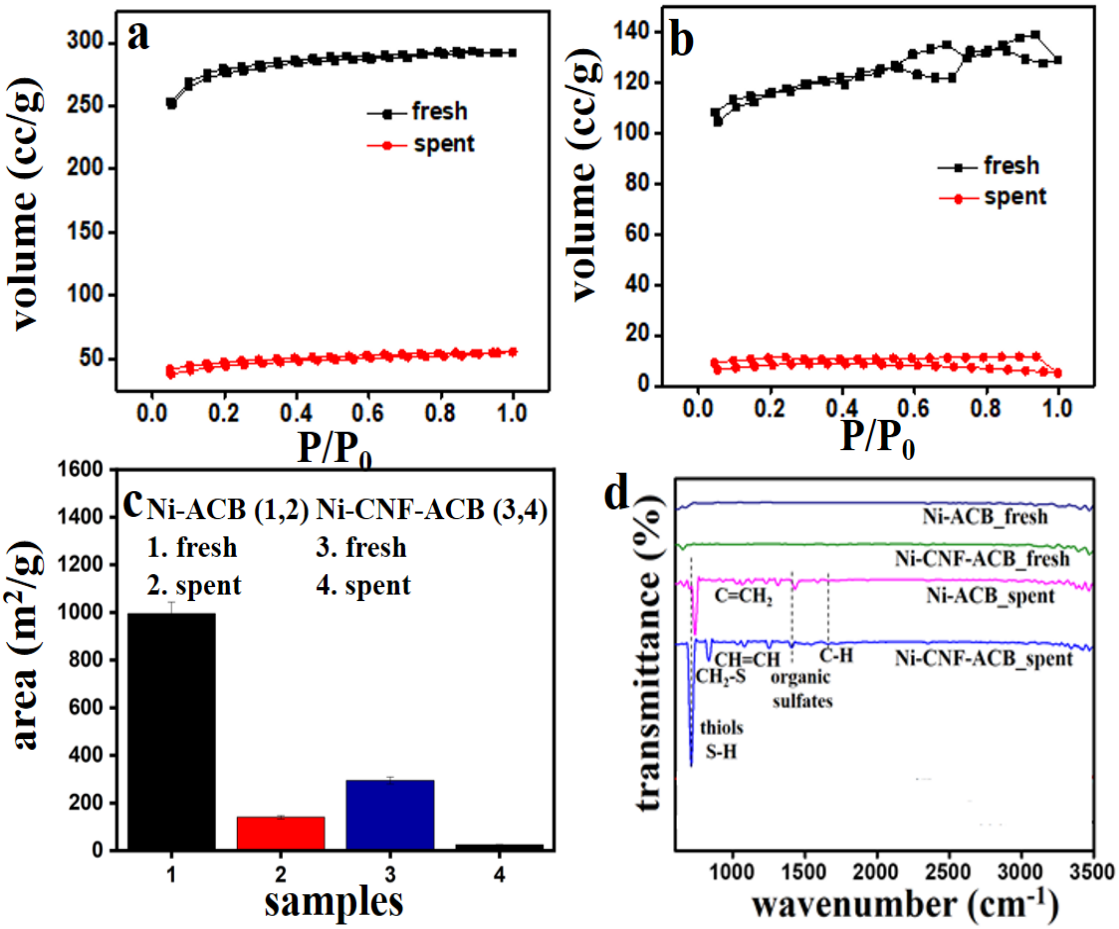

Fig 4.4: N_2 adsorption-desorption isotherms of fresh and spent (a) Ni-ACB and (b) Ni-CNF-ACB, (c) BET surface area of fresh and spent material, and (d) FI-IR analysis of fresh and spent adsorbents

4.4 Discussion

In this objective the adsorptive desulfurization of DBT and TH using Ni-doped activated carbon beads was performed. Prajapati and Verma, (2017) have also performed the adsorptive desulfurization test using the same adsorbent. The maximum removal of thiol compounds was achieved approximately 75 to 80 % of their initial concentration using four initial concentration 350, 500, 850 and 1200 ppm of DBT and TH. This study used Ni-CNF-ACB and Ni-ACB as adsorbents for tests of DBT and TH adsorption. Approximately 75 to 80% adsorption of thiol compounds (DBT/TH) was observed at four initial concentrations, which are 300, 600, 900, and 1200 ppm. In addition, after two hours of the desulfurization test, saturation in adsorption capacity was observed, which might be due to blocking of pores of the adsorbent material by thiol compound (DBT/TH) (Prajapati and Verma, 2017). SEM, FT-IR and BET analysis of spent adsorbent confirmed the adsorption DBT and TH.

Adsorption of thiol compounds was confirmed by characterizing spent (post desulfurization) adsorbent material. At lower magnification, spherical shape of beads indicating that no physical change in the adsorbent material. At higher magnification some large size shiny spherical dots confirm the adsorption of DBT onto the surface of Ni-ACB (Kim et al. 2006). In CNF containing beads, shiny dots on tips of the CNF confirmed the adsorption of TH onto the surface of Ni-CNF-ACB. A huge reduction in BET surface area of the spent adsorbent confirmed saturation in adsorption capacity or blocking of pores of the spent adsorbent. Apart from this, adsorption was also confirmed by FT-IR analysis. An FT-IR spectrum of spent adsorbent showed the same functional groups as found in DBT and TH, confirming adsorption of DBT/TH onto the adsorbent surface (Prajapati and Verma, 2018).

4.5 Conclusion

Approximately 75 – 80% thiol compound were removed using the adsorptive desulfurization process in four hours of the desulfurization test at four different initial concentration ranges between 300 to 1200 ppm. Physicochemical characterization of the spent adsorbent confirming successful adsorption of DBT and TH on Ni-doped activated carbon beads with no change in shape of the adsorbent (Ni-doped activated carbon beads).

Chapter V

Objective 3: Isolation, identification and characterization of desulfurizing-bacteria

5.1 Introduction

Combustion of sulfur compounds in fossil fuels release sulfur dioxide into the environment. The released sulfur cause adverse effect in heath, environment and economy. There are several technologies have been developed for the removal of sufur compound from the liquid fuels. Biodesulfurization is one of the developed technologies used to remove sulfur compound form the liquid fuels (Awadh et al. 2020).

In biodesulfurization microorganisms utilize the sulfur contain compounds as sulfur source and transform them to a non-sulfur containing product. In past years, several microorganism including bacteria and fungi have been isolated for desulfurization of liquid fuels (Bhatia and Sharma, 2010).

To date many bacteria species have reported for desulfurization. Some of them are *Bravibacterium*, *Pseudomonas*, *Anthrobactor*, *Gordona*, and *Rhodococcous* and their related species are capable in transformation of DBT for their metabolism (Grossman et al. 1999; Konishi et al. 1999). These bacterial transform the organosulfur compounds mainly in three ways as follow: (I) C-S bond braking (reductive), (II) C-C bond braking (oxidative), and (III) C-S bond breaking (oxidative). In most of the studies, DBT serves as an imitation compound for biodesulfurization studies (Kilbane and Jackowski, 1992). Some of the bacteria strains such as *Pesudomonas* showed approximately up to 90 % removal of sulfur in 24 h by C-S bond braking pathway (Kim et al. 1990; Borole et al. 2002; Nehlsen, 2006).

Some of the fungal species such as *Cunnighamella elegans* have also been used for desulfurization studies. However, the research on fungal desulfurization was

discontinued due to loss of desulfurization activity in fungus species (Holland et al. 1986; Crawford and Gupta, 1990).

Apart from these a mixture of yeast cells of *Hansenula* species have also used by Stevens and Burgess in 1989. Yeast cells enhances the desulfurization efficiency by secretion of surfactant like matrix. However, due to focusing on specific sulfur removal studies, further research on yeast cells was also discontinued (Stevens and Burgess, 1989).

The aim of this objective is to isolate, identify and characterize efficient desulfurizing bacteria for biodesulfurization of DBT and TH.

5.2 Materials and Methods

5.2.1 Materials

The sulfur containing compounds, namely, TH (99%) and DBT (98%) were purchased from Alfa Aesar and Spectrochem Pvt. Ltd, India. Peptone, beef extract powder, yeast extract powder, agar powder, were purchased from Himedia Pvt. Ltd, India. Bacterial media were prepared in ultrapure water from the Elix Mili Q system, USA.

5.2.2 Collection of Samples

Two samples designated as sample-1 (soil slurry) and sample-2 (wastewater/soil) were collected from two different sites of Indian Oil Petroleum Plant, Panki, Kanpur India. The samples were obtained with sterile bags and transported to laboratory in a cool-box.

5.2.3 Isolation and selection of desulfurizing bacteria

For isolation of bacteria from sample-1, 1 g of the soil sample was mixed with 10 mL of the sterilized distilled water. The mixture was serially diluted by 10 folds (i.e., 1 mL solution was mixed in 9 mL of the sterilized water). Approximately 0.1 mL of the diluted soil sample was spread over the nutrient agar plates containing 50 ppm DBT/TH. The plates were incubated for 24 h at 30 °C. The pure cultures were isolated by the streak plate method. Eight morphotypes were isolated and screened their ability to grow and degrade DBT and TH. One bacterial strain designated as R-2 was selected based on its fast efficiency to degrade DBT and TH.

Fig 5.1: Sampling site for the collection of oil contaminated samples

For isolation of bacteria from sample-2, approximately 1 g of oil-contaminated soil (slurry) was mixed in 100 mL of DBT/TH suspended broth in a flask under sterilized condition. The flasks were incubated at 30 °C for 24 h in shaking conditions.

The broth solution turned turbid. 1 mL of the solution was serially diluted with sterilized Milli-Q water up to ten folds and 0.1 mL of the highest dilution (10th dilution) was spread over the previously prepared nutrient agar plates using a sterilized glass spreader. The plates were incubated at 30 °C for 24 h. Different types of bacterial colonies observed in the plates were picked up using a sterilized inoculation loop. The selected colonies were streaked on a fresh sterilized nutrient agar plate using inoculation loops. The streaked colonies were purified and the purified bacteria were screened for their ability to grow and degrade DBT and TH. One bacterial strain designated as R5 was selected based on its rapid growth and fast efficiency to degrade DBT and TH.

5.2.4 Identification of bacterial strains R-2 and R5 by the 16S rRNA sequencing

To amplify the 16S rDNA, two primers were used, 8-27F (5'-AGAGTTTHATCCTGGCTAD-3') and 1492R (5'TACGGYTACCTTGTTA CGACTT-3'), respectively, complementary to the conserved regions at the 5' and 3' ends of the 16S rDNA sequence of *E. coli*. (Brosius et al. 1978). In 25 µl of PCR amplification reaction mix (BioBasic Inc., Ontario, Canada), 60-100 ng of genomic DNA, 2.5 µl of 10 X Tag polymerase buffer, 200 µM of each dNTP, and 1.0 µL of Taq DNA polymerase were added. In the amplification procedure, a thermocycler (Eppendorf, Hamburg, Germany) was used. The amplification program consisted of initially denaturing the samples at 94°C for 3 min, followed by 30 cycles of denaturing at 94°C for 1 min, annealing at 55°C for 1 min, extending at 70°C for 1 min, and extending at 72°C for 5 min. The reaction mix without any DNA template was also used for the negative control (PCR amplification). The PCR amplification was checked on a 1% Agrose gel. QIAquick or MinElute gel extraction kits (Qiagen, Germany) were used

to extract amplified products from the gel. Purified amplicons were sequenced by an automated DNA sequencer using Big Dye terminator cycle sequencing ready reaction kit (Applied Biosystems). Sequence electrophoretograms were checked for proper base calling, and the complete I6S rRNA sequences were assembled by joining the partial sequences that overlapped by at least 50-100 nucleotides. Gene runner and Microsoft Windows were used to compile the sequences. Using the software EzBioCloud, and BLAST, the sequence similarity of 16S rRNA genes of strain R-2 and R5 was determined. The sequences generated in this study were deposited in the GenBank database using the BANKT program accessible via the NCBI website.

5.2.5 Phylogenetic analysis

The 16S rRNA sequences of strain R-2 and strain R5 were compared with sequences from closely related organisms from the EzBioCloud database and the NCBI database. Alignment of sequence data was performed with CLUSTAL W I.8. Phylogenetic trees were constructed using the neighbour-joining method with MEGA 11. Evolutionary distances were calculated using the Kimura two-parameter model for neighbour-joining.

5.2.6 Morphological and Biochemical Characterization

Following one-day growth on Nutrient agar at 30°C, the bacterial colonies were observed for morphology. A Zeiss light microscope was used to study the cell morphology. In order to test mobility, methods described by Skerman, (1967) was used. Gram reaction was determined using HiMedia Gram Staining kit according to manufacturers' instructions. Spores were examined by heat treatment at 80°C for 10 min as well as phase contrast microscopy after bacteria had grown on different

sporulating media. The oxidase and catalase activities were determined using oxidase discs (Hi-Media) and 3% (v/v) H_2O_2, respectively, following the method described by Smibert (1994). Tests such as the methyl red test, Voges-Proskauer reaction, indole production, citrate utilization were performed according to standard procedures described by Cowan and Steel (1965).

The carbohydrate fermentation test was carried out using phenol red broth base containing pancreatic digest of casein (10 grams/l), NaCl (5 grams/l) and phenol red (0.018 grams/l). In a 500 mL flask, 1.5 g of phenol red broth base was added to 100 mL of distilled water. Next, the media was autoclaved and cooled to room temperature. After that, the media was poured into various sterilized test tubes. There was approximately 5 mL of media in each test tube. Then a filter sterilized solution of desired carbohydrate was added to test tube at 5 - 10%. In all test tubes, bacteria *Bacillus zhangzhouensis* R-2 or *Enterococcus faecium* strain R5 were inoculated. As a control, uninoculated test tubes were used. Further, tubes were incubated at 30 ^{O}C for 24 hours. Several sugars such as maltose, lactose, galactose, rhamnose, inositol, mannitol, sucrose, and arabinose were tested in this test.

5.3 Results

5.3.1 Isolation and selection of desulfurizing-bacteria

Two desulfurizing bacteria designated as strain R-2 and strain R5 were isolated from two different samples collected from Indian Oil Petroleum Plant, Panki, Kanpur India. These two strains were selected for further study.

5.3.2 Identification of strain R-2 and strain R5 by the 16S rRNA gene sequencing

Strain R-2 exhibited the highest 16S rRNA gene sequence (100%) similarity with *Bacillus zhangzhouensis* DW5-4 (MCCC 1A08372), followed by *Bacillus pumilus* ATCC 7061 (99.96%), *Bacillus australimaris* NH7I_1 (99.79%), *Bacillus safensis* subsp. *safensis* FO-36b (99.79%), *Bacillus safensis* subsp. *osmophilu*s BC09 (99.79%), *Bacillus altitudinis* 41KF2b (99.51%), *Bacillus xiamenensis* HYC-10 (99.44%). Table 5.1 summarized results of the 16S rRNA gene sequencing of strain R-2. The 16S rRNA sequences of strain R-2 was submitted to the Genbank, NCBI under accession number ON112198.

Strain R5 showed the highest 16S rRNA sequence similarity (99.85%) with *Enterococcus faecium* LMG 11423 (AJ301830), followed by *Enterococcus lactis* BT159 (98.61 %). It also showed significant similarity (>98.6%) with other species of *Enterococcus* including *Enterococcus durans* NBRC 100479, *Enterococcus thailandicus* DSM 21767, *Enterococcus hirae* ATCC 9790, *Enterococcus mundtii* DSM 4838, *Enterococcus canis* NBRC 100695, *Enterococcus hulanensis* 190-7, and *Enterococcus ratti* DSM 15687. In Table 5.2, analysis of the results of the 16S rRNA gene sequence of strain R5 is presented. Under the accession number ON112104, the 16S rRNA sequence of strain R5 was submitted to the Genbank, NCBI.

5.3.3 Phylogenetic analysis of strain R-2 and Strain R5

Phylogenetic analysis based on the 16S rRNA gene sequences of strain R-2 and the closely related species shows that strain R-2 belongs to the genus *Bacillus* and is in a clade with *Bacillus zhangzhouensis* DW5-4 (Fig 5.2).

On the basis of 16S rRNA gene sequence of strain R-2 and its phylogenetic analysis, strain R-2 was identified as *Bacillus zhangzhouensis* strain R-2.

Phylogenetic analysis based on the 16S rRNA gene sequences of strain R5 and the closely related species shows that strain R5 belongs to the genus *Enterococcus* and is in a clade with *Enterococcus faecium* LMG 11423 and *Enterococcus lactis* BT159 (Fig 5.3).

On the basis of 16S rRNA gene sequence of strain R5 and its phylogenetic analysis, strain R5 was identified as *Enterococcus faecium* R5.

5.3.4 Morphological and Biochemical Characterization

Gram staining of cells of *Bacillus zhangzhouensis* strain R-2 *and Enterococcus faecium* R5 showed that cells of strain R-2 were Gram-positive rods whereas cells of strain R5 were Gram-positive cocci (Fig 5.4). Spore staining showed that endospore was present in cells of *Bacillus zhangzhouensis* strain R-2 whereas no spores were detected in strain *Enterococcus faecium* R5. Cells of the *Bacillus zhangzhouensis* strain R-2 was catalase and oxidase positive whereas cells of *Enterococcus faecium* strain R5 were negative for both the test. *Bacillus zhangzhouensis* strain R-2 showed positive results for indole production, citrate utilization, MR test, and urease test whereas *Enterococcus faecium* strain R5 was negative for these tests. Cells of *Bacillus zhangzhouensis* strain R-2 strains were negative for VP test whereas positive for *Enterococcus faecium* strain R5. Cells of *Bacillus zhangzhouensis* strain R-2 produced acids from maltose, galactose, rhamnose, inositol and arabinose whereas cells of *Enterococcus faecium* strain R5 produced acids from lactose, mannitol and sucrose.

Table 5.1: 16S rRNA gene sequence similarity of strain *Bacillus zhangzhouensis* R-2 with valid published species

S. No.	Bacteria	Similarity (%)
1	*Bacillus zhangzhouensis* DW5-4 (JOTP01000061)	100
2	*Bacillus pumilus* ATCC 7061 (ABRX01000007)	99.86
3	*Bacillus australimaris* NH7I_1 (JX680098)	99.79
4	*Bacillus safensis* subsp. *safensis* FO-36b (ASJD01000027)	99.79
5	*Bacillus safensis* subsp. *osmophilus* BC09 (KY990920)	99.79
6	*Bacillus altitudinis* 41KF2b (ASJC01000029)	99.51
7	*Bacillus xiamenensis* HYC-10(AMSH01000114)	99.44
8	*Bacillus atrophaeus* JCM 9070 (AB021181)	97.29
9	*Bacillus siamensis* KCTC 13613 (AJVF01000043)	97.08
10	*Bacillus subtilis* NCIB 3610 (ABQL01000001)	97.01
11	*Bacillus nakamurai* NRRL B-41091 (LSAZ01000028)	97.01
12	*Bacillus velezensis* CR-502 (AY603658)	97.00
13	*Bacillus tequilensis* KCTC 13622 (AYTO01000043)	96.94
14	*Bacillus halotolerans* ATCC 25096 (LPVF01000003*)*	96.94
15	Bacillus stercoris JCM 30051(MN536904)	96.94
16	*Bacillus spizizenii* NRRL B-23049 (CP002905)	96.94
17	*Bacillus vallismortis* DV1-F-3 (JH600273)	96.87
18	*Bacillus amyloliquefaciens* DSM 7 (FN597644)	96.87
19	*Bacillus cabrialesii* TE3 (MK462260)	96.80
20	*Bacillus inaquosorum* KCTC 13429 (AMXN01000021)	96.80
21	*Bacillus mojavensis* RO-H-1 (JH600280)	96.80
22	*Bacillus paralicheniformis* KJ-16(KY694465)	96.38
23	*Bacillus swezeyi* NRRL B-41294 (MRBK01000096)	96.38
24	*Bacillus glycinifermentans* GO-13 (LECW01000063)	96.31
25	*Bacillus licheniformis* ATCC 14580 (AE017333)	96.17
26	*Bacillus sonorensis NBRC 101234 (AYTN01000016)*	96.17
27	*Bacillus haynesii* NRRL B-41327 (MRBL01000076)	96.17
28	*Bacillus salacetis* SKP7-4 (LC367333)	95.63

Table 5.2: 16S rRNA gene sequence similarity of *Enterococcus faecium* strain R5 with valid published species

S. No.	Bacteria	Similarity (%)
1	*Enterococcus faecium* LMG 11423 (AJ301830)	99.85
2	*Enterococcus lactis* BT159 (GU983697)	99.61
3	*Enterococcus durans* NBRC 100479 (BCQB01000108)	99.54
4	Enterococcus thailandicus DSM 21767 (JXLE01000039)	99.46
5	*Enterococcus hirae* ATCC 9790 (CP003504)	99.38
6	*Enterococcus mundtii DSM 4838 (JXKV01000056)*	99.00
7	*Enterococcus canis* NBRC 100695 (BCQJ01000024)	98.84
8	*Enterococcus hulanensis* 190-7 (LC473138)	98.84
9	*Enterococcus ratti* DSM 15687 (JXLB01000051)	98.76
10	Enterococcus ratti DSM 15687 (JXLB01000051)	98.76
11	*Enterococcus villorum* ATCC 700913 (AJAN01000023)	98.69
12	*Enterococcus avium* ATCC 14025 (KE136366)	98.69
13	*Enterococcus gilvus* ATCC BAA-350 (AJDQ01000009)	98.69
14	*Enterococcus malodoratus ATCC 43197 (ASWA01000002)*	98.61
15	*Enterococcus viikkiensis IE3.2 (HQ378515)*	98.61
16	*Enterococcus pseudoavium* NCFB 2138 (Y18356)	98.61
17	*Enterococcus devriesei* LMG 14595 (AJ891167)	98.61
18	*Enterococcus xiangfangensis* 11097 (HF679036)	98.53
19	*Enterococcus pingfangensis* 241-2-2 (LC438519)	98.53
20	*Enterococcus dongliensis* 63-4 (LC438513)	98.30
21	*Enterococcus phoeniculicola* ATCC BAA-412 (AJAT01000017)	98.22
22	*Enterococcus florum* Gos25-1 (LC428281	97.99
23	*Enterococcus gallinarum* NBRC 100675 (BCQE01000074)	97.91
24	*Enterococcus casseliflavus* MUTK 20 (AF039903)	97.91

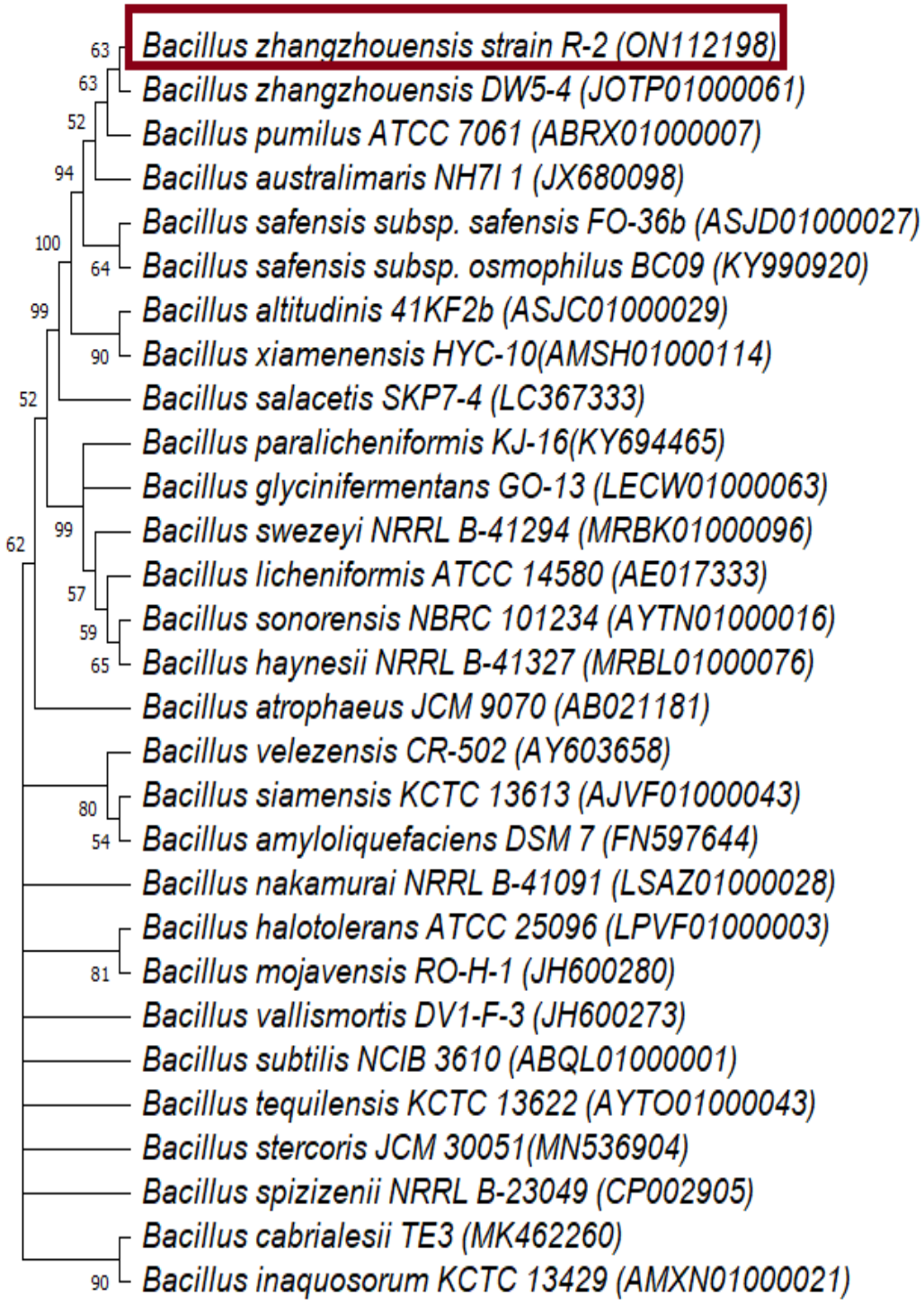

Fig 5.2: Neighbour-joining phylogenetic tree based on 16S rRNA gene sequences showing the positions of *Bacillus zhangzhouensis* strain R-2 and other related taxa. Bootstrap values (expressed as percentages of 1000 replications) of >50 % are shown at branch points

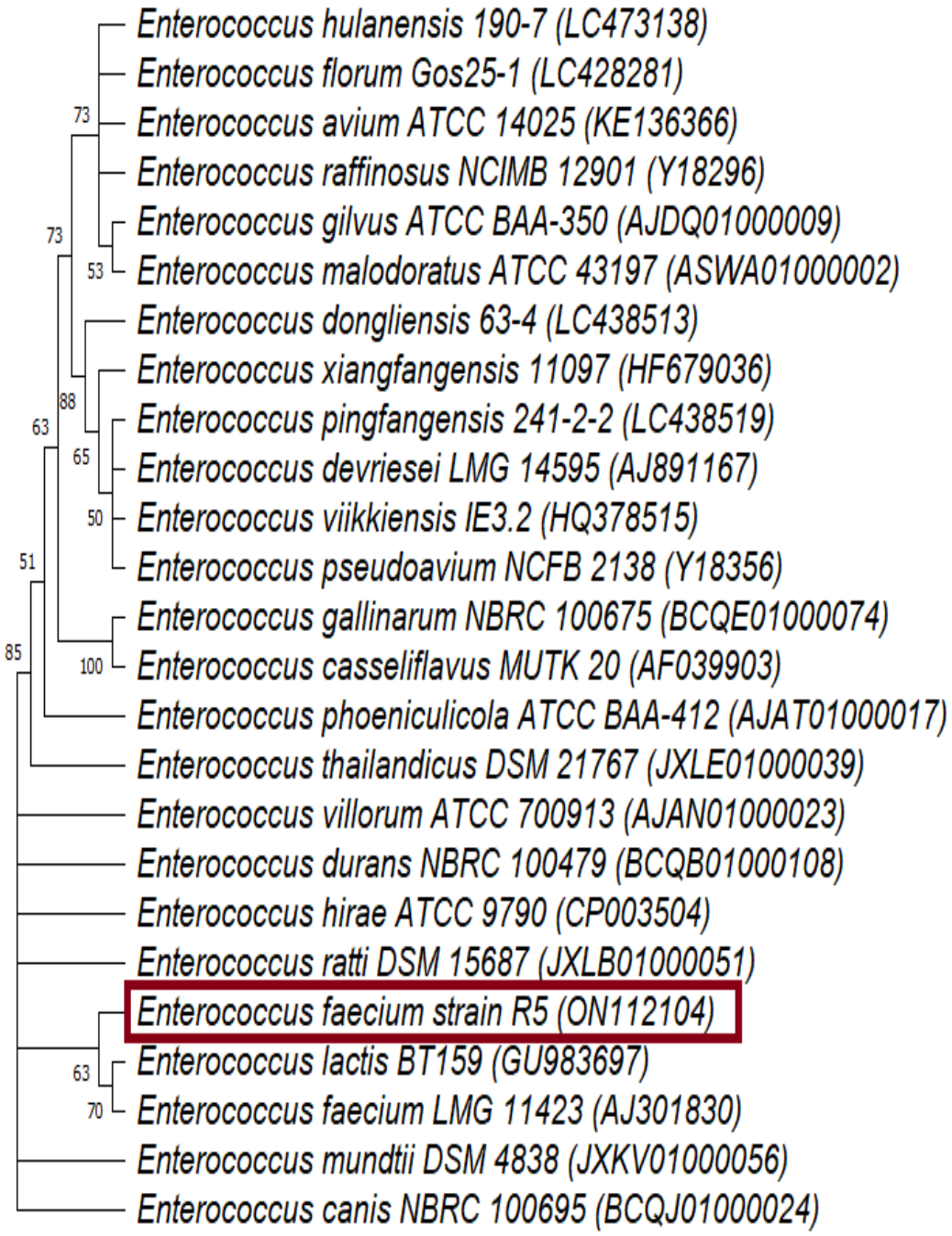

Fig 5.3: Neighbour-joining phylogenetic tree based on 16S rRNA gene sequences showing the positions of *Enterococcus faecium* strain R5 and other related taxa. Bootstrap values (expressed as percentages of 1000 replications) of >50 % are shown at branch points

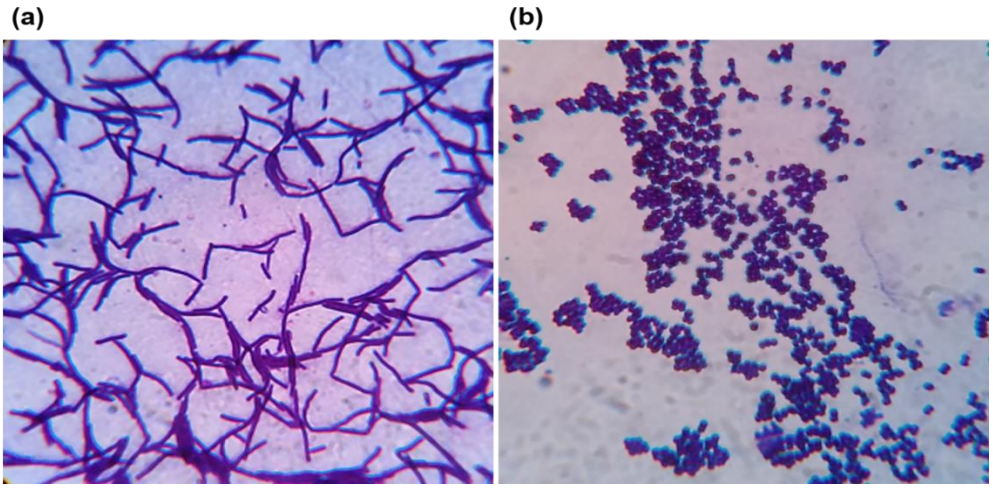

Fig 5.4. Gram staining of *Bacillus zhangzhouensis* strain R-2 (a) and *Enterococcus faecium* strain R5 (b)

The morphological and biochemical characterization of *Bacillus zhangzhouensis* strain R-2 and *Enterococcus faecium* strain R5 were summarized in Table 5.3 and Fig 5.5.

Table 5.3: Morphological characteristics of *Bacillus zhangzhouensis* strain R-2 and *Enterococcus faecium* strain R5

Characteristics	***Bacillus zhangzhouensis* strain R-2**	***Enterococcus faecium* strain R5**
Gram Staining	+	+
Shape	Rods	Cocci
Spore	+	–
Catalase	+	-
Oxidase	+	-
Citrate utilization	+	-
Voges-Proskauer test	-	+
Indole	+	-
Urease	+	-

Methyl red test	+	-
Acids from carbohydrates		
Maltose	+	-
Lactose	-	+
Galactose	+	-
Rhamnose	+	-
Inositol	+	-
Mannitol	-	+
Sucrose	_	+
Arabinose	+	-

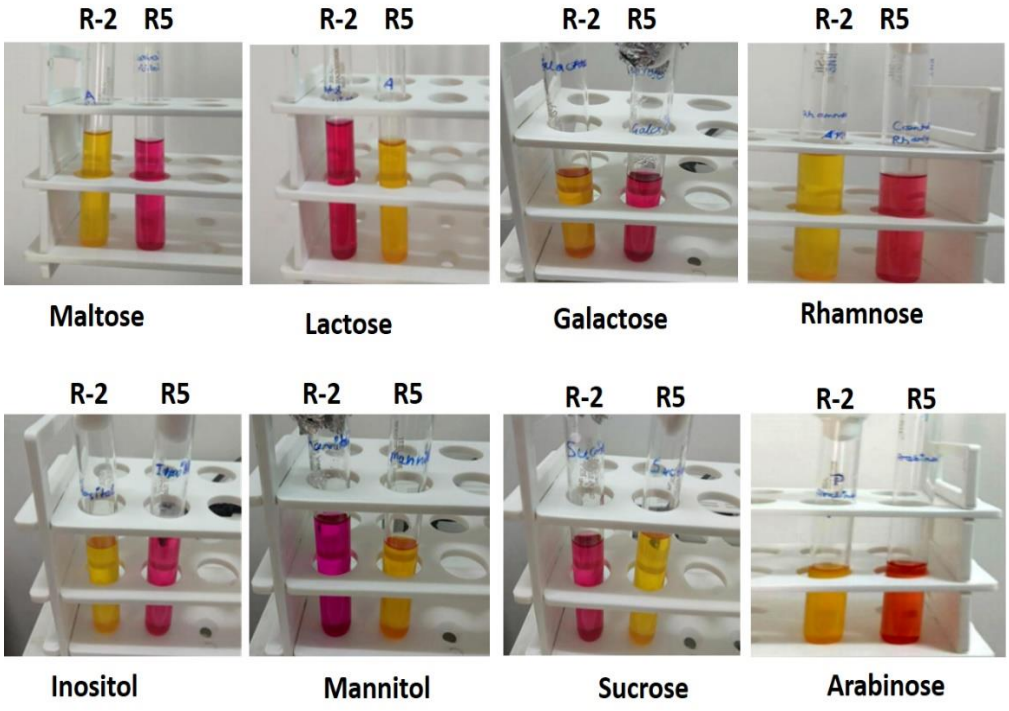

Fig 5.5: Biochemical characterization of *Bacillus zhangzhouensis* strain R-2 and *Enterococcus faecium* strain R5

5.4 Discussion

In this study, two desulfurizing-bacteria strain R-2 and strain R5 isolated from two different samples collected from Indian Oil Petroleum Plant, Panki, Kanpur, India were identified as *Bacillus zhangzhouensis* and *Enterococcus faecium* respectively based on their 16S rRNA gene sequences and phylogenetic analysis.

Cells of *Bacillus zhangzhouensis* strain R-2 were Gram-positive, rod-shaped, and motile and spore producing whereas cells of *Enterococcus faecium* strain R5 were Gram-positive, cocci-shaped, non-motile and non-spore producing.

Cells of *Bacillus zhangzhouensis* strain R-2 were catalase and oxidase positive whereas *Enterococcus faecium* strain R5 were negative for oxidase and catalase activities.

Bacillus zhangzhouensis strain R-2 belongs to the genus *Bacillus* that comprises of 293 species/subspecies of *Bacillus* (Arora, 2020). Rod-shaped bacteria that form endospores belong to this genus. They can be aerobic or facultatively anaerobic. Similarly, *Bacillus zhangzhouensis* strain R-2 forms endospores and rods. There are numerous sources of *Bacillus*, including soil, sewage sludge (Demharter and Hensel, 1989), ocean sediments (Rüger et al. 2000), and salt water (Smibert, 1994). *Bacillus zhangzhouensis* strain R-2 was isolated from soil slurry containing oil.

Bacillus zhangzhouensis strain R-2 has the ability to desulfurize DBT and TH. Many species of *Bacillus* have been reported to degrade various toxic compounds, including petroleum hydrocarbons, polycyclic aromatic compounds, dyes, drugs and heavy metals. *Bacillus* spp. are, therefore, considered to be potential bioremediation agents

Enterococcus faecium strain R5 belongs to the genus *Enterococcus* that comprises of more than 75 species. *Enterococci* are non-spore-forming ovoid bacteria that can exist in pairs, chains, or groups (García-Solache and Rice, 2019). *Enterococcus faecium* strain R5 also a non-spore forming strain that produces single, in pairs and in chains of cocci. *Enterococci* are chemo-organotrophic facultative anaerobes. *Enterococci* are usually catalase- and oxidase-negative. *Enterococcus faecium* strain R5 was also catalase and oxidase negative.

Few *Enterococcus* spp. are known for their bioremediation and biodegradation capabilities. *E. faecium* CCDM 922A accumulated and bio-transformed inorganic selenium (Hyrslova et al. 2022). Mate and Pathade, (2012) studied degradation of dye Reactive Red 195 by *Enterococcus faecalis* strain YZ66. In this study, *Enterococcus faecium* strain R5 desulfurized DBT and TH.

5.5 Conclusion

Two desulfurizing-bacteria strains R-2 and R5 were isolated from two samples collected from Indian Oil Petroleum Plant, Panki, Kanpur, India. Based on their 16S rRNA gene sequences and phylogenetic analysis, strains R-2 and R5 were identified as *Bacillus zhangzhouensis* and *Enterococcus faecium*, respectively. *Bacillus zhangzhouensis* strain R-2 and *Enterococcus faecium* strain R5 will be used for the study of desulfurization of DBT and TH.

Chapter VI

Objective 4: Desulfurization test for Dibenzothiophene and Thiophene by bacterial isolates

6.1 Introduction

The combustion of liquid fuels releases several pollutants into atmosphere. Among all the pollutants, sulfur dioxide (SO_2) is one of the hazards gas releases into the environment (Buzanello et al. 2010). The main cause of releasing SO_2 into atmosphere is the presence of sulfur containing compound in liquid fuels. SO_2 reacts with environmental moisture and other gases in atmosphere to form the sulfuric acid (H_2SO_4). H_2SO_4 cause air pollution and comes down to the earth with rainy water and cause acid rains. Also, showed adverse effects in human health (Lee et al. 2018). These sulfur compounds are present in aliphatic and aromatic form. The aliphatic sulfur removed during distillation process of crude oil. However, aromatic forms having complex structure therefore, they are difficult to remove (Kirimura et al. 2001).

To overcome this problem several desulfurization technologies have been developed to remove sulfur from the liquid fuels. These technologies are hydrodesulfurization (HDS), oxidative desulfurization (ODS), extractive desulfurization (EDS) adsorptive desulfurization (ADS), and biodesulfurization (BDS) (Shang et al. 2013). All the developed techniques are efficient in different aspects. However, they require sever and sophisticated conditions and expensive chemicals for sulfur removal. These conditions make the process economic inefficient (Li et al. 2007). Biodesulfurization is the most economic efficient process for desulfurization of liquid fuels. In biodesulfurization, microorganism utilize sulfur through their metabolic pathway and transform the sulfur containing compound to non sulfur product without losing the calorific value of liquid fuel. In addition, BDS does not required the sophisticated conditions or expensive chemicals (Pacheco et al. 2019).

In this objective, the desulfurization of DBT and TH was performed in nutrient-rich medium using the uninduced and induced cells of *Bacillus zhangzhouensis* strain R-2 and *Enterococcus faecium* strain R5 bacterial strains.

6.2 Materials and methods

6.2.1 Materials

The sulfur containing compounds, namely, TH (99%) and DBT (98%) were purchased from Alfa Aesar and Spectrochem Pvt. Ltd, India. Peptone, beef extract powder, yeast extract powder, agar powder, were purchased from Himedia Pvt. Ltd, India. Bacterial media were prepared in ultrapure water from the Elix Mili Q system, USA.

6.2.2 Bacterial growth studies

For growth study, *Bacillus zhangzhouensis* strain R-2 and *Enterococcus faecium* strain R5 were grown on 100 mL nutrient broth medium enriched with DBT or TH. Samples were taken at regular intervals and bacterial growth was monitored by taking optical density at 630 nm by UV-Vis spectroscopy (Varian, Cary 100, USA).

6.2.3 Bacterial growth in presence of beads

Effect of beads on *Bacillus zhangzhouensis* strain R-2 and *Enterococcus faecium* strain R5 was determined by growing them in presence and absence of prepared beads. The flasks containing nutrient broth medium, bacterial cells and prepared beads were incubated. Samples were collected at regular intervals and

filtered by Whatman filter paper. The bacterial growth was determined by measuring optical density at 630 nm by UV – Vis spectroscopy (Varian, Cary 100, USA).

6.2.4 Bacterial desulfurization using uninduced cells.

The bacterial desulfurization test was performed in conical flask containing 100 mL nutrient broth medium enriched with DBT and TH at the concentration of 300 ppm. The bacterial strains (*Bacillus zhangzhouensis* strain R-2 or *Enterococcus faecium* strain R5) were inoculated in the medium containing flask. The flasks were incubated for 15 h at 30^{O} C under shaking condition at 100 rpm. Initial and final concentration of DBT and TH in flasks were determined using gas chromatography analysis equipped with the flame ionization detector (Nucleon-5700, India).

6.2.5 Bacterial desulfurization test by induced cells

Bacterial desulfurization test was performed in conical flask. Approximately 20 mL of nutrient broth medium containing DBT/TH was taken in a flask. Pellet of approximately 5 mL of resting bacterial cells was inoculated into same flask containing DBT/TH enriched nutrient broth medium. The flasks were incubated for 4 h under shaking condition at 100 rpm. The DBT/TH concentrations were measured every 30 min using a gas chromatography equipped with the flame ionization detector (Nucleon-5700, India). Some amounts of samples were taken at 0, 2 and 4 h to check the bacterial growth during the desulfurization test. Approximately 0.1 mL of the collected sample was spread on the prepared nutrient agar plates. The plates were incubated at 30 ^{O}C for 24 h. After bacterial growth colony was counted and colony forming unit (CFU) was calculated using the following formula:

CFU = (number of colonies x dilution factor) / volume of the sample

6.3 Results

6.3.1 Bacterial growth in presence and absence of beads.

The isolated bacteria were subjected to growth study. Growth was observed in nutrient broth medium enriched with thiol compound (300 ppm) for 35 h at 30 ^{O}C. The bacterial strains (R-2 or R5) showed approximately similar growth (O.D. of R-2 1.771 and 1.883 in presence and absence of DBT/TH respectively and O.D. of R5 1.574 and 1.713 in presence and absence of DBT/TH respectively at 35h of incubation respectively) in presence and absence of thiol compounds (DBT/TH), confirming that both the strains are capable to grow efficiently in presence of thiol compounds (Fig. 6.1a-b). Further R-2 and R5 was also checked for the effect of beads. The bacterium was grown in nutrient broth medium in presence and absence of Ni doped beads at 30 ^{O}C. In presence of beads, growth was approximately similar to the growth in absence of beads (O.D. of R-2 1.774 and R5 1.751at 35 h in presence of beads and 1.783 in absence of beads) (Fig. 6.1c), which confirms that the Ni doped beads were showed no effect in the growth of R-2 and R5 bacterial cells.

6.3.2 Bacterial desulfurization using uninduced cells

The bacterial desulfurization was performed using DBT and TH in nutrient broth medium. Initial and final concentration of DBT and TH was determined through gas chromatographic analysis equipped with flame ionization detector. The results of desulfurization test were showed in fig 6.2. Data in the graph was showing complete removal of DBT and TH in 15 h of incubation. Therefore, data of the desulfurization

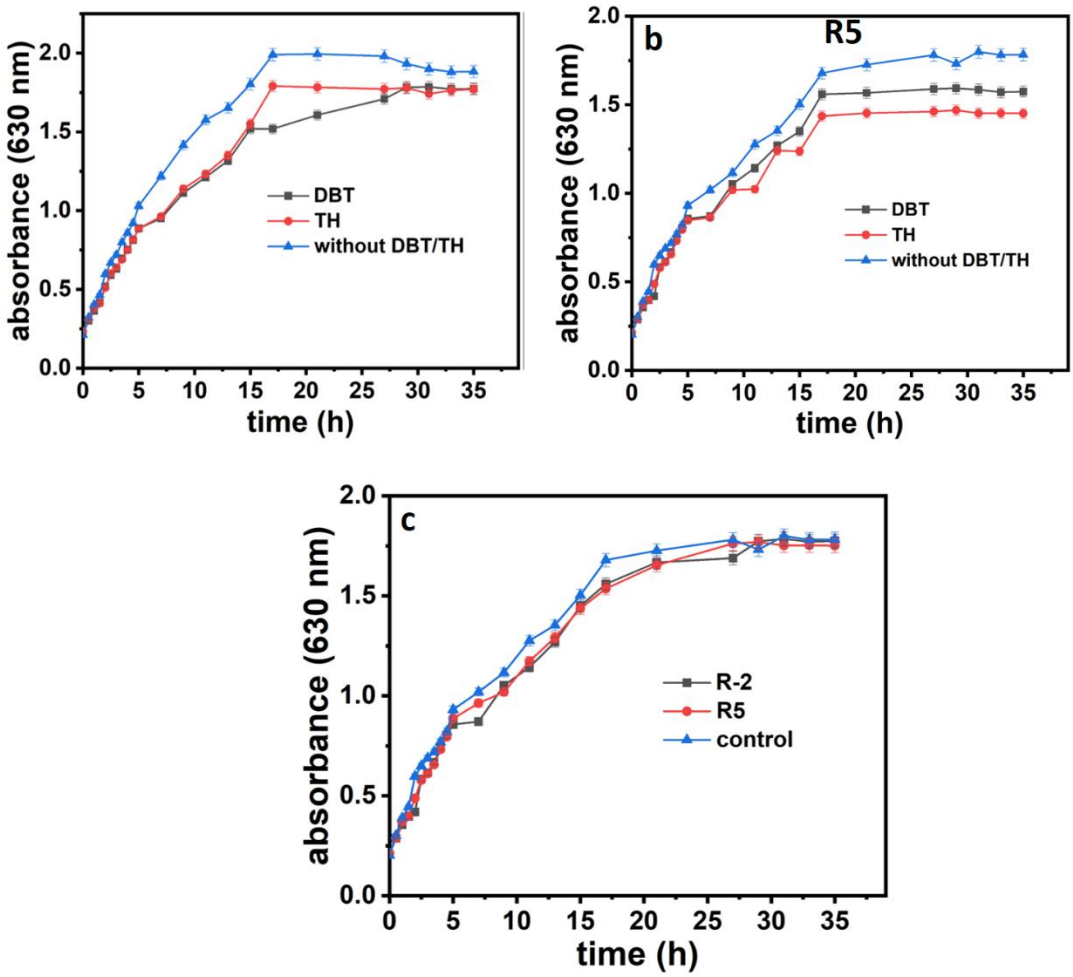

Fig 6.1: (a-b) Growth study of R-2 and R5 in presence/absence of thiol compounds and, (c) in presence/absence of beads

test indicating that the strains (*Bacillus zhangzhouensis* strain R-2 or *Enterococcus faecium* strain R5) are capable of desulfurizing DBT and TH efficiently at the initial concentration of 300 ppm in 15 h of incubation at 30 ^{O}C under shaking condition at 100 rpm.

6.3.3 Bacterial desulfurization test using induced cells of *Bacillus zhangzhouensis* strain R-2

Bacterial desulfurization tests were performed at four different initial concentrations (50 – 400 ppm) (Fig 6.3). These concentrations were selected to be

approximately the equilibrium (final) concentration values attained during the adsorption tests described earlier.

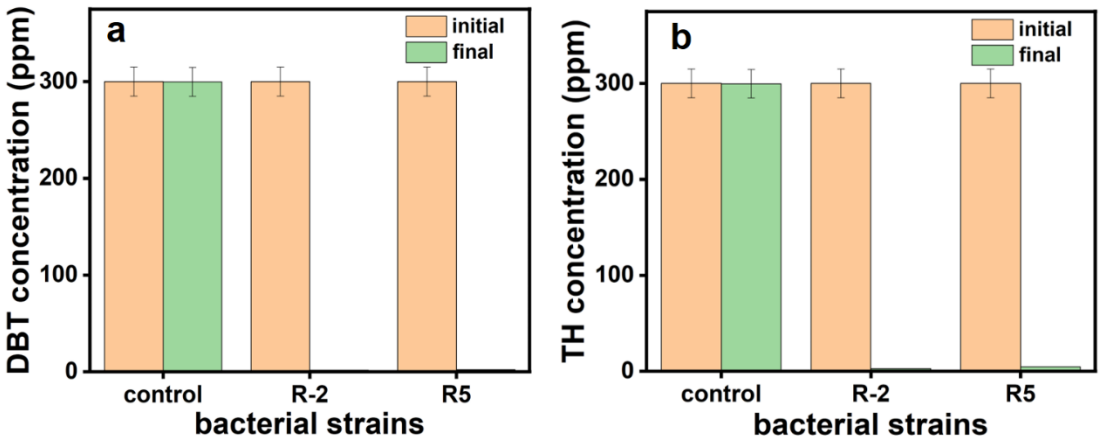

Fig 6.2: Bacterial desulfurization test using uninduced cells of *Bacillus zhangzhouensis* strain R-2 and *Enterococcus faecium* strain R5

Although removal rates for DBT were relatively faster or rapid, less than 10 ppm concentrations were measured in both test liquids (DBT and TH) in 4 h (Fig 6.4). The initial and final concentrations of DBT/TH for the other cases are mentioned in table 6.1. Bacterial growth was also observed using the plate count method in 0, 2 and 4 h of the tests. The calculated CFU were approximately 150×10^5, 110×10^6, and 175×10^8 in 0, 2 and 4 h, respectively, in both spent liquids (Fig 6.5). The data indicate an exponential growth of the bacteria during the test, which was also confirmed by the earlier measured growth curved in the presence/absence of DBT and TH. The selected isolates were found to be a fast grower in the thiol compound-containing medium. Although some amounts of sulfur (< than 10 mg L^{-1}) were left in the spent liquids, the test results indicated that the selected *Bacillus zhangzhouensis* strain R-2 bacterium can efficiently remove the thiol compounds from the liquids medium.

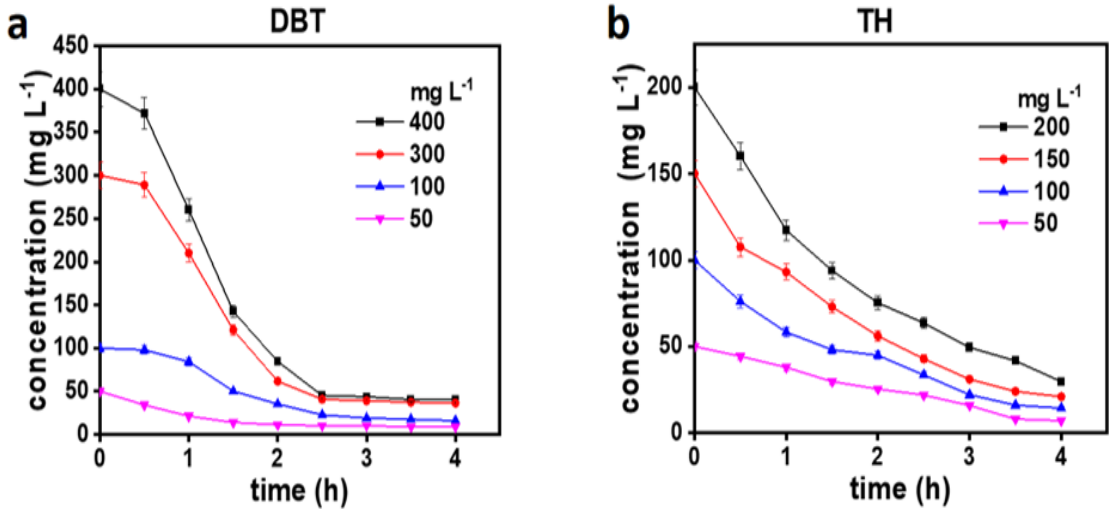

Fig 6.3: Bacterial desulfurization test of (a) DBT and (b) TH using induced cells of *Bacillus zhangzhouensis* strain R-2

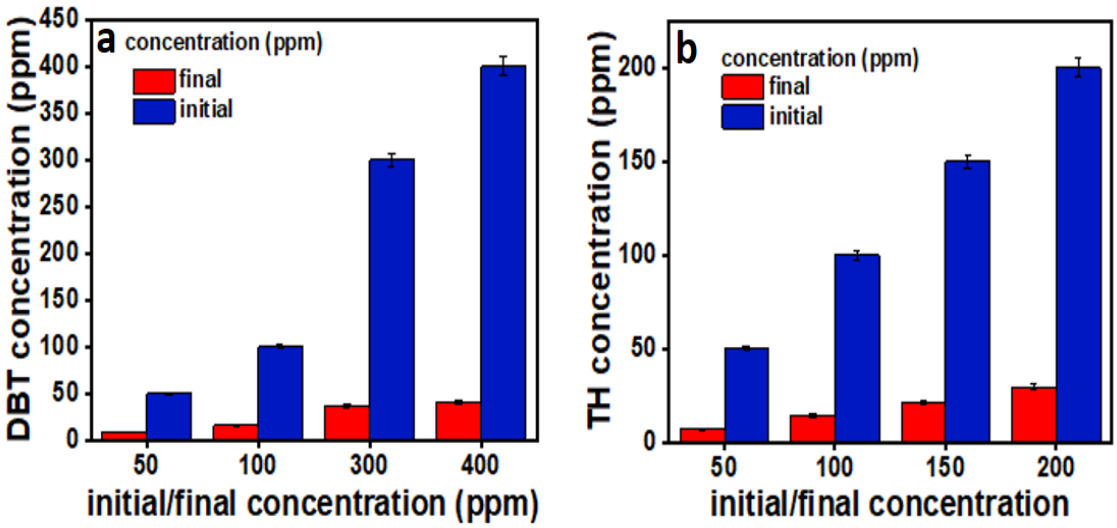

Fig 6.4: Summarized results of bacterial desulfurization test of (a) DBT, and (b) TH using induced cells of *Bacillus zhangzhouensis* strain R-2

Table 6.1: Initial/final concentrations in bacterial desulfurization test (using induced cells of *Bacillus zhangzhouensis* strain R-2)

S. No.	Initial concentration of DBT (mg L^{-1})	Initial concentration of TH (mg L^{-1})	Final concentration of DBT (mg L^{-1})	Final concentration of TH (mg L^{-1})
1	400	200	40.35	29.62
2	300	150	36.39	20.85
3	100	100	15.89	14.24
4	50	50	8.80	6.97

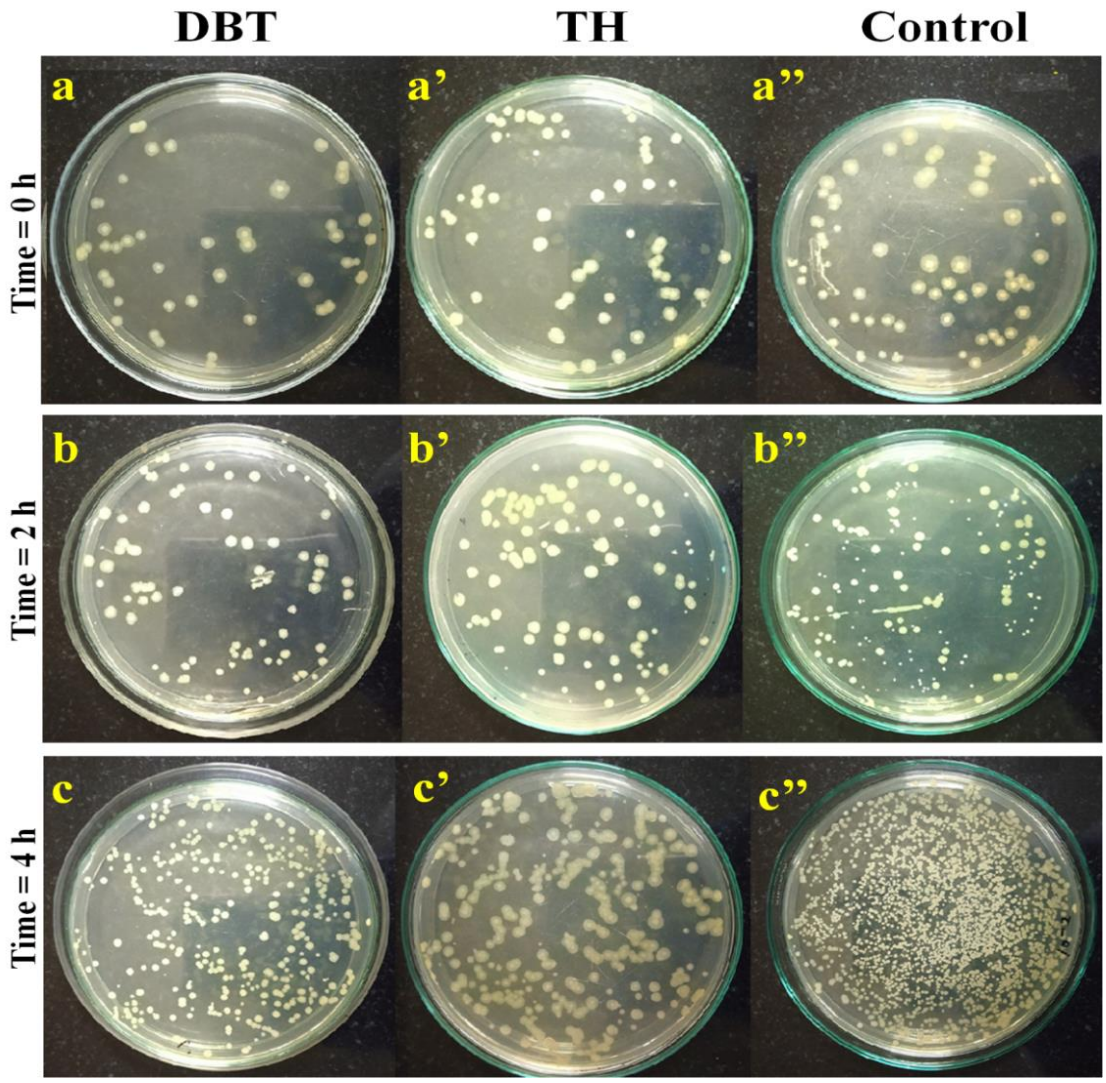

Fig 6.5: Bacterial growth of *Bacillus zhangzhouensis* strain R-2 during desulfurization test (a) at 0 h, (b) 2 h and (c) after 4 h of the experiment

6.3.4 Bacterial desulfurization test using induced cells of *Enterococcus faecium* strain R5

The bacterial desulfurization tests were performed at four different concentrations (50–400 ppm) of DBT and TH to check the desulfurization efficiency of the *Enterococcus faecium* strain R5 (Fig. 6.6). The concentrations used for the bacterial desulfurization was the approximate concentration reaches after 1.5 - 2 h of the adsorption experiment. All the tests were performed for 4 h. After 4 h of the

bacterial desulfurization test the concentration of DBT and TH reaches approximately < 10 ppm, confirming the selected bacterium was capable to remove the thiol compounds efficiently. The removal rate was observed faster in DBT in comparative to TH (Fig 6.7). Initial and final concentrations of DBT and TH were mentioned in Table 6.2. During the bacterial desulfurization test, bacterial growth was also observed at the initial (0 h), middle (2 h), final (4 h) stage of the experiment using plate count method (Fig. 6.8). The calculated CFU was 38 x 10^{13}, 69 x 10^{14}, and 178 x 10^{15} in 0 h, 2 h, and 4 h respectively in spent liquid. CFU data confirms the exponential growth of bacterium during desulfurization test. Bacterial desulfurization test and CFU data confirms that the selected bacterium was fast growing in presence of thiol compounds which was also confirmed earlier by determining bacterial growth in presence/absence of DBT/TH, and capable to efficiently remove the thiol compounds from liquid medium. However, some amount of thiol compounds (<10 ppm) was left in the spent liquid medium.

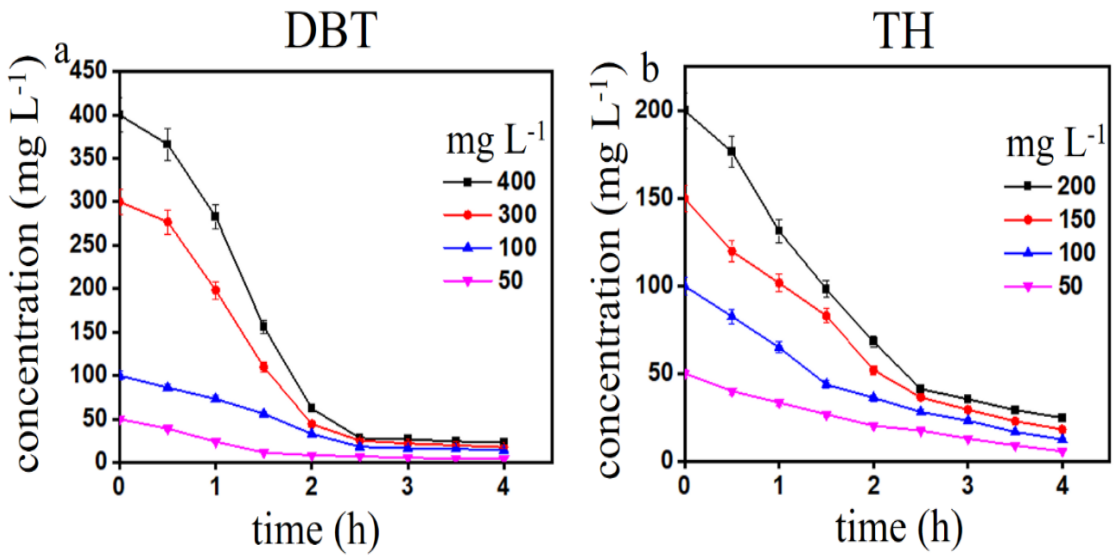

Fig 6.6: Bacterial desulfurization test of (a) DBT and (b) TH using induces cells of *Enterococcus faecium* strain R5

Table 6.2: Initial/Final concentrations in bacterial test (Using induced cells of *Enterococcus faecium* strain R5)

S. No.	Initial concentration of DBT (mg L^{-1})	Initial concentration of TH (mg L^{-1})	Final concentration of DBT (mg L^{-1})	Final concentration of TH (mg L^{-1})
1	400	200	23.02	24.77
2	300	150	17.53	18.14
3	100	100	14.17	12.38
4	50	50	3.97	5.65

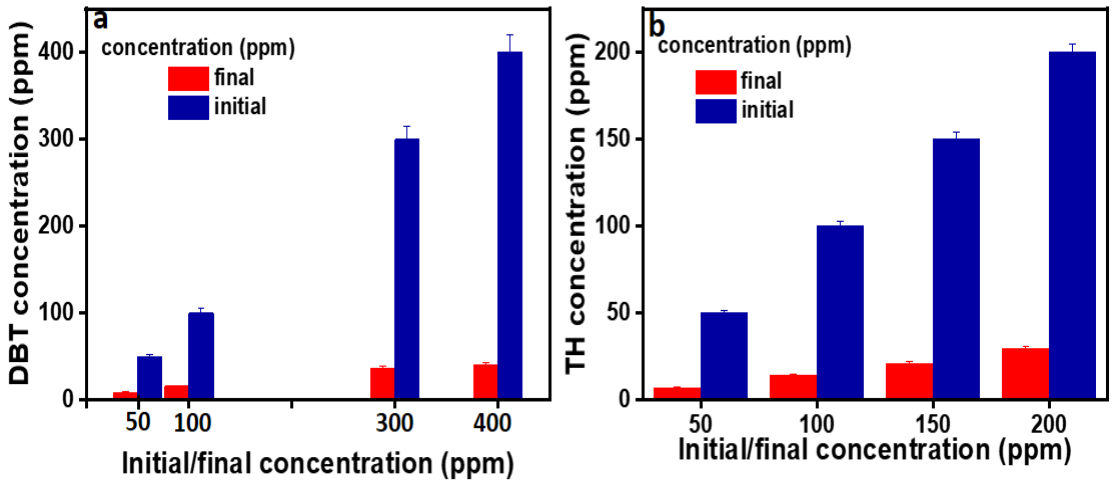

Fig 6.7: Summarized results of desulfurization test of (a) DBT, and (b) TH using induced cells of *Enterococcus faecium* strain R5

The bacterial desulfurization test was performed using both the strain separately. Results showing approximately 98% and 96% removal of DBT/TH using *Bacillus zhangzhouensis* strain R-2 and *Enterococcus faecium* strain R5, respectively at four different initial concentrations, which were 50, 100, 200 and 300 ppm. Caro et al. (2007) have shown the desulfurization of DBT using *Pseudomonas putida* and showed approximately 75 % removal of its initial concentration (200 ppm) in 24 h. Similarly, Chen et al. (2008) showed desulfurization of TH using *Mycobacterium* species and showed complete removal of its initial concentration (0.5 mM) in 56 h.

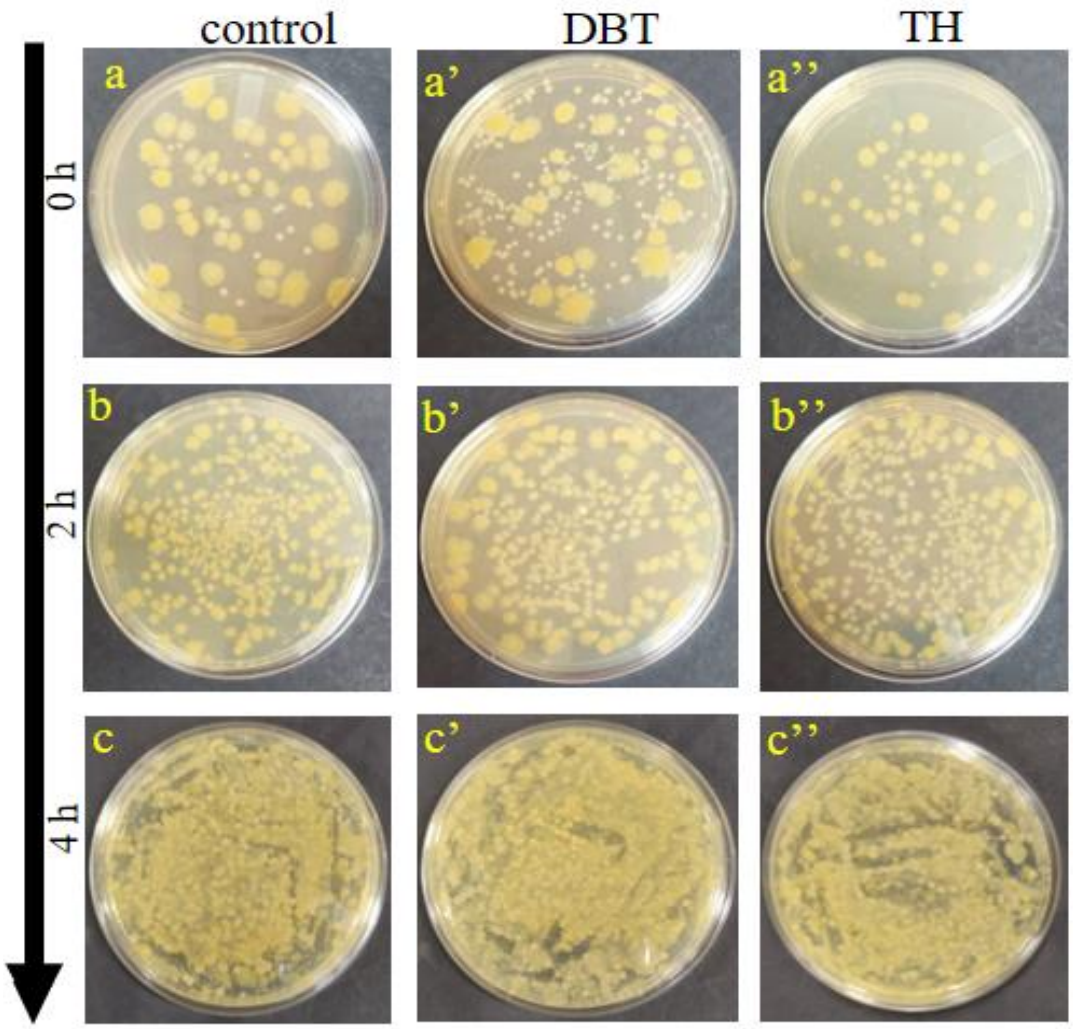

Fig 6.8: Bacterial growth of *Enterococcus faecium* strain R5 during desulfurization test (a) at 0 h, (b) 2 h and (c) after 4 h of the experiment

6.4 Discussion

In this study, both bacterial strains showed the approximately complete desulfurization of DBT and TH in 15 h of incubation. Few researchers have also shown the desulfurization of DBT by bacterial cells (Tanaka. et al. 2002; Boshagh. et al. 2014). However, in their study the maximum desulfurization was achieved up to 60 -65 % at the initial concentration of 100 ppm after three to four days of incubation. In a study Martinez et al. (2016) have also desulfurize the DBT using induced/resting cells of *Pseudomonas putida* and achieved complete desulfurization in 90 min of the

desulfurization. Hence, in this study the bacteria selected for desulfurization were found more efficient than other reported studies. After the desulfurization test the bacterial cells were separated by 0.22 µm syringe filter. The spent solution was found free from sulfur compounds and inoculated bacterial cells.

6.5 Conclusion

The bacterial strains namely *Bacillus zhangzhouensis* strain R-2 or *Enterococcus faecium* strain R5 grew well in presence of DBT or TH. No effect of beads was observed in bacterial growth. The bacterial strains (*Bacillus zhangzhouensis* strain R-2 or *Enterococcus faecium* strain R5) showing complete removal of DBT and TH in 15 h of the desulfurization test using uninduced cells. However, rate of desulfurization enhanced using induced cells of both the strains. The induced cells showed complete desulfurization of DBT and TH in 4 h of desulfurization test.

Chapter VII

Objective 5: Complete desulfurization of DBT and TH in liquid fuel using Ni-doped carbon beads followed by an isolated bacterial strain

7.1. Introduction

Sulfur is the third most abundant element present in liquid fuels after carbon and hydrogen. It persists in aliphatic and aromatic form. The aliphatic form of sulphur removes during the refining process however, aromatic form having the complex structure therefore, it is difficult to remove. Removal of sulfur from the liquid fuels necessary because it causes environmental pollution on combustion of the liquid fuels (Betiha et al. 2018).

There are several methods have been developed for removal of aromatic sulphur compound from the liquid fuel such as hydrodesulfurization (HDS), oxidative desulfurization (ODS), extractive desulfurization (EDS), adsorptive desulfurization (ADS), and biodesulfurization (BDS) (Danmaliki et al. 2017). These desulfurization techniques are efficient in several aspects. However, they have several limitations and drawbacks such as hydrodesulfurization requires severe conditions such as high temperature and pressure, oxidative desulfurization is a multistep process also selection of suitable oxidizing agent is challenging. Separation of ionic liquid from the spent (desulfurized) is difficult in extractive desulfurization process (Abro et al. 2014). Adsorptive desulfurization can be done at room temperature i.e., does not require severe conditions. Also, separation of spent adsorbent from the spent liquid fuel is much easier than other desulfurization techniques. Adsorptive desulfurization technique is efficient for removal of sulfur compound in high concentration however, at lower concentration adsorption becomes saturated (Prasad et al. 2008). Biodesulfurization is an efficient desulfurization technique for low concentration of sulfur compounds because microorganism cannot tolerate higher concentration of sulfur compounds. Therefore, observing all the drawbacks of different desulfurization

techniques, a new desulfurization approach has been developed for complete removal of sulfur compounds from liquid fuel in this work. In this new approach, two different desulfurization technique namely adsorptive desulfurization and biodesulfurization were integrated in a sequence for complete removal of sulfur compounds from liquid fuels (Lee and Valla, 2019; Houda et al. 2018; Ibrahim et al. 2017; Dasgupta et al. 2013).

In this objective, the sequential desulfurization test of DBT and TH was performed using the prepared Ni-doped activated carbon beads and isolated bacterial strains for complete removal to DBT and TH in liquid fuels. The spent adsorbent was characterized to confirm the adsorption of DBT and TH on prepared adsorbent (Ni-doped activated carbon beads). In addition, regeneration of the spent adsorbent was also done using the bacterial regeneration method. The regenerated adsorbent was further physicochemically characterized and compared with the physicochemical properties of the fresh adsorbent to confirm the successful regeneration of the spent adsorbent.

7.2 Materials and methods

7.2.1 Materials

n-octane (> 99%) and ethanol (99%) were purchased from Merck, Germany. The sulfur containing compounds, namely, TH (99%) and DBT (98%) were purchased from Alfa Aesar and Spectrochem Pvt. Ltd, India. Nutrient broth and agar were purchased from Himedia Pvt Ltd, India. All gases used in the study were zero grade

and purchased from Sigma Gases, India. Bacterial media were prepared in ultrapure water from the Elix Mili Q system, USA.

7.2.2. Complete (sequential) desulfurization test

The sequential desulfurization test was performed in the same equipment and at the same physical condition used for adsorption test. Briefly, A high pressure vassal (I.D. = 45 mm, O.D. = 80 mm, height = 60) was used to perform the test. Vessel was equipped with a PID temperature controller and an electric heater. A stainless steel (SS) agitator cum beads holder (basket) diameter = 40 mm, height = 15 mm, side wall pore = 0.5 mm, was especially fabricated which was fitted to the bottom end to vertical shaft of the motor. The agitator allows the movement of liquid throughout the beads also prevents the escaping of beads outside the bead holder.

All the tests were performed at room temperature (~30 ^{O}C). Approximately 0.1 g of beads (Ni-ACB/Ni-CNF-ACB) was placed into the sample holder. Approximately 20 mL of model/test oil (n-octane) containing DBT/TH (depending on the type of beads, viz Ni-ACB/Ni-CNF-ACB respectively) was taken into the vessel. The mixture was stirred at 200 rpm for approximately 1.5 h. After that approximately 5 mL of centrifuged induced bacterial cells of *Bacillus zhangzhouensis* strain R-2 or *Enterococcus faecium* strain R5 was transferred to the reactor vessel. The mixture was stirred for another 2.5 h. The DBT/TH concentrations were measured every 30 min, using a gas chromatography. After 4 h (1.5 + 2.5 h) stirring was stopped and solid beads were separated using filter paper (Whatman ashless, grade no. 42). The spent adsorbent was used for the regeneration. Bacterial cells from the spent liquid were

separated using syringe filter (0.22 µm). The filtered spent liquid was checked for bacterial counts using the colony count method.

7.2.3 Gas chromatography

The concentration of DBT and TH in oil before and after desulfurization was determined using gas chromatography (Nucleon-5700, India). The chromatography was equipped with flame ionization detector and Ch. W. hp column. Nitrogen at the frow rate of 200 sccm was used as carrier gas. However, hydrogen in combination with air was used for flame ionization. Approximately 2 µl of each sample was taken for GC analysis.

7.2.4 Spent characterization by FE-SEM

Surface morphology of the spent adsorbent samples was observed using the field emission high resolution field emission microscope (FE-SEM) (MIRA-3 TESCAN, Brno, Czech Republic) by capturing the electronic images.

7.2.5 Bacterial regeneration

Separated spent adsorbent was collected in clean and dry falcon tube and subjected to successively wash with 70% ethanol and sterilized milli Q water to remove adhered bacterial cells. Further adsorbent was transferred into a flask containing 25 mL active bacterial culture in nutrient broth medium. Flask containing beads and bacterial cell into the nutrient broth medium was incubated at 30 ^{O}C for five days under shaking condition. After five days beads were separated using wire mesh. Separated beads were washed 2-3 times with 70% ethanol then finally with milli Q

water to remove the adhered bacterial cells. These beads were dried at 100 ^{O}C for 12 h to remove all the moisture content from the beads. Dried beads were used for the fresh desulfurization experiment.

7.2.6 Spent and regenerated adsorbent characterization

Spent and regenerated adsorbent were physicochemically characterized by BET and FT-IR analysis to confirm adsorption and desorption of sulfur compound from spent and regenerated adsorbent respectively.

7.3 Result

7.3.1 Complete (sequential) desulfurization test (using *Bacillus zhangzhouensis* strain R-2)

Sequential tests were performed at the same initial concentrations as those used in the (single-step) adsorption tests for DBT and TH. The tests were started initially using the prepared adsorbents. After approximately 1.5 - 2 h, when the concentration levels decreased to ~ 80% of the initial concentration levels in each test, the prepared bacterial cells were inoculated in the test setup. The tests were continued under the same conditions as used in the (single-step) bacterial tests. Approximately 99 ± 0.5% of DBT/TH removal was determined within the next 2 h in each test (Fig 7.1). The initial and final concentrations of DBT/TH are mentioned in Table 7.1. Mechanistically, post saturation or near saturation of the adsorption sites in the materials, the bacterial cells removed the remaining thiol compounds from the oil. The process was expeditious, attributed to the simultaneous desulfurization actions of both, the adsorbents as well as cells. A synergistic effect between the carbon substrate

in the adsorbents and the bacterial cells also played a role in completely desulfurizing the liquid fuels (Fig 7.2). Fig 7.3 and 7.4 represents the GC chromatogram of DBT and TH respectively at their initial and final stages of treatment. The SEM images of the spent adsorbents and growth of the bacterial cells during the tests confirmed the non-toxic effects of the adsorbents on the bacterial cells. The spent/treated oils (post sequential tests) were filtrated using a syringe filter and CFUs were calculated. Whereas the CFU value was calculated to be approximately 134×10^8 in the pre-filtered liquids, only 6 - 13 units were measured in the DBT post-filtration even after 24 h. No colony was observed in the filtered TH (Fig 7.5). Therefore, approximately all bacterial cells were separated from the treated oils, and the filtered oils were considered to be free from bacterial cells. Also, the metal (Ni) or carbon was not detected/measured in the treated liquids, indicating the prepared metal-carbon based-adsorbents to be stable without leaching. Thus, the treated oils were ready to be used without further treatment.

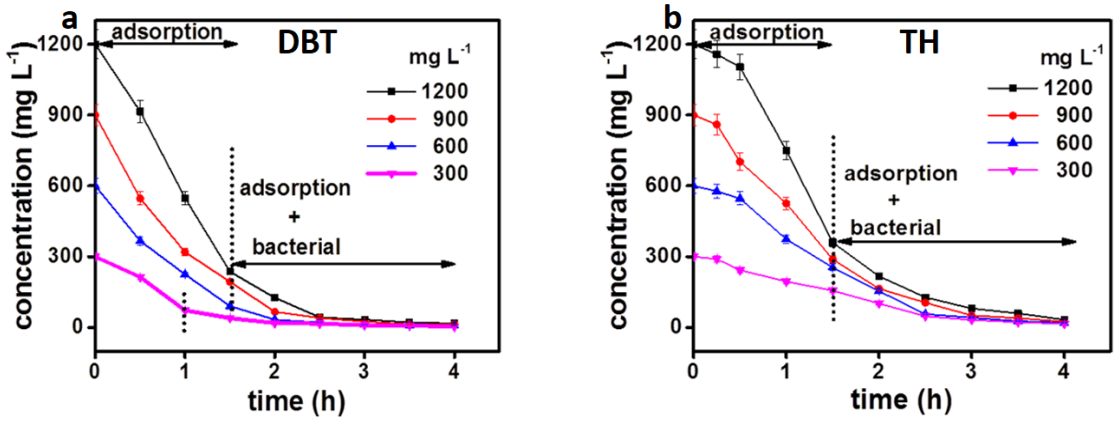

Fig 7.1: Complete desulfurization test of (a) DBT and (b) TH using carbon beads and *Bacillus zhangzhouensis* strain R-2

Table 7.1: Initial/final concentrations in sequential test (*Bacillus zhangzhouensis* strain R-2)

S. No.	Initial concentration of DBT/TH (mg L^{-1})	Final concentration of DBT (mg L^{-1})	Final concentration of TH (mg L^{-1})
1	1200	14.07	16.32
2	900	12.23	12.88
3	600	6.28	8.46
4	300	2.28	3.27

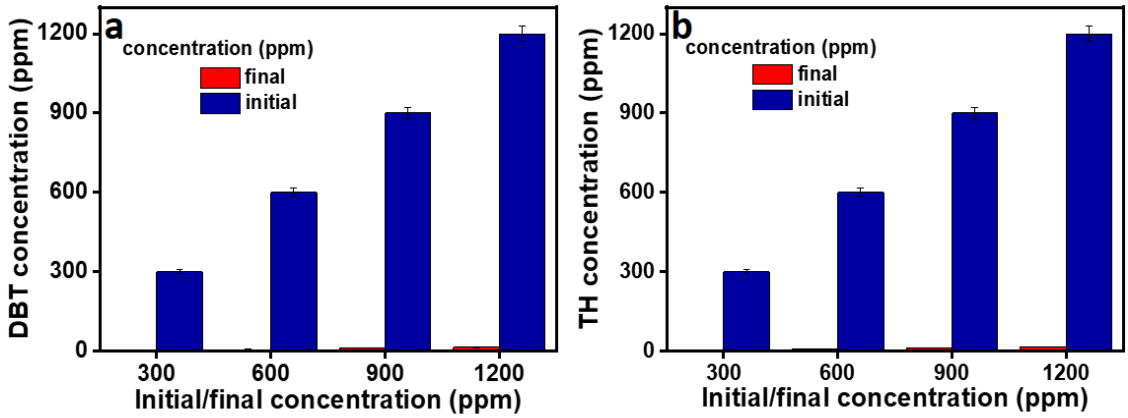

Fig 7.2: Summarized outcome graph of complete desulfurization test of (a) DBT and (b) TH using carbon beads and *Bacillus zhangzhouensis* strain R-2

7.3.2 Complete (sequential) desulfurization test (Using *Enterococcus faecium* strain R5)

Sequential tests were performed at four different initial concentrations of DBT and TH (Fig 7.6). Initially, tests were started using the prepared fresh adsorbent. After approximately 1.5 h the concentration decreased up to ~80 % of the initial concentration of DBT and TH. In further, the prepared bacterial cells were inoculated into the test solution in a previously used dose. The time of bacterial inoculation is not the exact time. It can be delayed or advanced, depends on the decrement in DBT/TH concentration, which should decrease up to ~80 % of the initial concentration through

adsorption test and the adsorption process stated slowing down in left (~20 %) concentration of DBT/TH in the test oil.

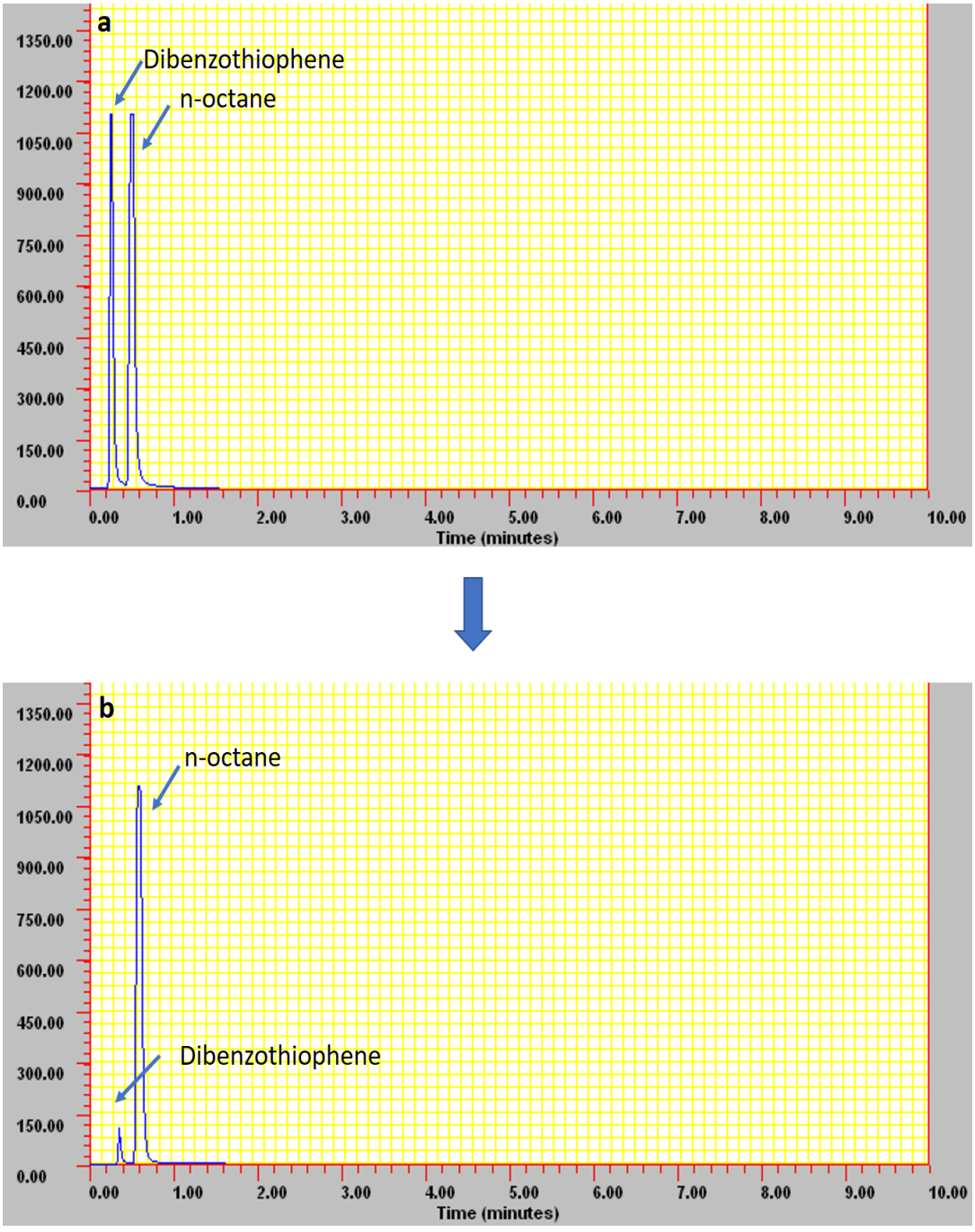

Fig 7.3: GC chromatogram of DBT (a) before desulfurization and (b) after desulfurization using *Bacillus zhangzhouensis* strain R-2

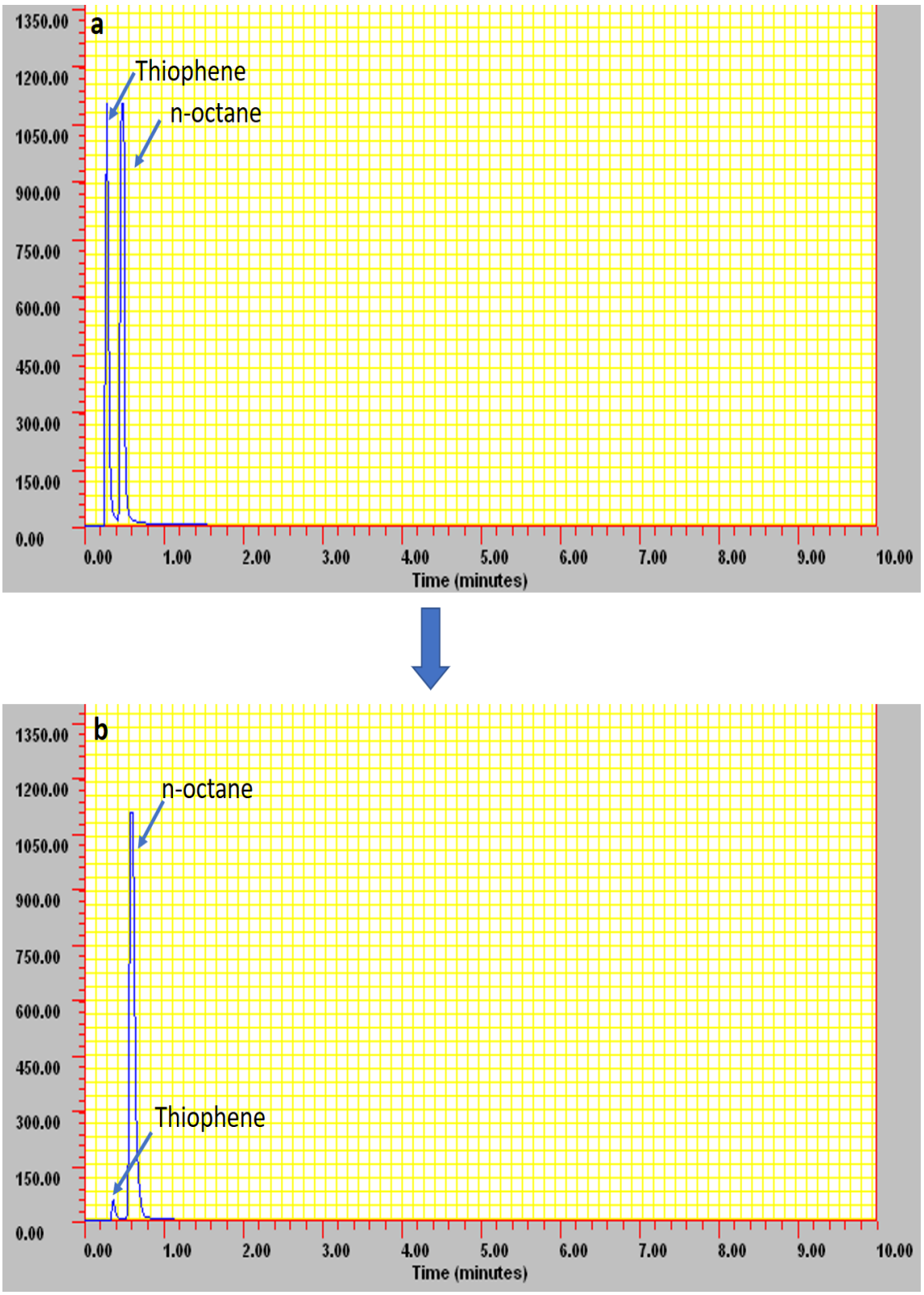

Fig 7.4: GC chromatogram of TH (a) before desulfurization and (b) after desulfurization using *Bacillus zhangzhouensis* strain R-2

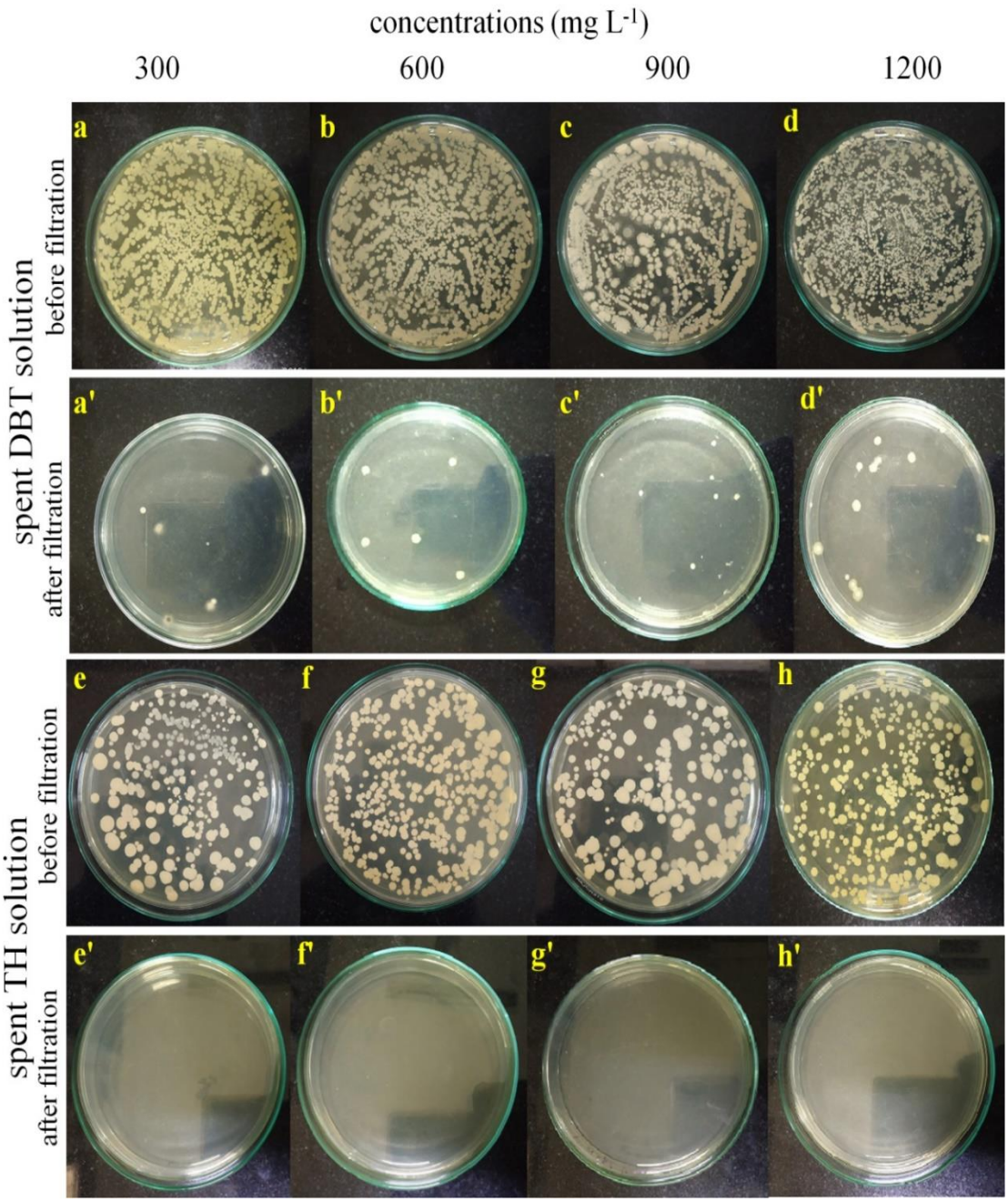

Fig 7.5: Bacterial colonies in spent solution (after desulfurization), before and after filtration at each concentration of (a-d') DBT and (e-h') TH

The tests were continued till next 2.5 h. Approximately 99 ± 5 % of DBT/TH concentration removed was determined after a complete 4 h sequential test (1.5 + 2.5 h) (Fig. 7.7). The initial and final concentrations of DBT and TH represented in table

7.2. Fig 7.8 and 7.9 represents the GC chromatogram of DBT and TH respectively at their initial and final stages of desulfurization.

After each sequential test the treated oil was filtered with 0.22 µm sized syringe filter to remove the bacterial cells used for the desulfurization test. The CFU count before filtration was determined approximately between 176 x 10^{14} and 193 x 10^{14} which decreased to 5 - 9 units of the cells post filtration of the spent oil samples even after 24 h of incubation (Fig. 7.10). Therefore, approximately all bacterial cells were removed from the spent oil, and the filtered oil was considered to be free from the bacterial cells. Also, the treated spent oil was detected/measured free from carbon or Ni, indicating the Ni-doped carbon-based adsorbents were stable without leaching of the metal in the oil, and therefore, the treated oil was ready to be used without any further treatment.

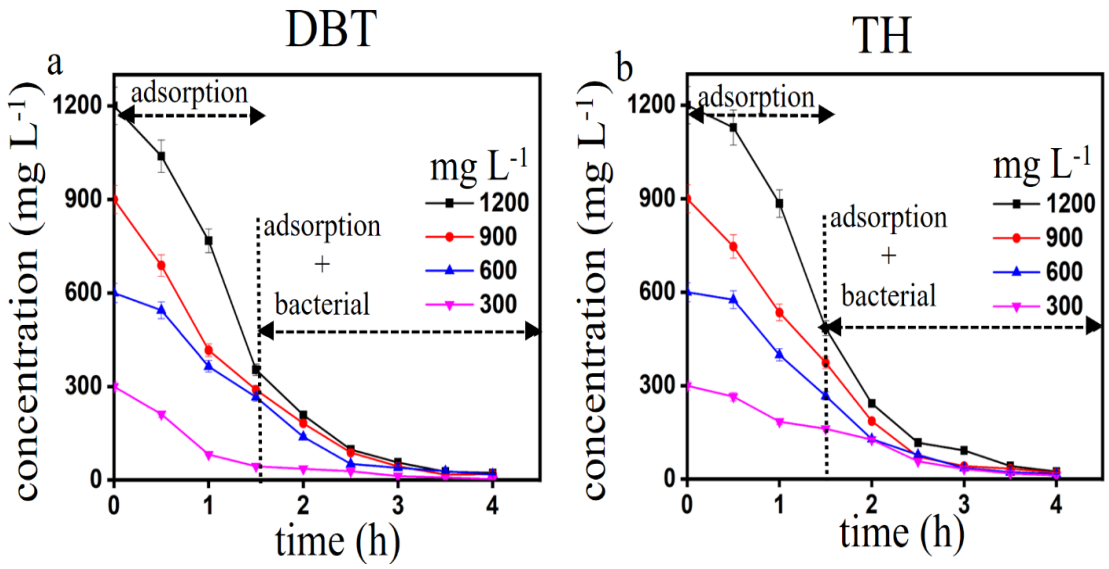

Fig 7.6: Complete desulfurization test of (a) DBT and (b) TH using carbon beads and *Enterococcus faecium* strain R5

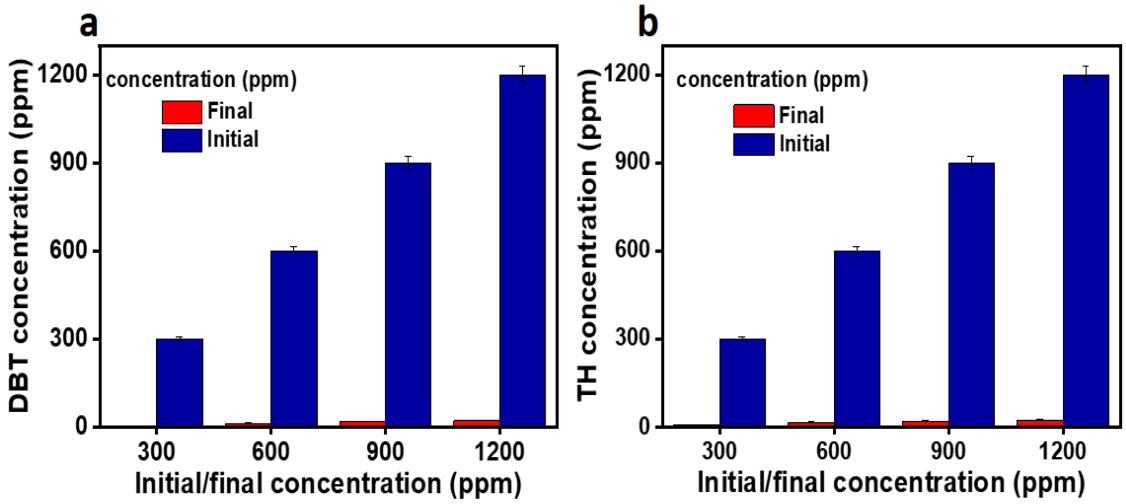

Fig 7.7: Summarized outcome graph of complete desulfurization test of (a) DBT and (b) TH using carbon beads and *Enterococcus faecium* strain R5

Table 7.2: Initial/final concentrations in sequential test (*Enterococcus faecium* strain R5)

S. No.	Initial concentration of DBT/TH (mg L^{-1})	Final concentration of DBT (mg L^{-1})	Final concentration of TH (mg L^{-1})
1	1200	22.8	24.26
2	900	19.04	20.69
3	600	13.1	16.65
4	300	3.29	8.52

7.3.3 FE-SEM analysis

The SEM images of the spent beads after the sequential test (adsorption + bacterial) are shown in Fig 7.11 (a-b'). The external surface of the spent beads, post-sequential test, appeared to be smooth, with coverage of the secretion of some bacterial exopolysaccharides (Fig. 7.11b). The materials were completely covered with the bacterial colonies.

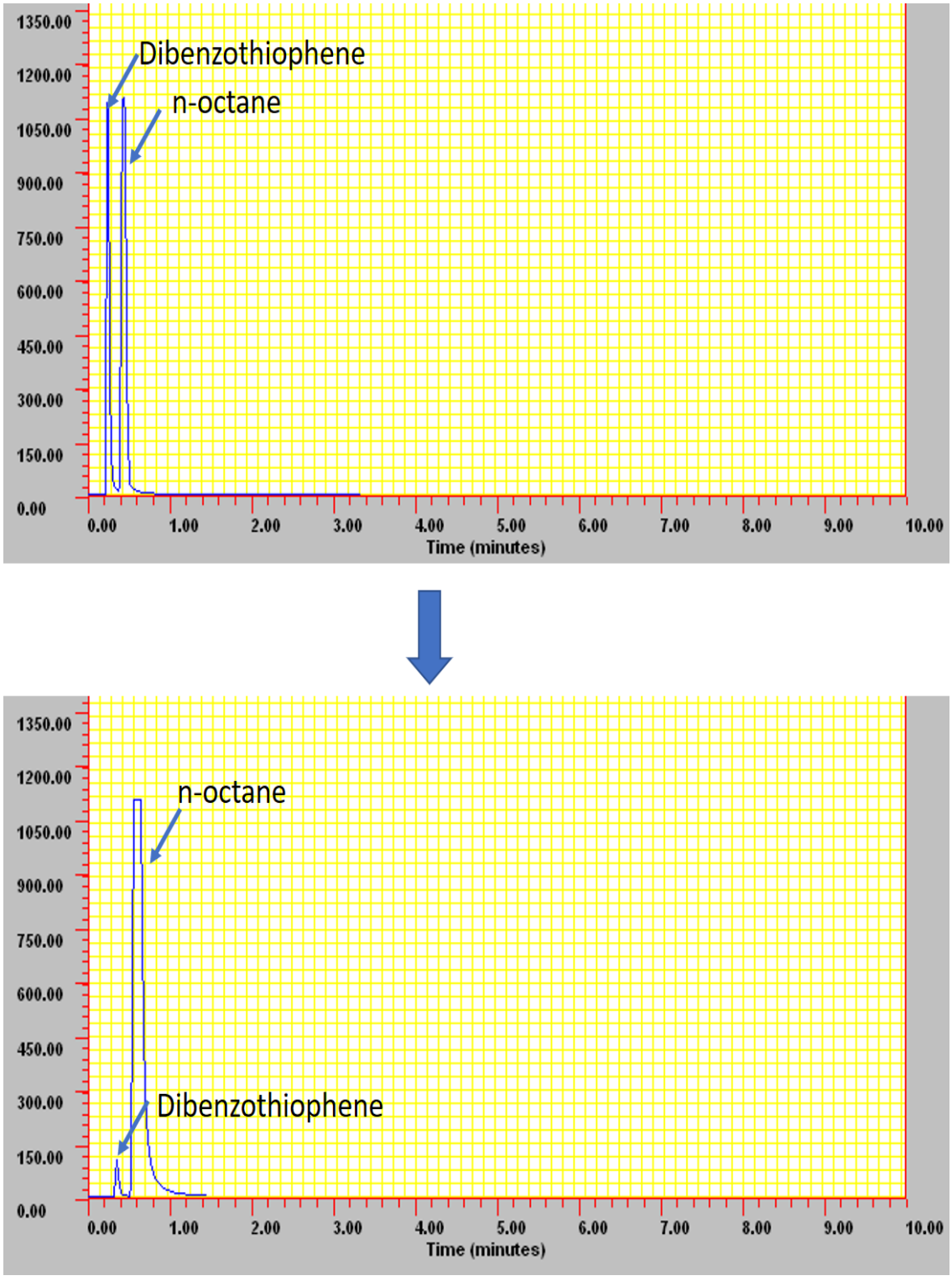

Fig 7.8: GC chromatogram of DBT (a) before desulfurization and (b) after desulfurization using *Enterococcus faecium* strain R5

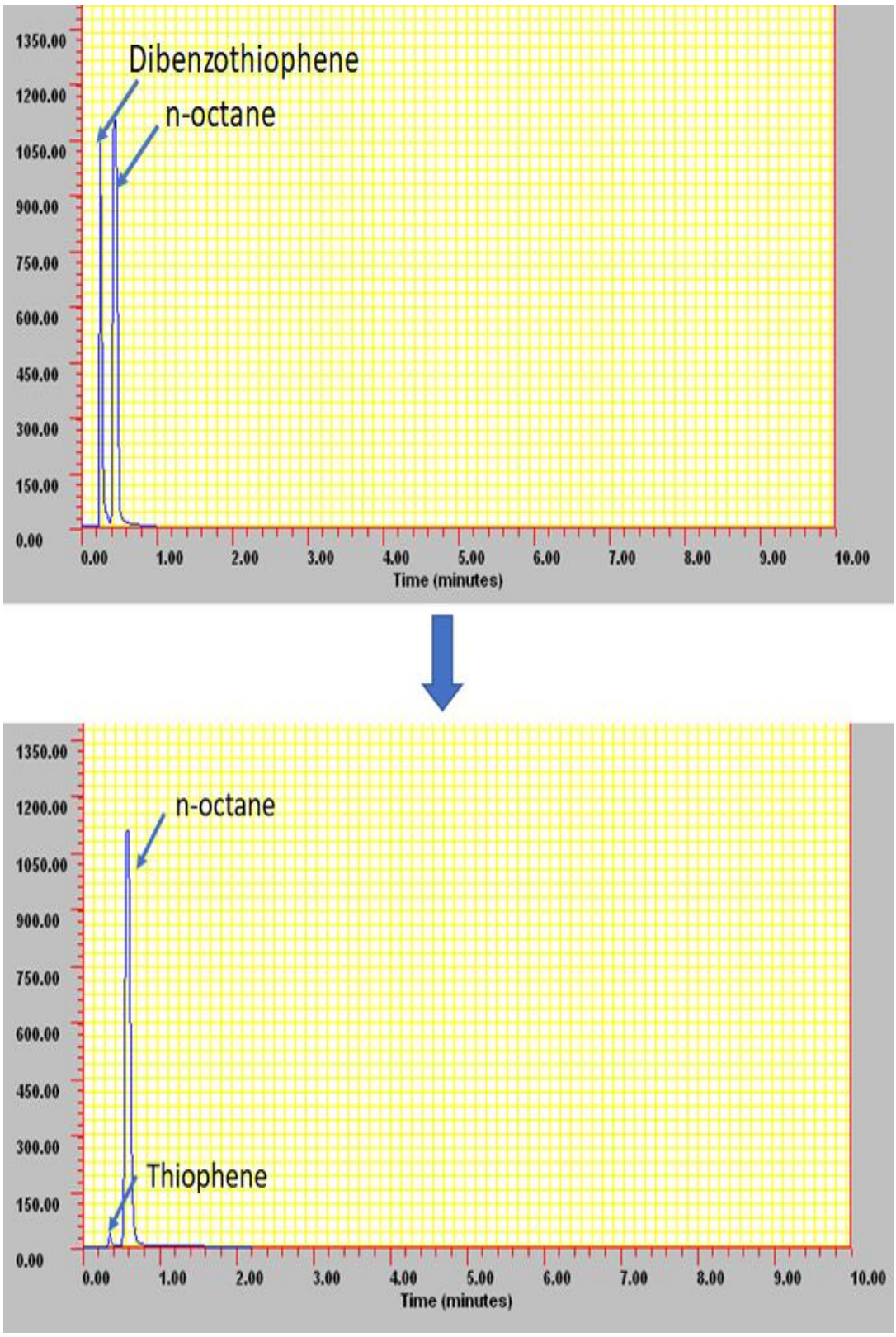

Fig 7.9: GC chromatogram of TH (a) before desulfurization and (b) after desulfurization using *Enterococcus faecium* strain R5

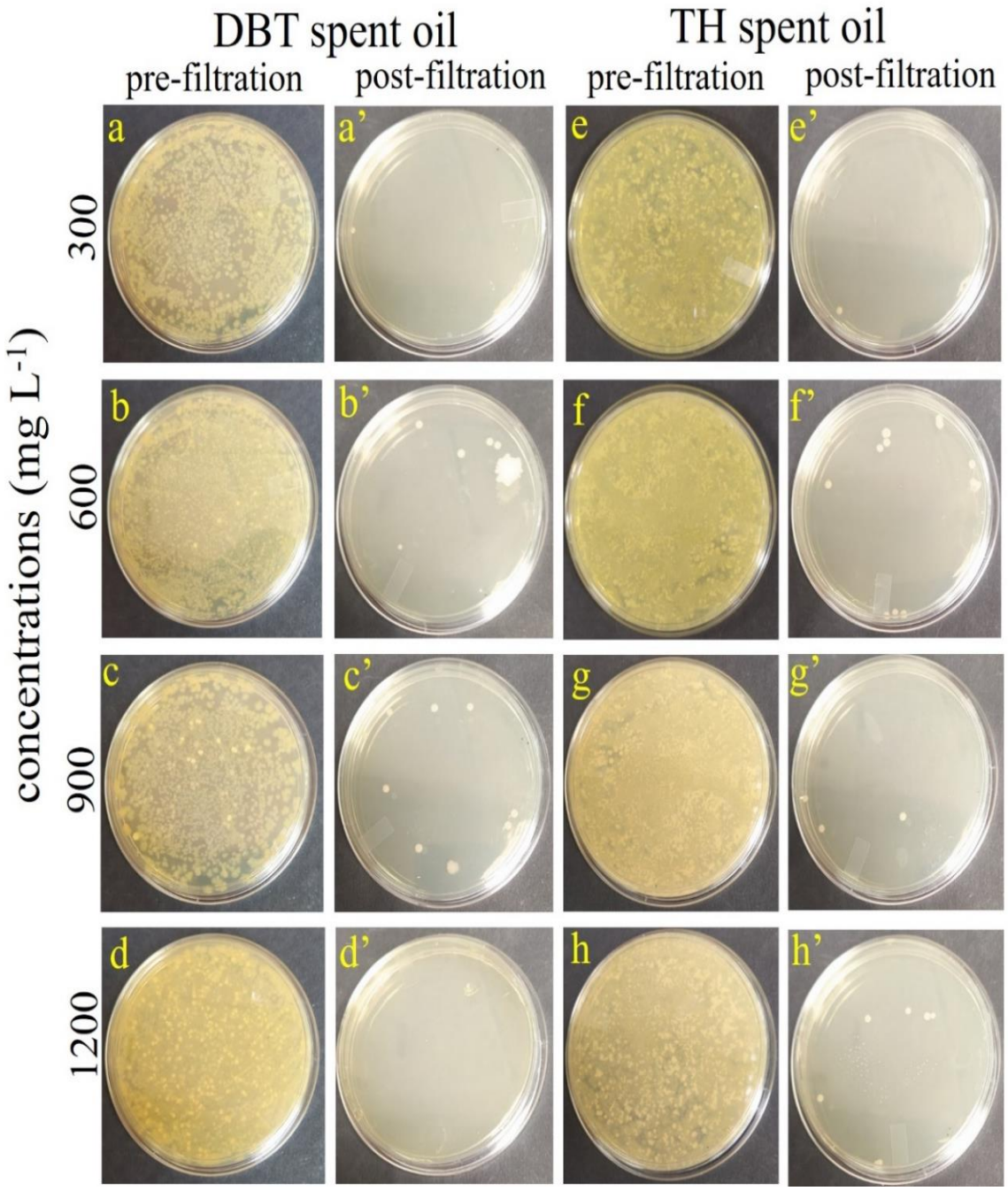

Fig 7.10: Bacterial colonies in spent solution (after desulfurization) before and after filtration at each concentration of (a-d') DBT and (e-h') TH

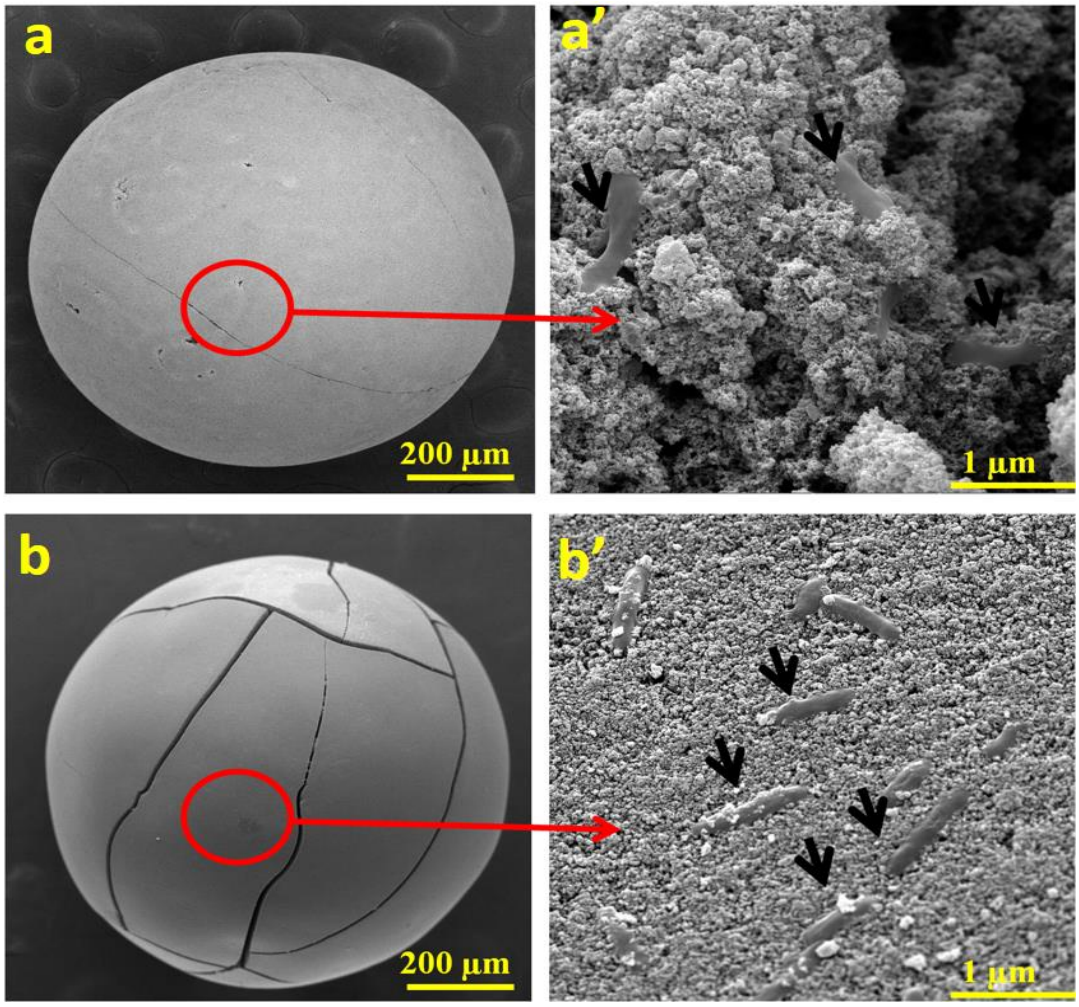

Fig 7.11: SEM images of spent (post desulfurization) adsorbent (a-a') Ni-ACB, and (b-b') Ni-CNF-ACB

7.3.4 Complete desulfurization test using regenerated adsorbent

Some other tests were performed using the same four concentrations (used in fresh sequential test) of DBT and TH. At initial stage of the test (during adsorption test) the regenerated adsorbents were used instead of the fresh adsorbent (Fig. 7.12). The test was performed using the same condition used in fresh sequential test. After 1.5 h of the test, DBT and TH was removed up to approximately concentration same as in fresh sequential test. The bacterial cells of *Bacillus zhangzhouensis* strain R2 or

Enterococcus faecium strain R5 were inoculated into the test solution. After next 2.5 h the concentration of DBT and TH in each test was determined approximately same as the fresh sequential experiment. The initial and final concentrations of DBT and TH were given in Table 7.3. A summarized comparative data of the fresh and regenerated sequential tests are also presented in Fig. 7.13. The determined data concluded that the adsorbent was successfully regenerated and shows the same desulfurization efficiency as compare to fresh adsorbent.

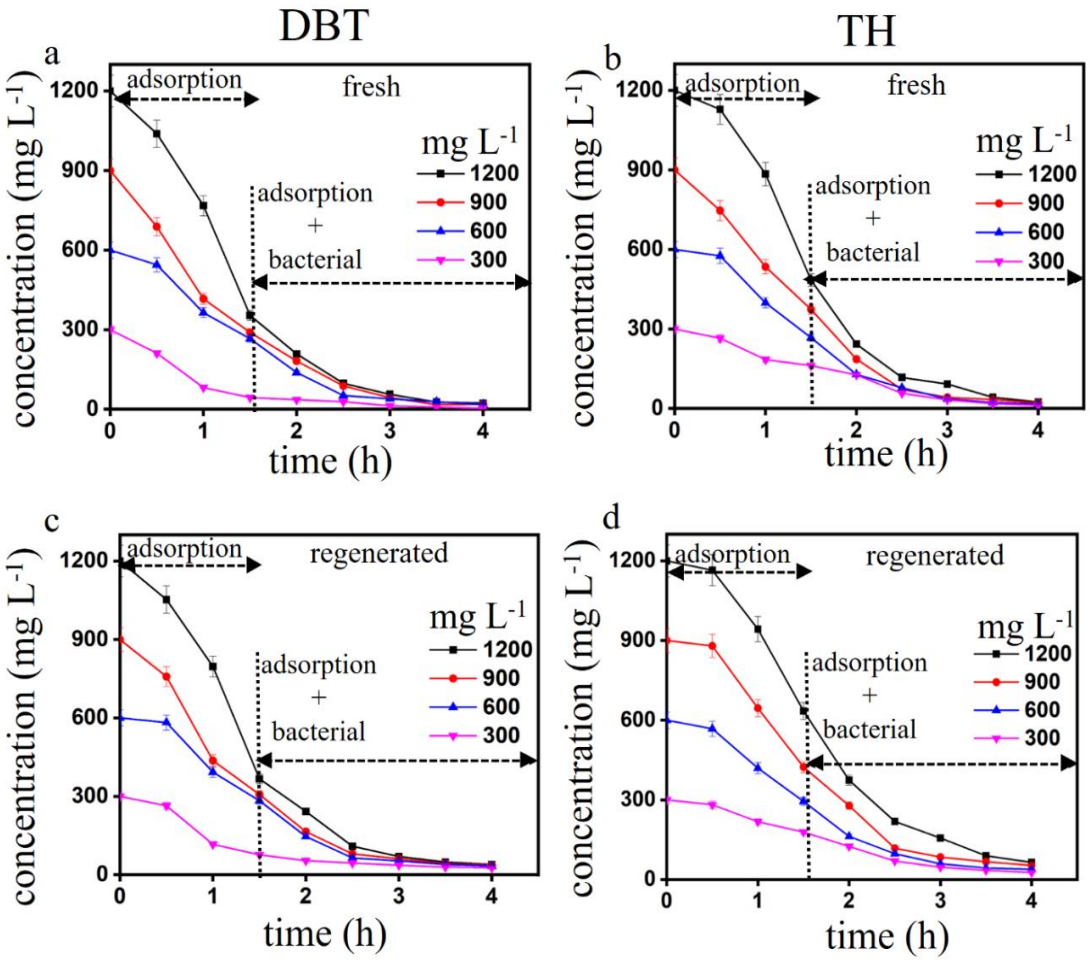

Fig. 7.12: Sequential desulfurization experiment using (a-b) fresh adsorbent and (c-d) regenerated adsorbent (conditions: 30 ^{O}C, 1 atm, adsorbent dose = 5g/L)

Table 7.3: Initial/final concentrations in sequential test using regenerated adsorbent

S. No.	Initial concentration of DBT/TH (mg L^{-1})	Final concentration of DBT (mg L^{-1})	Final concentration of TH (mg L^{-1})
1	1200	39.13	64.65
2	900	36.28	53.36
3	600	33.32	38.26
4	300	26.57	26.83

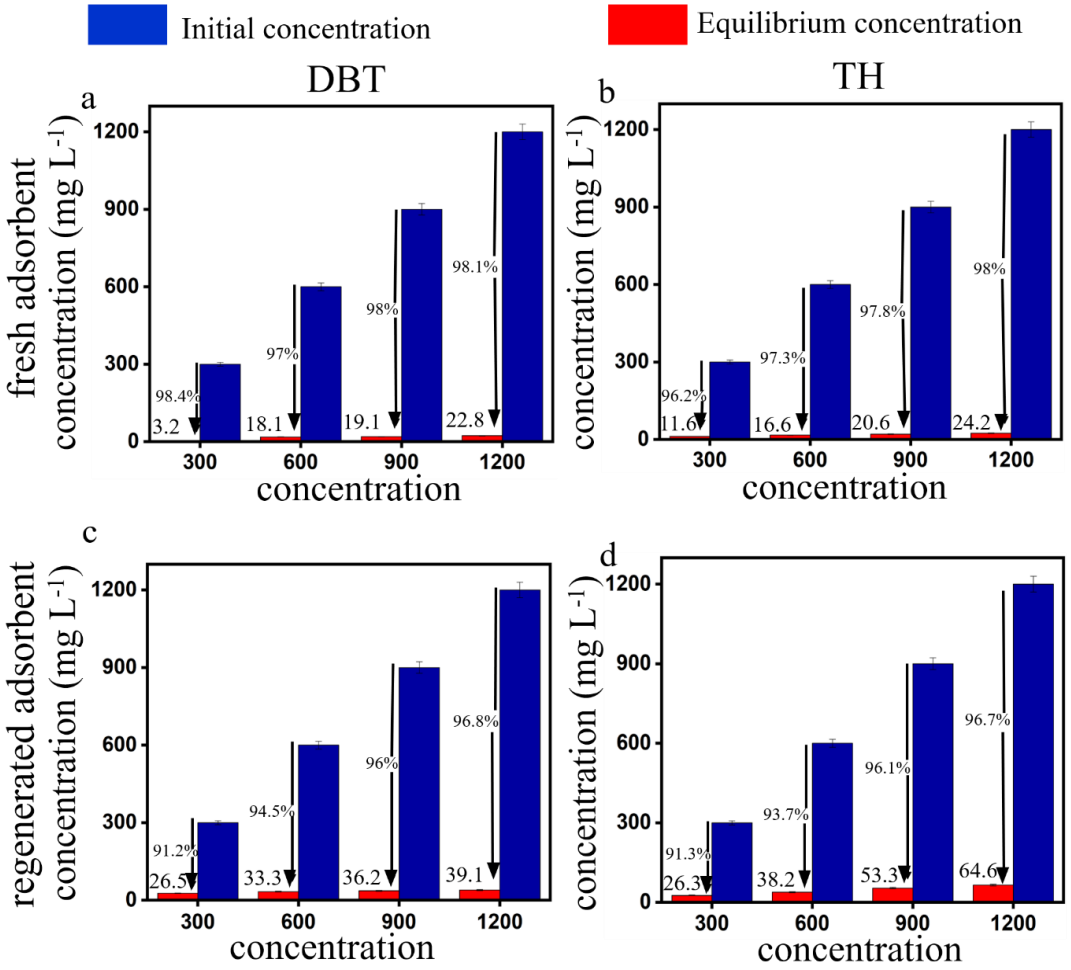

Fig. 7.13: Initial and final/equilibrium concentrations of sequential test in fresh adsorbent (a) DBT; (b) TH and with regenerated adsorbent; (c) DBT and; (d) TH after 4 h of the test

7.3.5 BET analysis

Fig. 7.14a and 7.14b shows the adsorption desorption isotherm of Ni-ACB and Ni-CNF-ACB respectively. The N_2 adsorption was rapidly increased up to 0.2 relative pressures then becomes constant in fresh and regenerated adsorbents (Ni-ACB and Ni-CNF-ACB), however in the N_2 adsorption was slightly increased in Ni-ACB and constant in Ni-CNF-ACB spent adsorbents, indicating the type 1 isotherm. The decrement of N_2 adsorption in spent adsorbent indicating the saturation of adsorption capacity of adsorbent, which was regained after the regeneration of the spent adsorbents (Fig 7.14 a-b). Fig. 7.14c shows the S_{BET} surface area of the adsorbent at different stages. The maximum surface area (1090.6 m^2/g) was determined in Ni-ACB (Fig. 7.14c, Table 7.4) due to formation of pore onto the surface of the material during the steam activation process. The surface area was decrease (140.4 m^2/g) in spent adsorbent confirming the adsorption of the sulfur compounds or blocking the mouths of pores of the material by sulfur compounds. After regeneration the surface area was again increased (881.1 m^2/g) up to approximately same as in fresh material, confirming the successful regeneration of the material. In Ni-CNF-ACB the surface area was decreased (284.1 m^2/g) due to growth of CNF onto the surface of the material which occupied some of the pores of the material. After desulfurization tests (in spent adsorbent) the surface was decreased (24.5 m^2/g) confirming the successful adsorption of TH on the adsorbent surface. The surface area of the regenerated adsorbent again increased (336.8 m^2/g) confirming the efficient regeneration of adsorbent. The adsorption and regeneration were also further confirmed by FT-IR analysis.

7.3.6 FT-IR analysis

The FT-IR analysis was performed for the fresh, spent and regenerated adsorbent (Fig. 7.14d). In fresh adsorbents (Ni-ACB and Ni-CNF-ACB) none of the vibrational peak was observed. It might be due to the loss of all the surface functional groups at the during the carbonization process, in which the material was converted to carbon. In spent adsorbent at ~782, 993, 1450, and 1750 cm^{-1} wavelengths represents the sulfone group, benzene ring of DBT and TH, organic sulfates and aromatic carbons respectively, confirming the successful adsorption of sulfur compounds on the surface of the material. After regeneration the all the vibrational peaks were disappear and the spectra was similar to the fresh material confirming efficient regeneration of the spent adsorbent. A vibration broad range after 3000 cm^{-1} wavenumber was observed in all the materials, attributed to moisture or –OH groups in the material.

Table 7.4: S_{BET} surface area of adsorbents

Adsorbent stages	Ni-ACB (Area in m^2/g)	Ni-CNF-ACB (Area in m^2/g)
Fresh	994.6	284.1
Spent	140.4	24.59
Regenerated	981.1	336.82

7.3.7 Multiple regeneration cycles

The spent adsorbent of the regenerated sequential test was again regenerated multiple times up to 3 cycles. The adsorbent was regenerated by the same regeneration procedure and checked for the fresh sequential desulfurization test up to 3 cycles. The multiple regeneration cycles were tested in a single concentration, 600 ppm

(approximately middle concentration of all four concentrations) of DBT and TH (Fig. 7.15a-b).

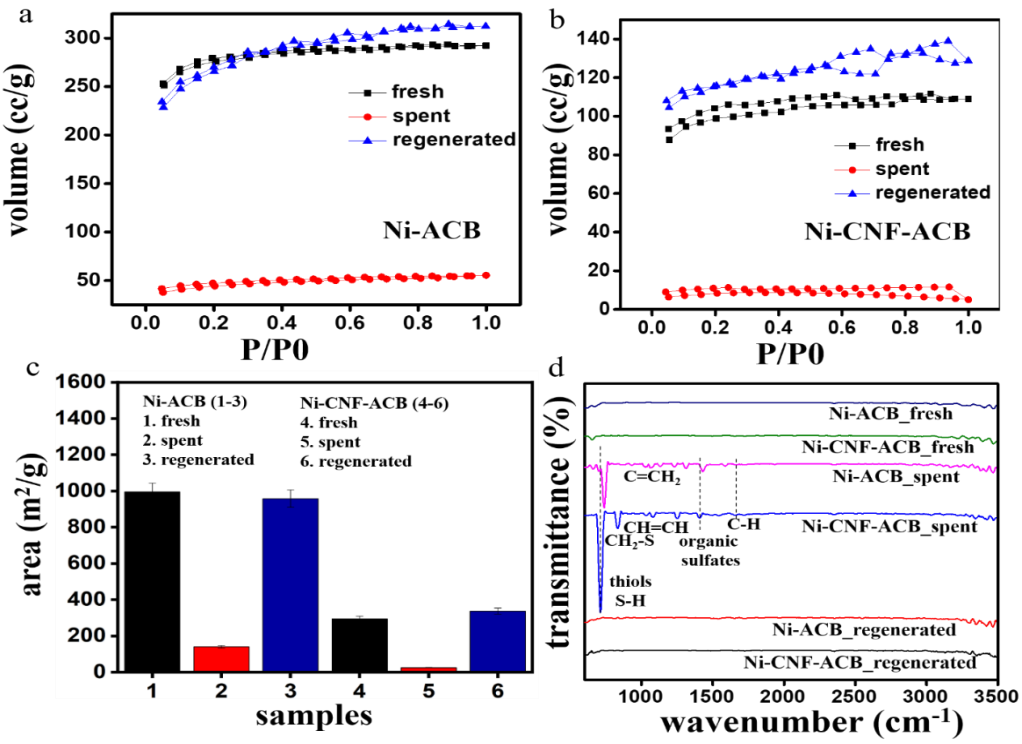

Fig. 7.14: BET isotherm of (a) Ni-ACB, and (b) Ni-CNF-ACB, (c) surface area of all the materials, and (d) FT-IR spectra of all the material before and after regeneration

The data showed that, after multiple regeneration of the adsorbent the desulfurization efficiency was approximately similar to the fresh desulfurization test. The final concentrations of DBT and TH after every cycle are mentioned in Table 7.5. It was observed that on regeneration of adsorbents the desulfurization efficiency was slightly decreased (especially in TH) which might be due to loss of some pore/nanofibers during the washing in regeneration process. A summarized data of multiple regeneration cycles of DBT and TH was presented in Fig. 7.15c-d. The data suggested that the regeneration process was determined more efficient in Ni-ACB in

comparative to Ni-CNF-ACB, which might be due to loss of some nanofibers during the washing of spent adsorbents.

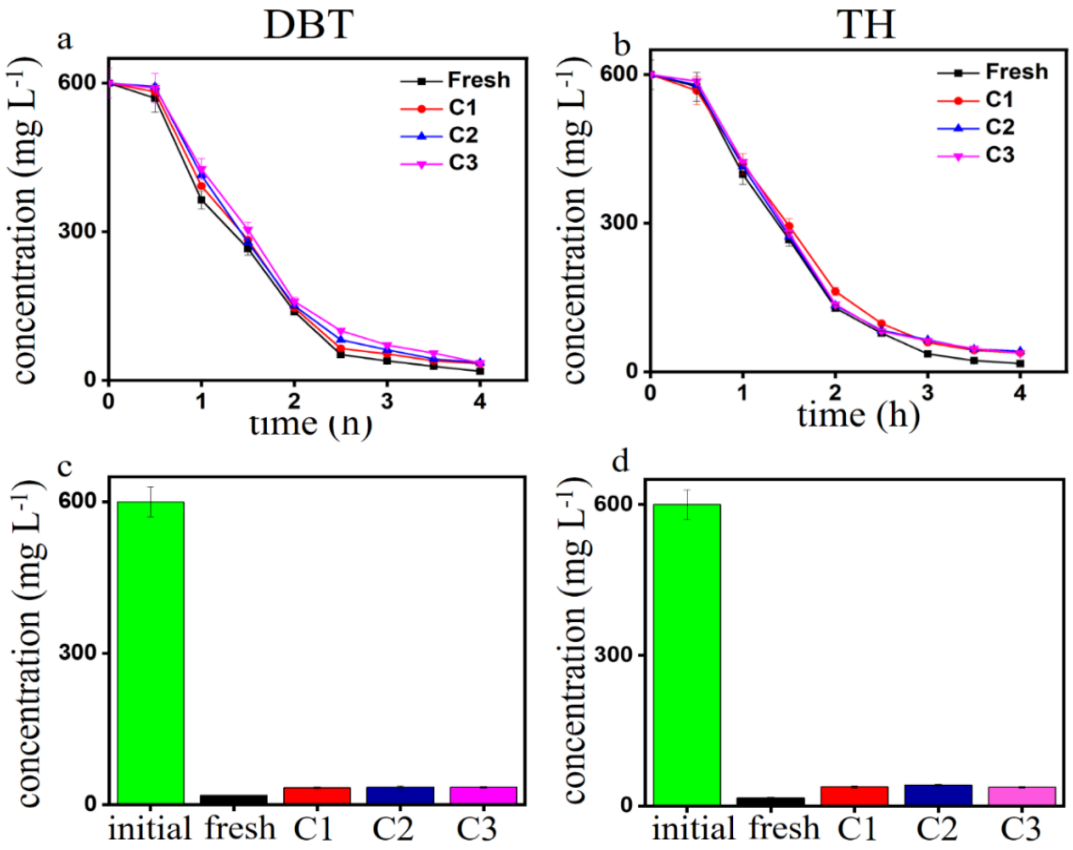

Fig. 7.15. Sequential desulfurization experiment using regenerated adsorbent for multiple regeneration cycles, (a-b) in respect of time, and (c-d) in respect of initial and final/equilibrium concentrations, at the initial concentration of 600 mg L^{-1}

Table 7.5: Final concentrations in regenerated sequential test in multiple cycles at the initial concentration of 600 mg L^{-1}

S. No.	No of cycles	Final concentration of DBT (mg L^{-1})	Final concentration of TH (mg L^{-1})
1	1	33.32	38.26
2	2	35.36	41.58
3	3	34.84	37.78

7.4 Discussion

Complete desulfurization test was performed using the prepared adsorbent (Ni-ACB and Ni-CNF-ACB) and the selected bacterial isolates (*Bacillus zhangzhouensis* strain R-2 or *Enterococcus faecium* strain R5) in a sequence. In the desulfurization test approximately 97 – 99% removal of DBT was achieved using *Bacillus zhangzhouensis* strain R2 and approximately 96 – 98% removal of DBT was achieved using *Enterococcus faecium* strain R5 strain at the initial concentration range between 300–1200 ppm. In case of TH approximately 96 – 98 % removal of TH was achieved in both the strains at the initial concentration range of 300 – 1200 ppm. Olajire et al. (2017) have performed the adsorption study of DBT using silver doped adsorbent and showed approximately 70% adsorption of DBT at the initial concentration of 600 ppm. Similarly, De et al. (2018) have performed the adsorption of TH using zinc-doped adsorbent and showed 73% adsorption of TH at the initial concentration of 250 ppm. In bacterial desulfurization studies, Caro et al. (2007) have performed the bacterial desulfurization of DBT using *Pseudomonas putida* and showed approximately 75% removal of DBT at the initial concentration of 200 ppm. In a study Martinez et al. (2016) have also desulfurize the DBT using induced/resting cells of *Pseudomonas putida* and achieved complete desulfurization in 90 min of the desulfurization. Alves et al. (2005) have performed the bacterial desulfurization of TH using *Gordonia alkanivorans* and showed approximately 90% removal of TH at the initial concentration of 1 mM. Therefore, separate studies of adsorption and bacterial desulfurization test were found inefficient for complete desulfurization of liquid fuels. Also, most of the adsorption studies requires certain temperature (i.e., not done at room temperature). Each separate methods have their own drawbacks such as in

adsorption study, the adsorbent becomes saturated after several hours. In bacterial desulfurization test, bacterial cells cannot tolerate the higher concentration of sulfur compounds. Therefore, integration of two different desulfurization approaches i.e., adsorption and bacterial desulfurization was found efficient than the other alone desulfurization and capable to remove approximately 99% of DBT and TH from a very high concentration i.e., 1200 ppm. After desulfurization test all the bacterial cells were separated using 0.22 µm syringe filter and the spent oil was declared free from sulfur and bacteria.

For the purpose of industrial application, regeneration of spent adsorbent is necessary in prospects of economic efficiency. Several methods including thermal, chemical, and combining thermal and chemical were already developed for regeneration of spent adsorbent. Danmaliki et al. (2017) have regenerated the spent adsorbent by heat treatment and showed 63 % adsorption efficiency was regained up to 3 cycles. Mahmoudian et al. (2020) have regenerated the spent adsorbent by successive washes through different chemical and showed 85% adsorption efficiency was regained up to 3 cycles. Yang et al. (2018) have used a combination of thermal and chemical method for regeneration. In this method primarily the spent adsorbent was heat treated and then washed by several chemicals and showed approximately 92 % adsorption efficiency was regained up to five cycles using this method. Apart from these methods, Li et al. (2009) are the only researcher, have performed the bioregeneration of oil spent adsorbent, using an environmentally isolated bacterium and showed 100 % adsorption efficiency was regained up to one cycle. The bioregeneration method was efficient and cost effective, however it was limited up to one cycle only. The other methods of regeneration also having some drawbacks in

different prospective such as, thermal regeneration method require high temperature which make the method energy and cost inefficient, also high temperature could disrupt the physical properties of adsorbent (Danmaliki et al. 2017), chemical method was not as much efficient than thermal method, also requires lot of chemicals and solvents which makes the method cost inefficient. In thermal–chemical method, it requires high temperature as well as different chemicals, therefore the process is cost and energy efficient. Apart from this all the methods are limited up to 3–5 cycles of regeneration. In addition, for regeneration it is necessary to characterize the fresh, spent and regenerated adsorbent to compare the physicochemical properties of adsorbent. In the reported studies most of the regeneration was performed without characterizing the adsorbent at different stages, which makes the study incomplete. Following Li et al. (2009), this study used the same regeneration method using *Enterococcus faecium* strain R5 for regeneration of spent adsorbent. In first, the spent adsorbent was characterized by SEM, BET and FT-IR analysis. The SEM images showing spherical structure of beads confirming no physical changes were happened during desulfurization test. However, some of the bacterial cells were adhered onto the surface of the spent adsorbent during desulfurization, can be clearly seen in SEM images. The FT-IR spectra showing the similar functional groups present in DBT and TH confirming the adsorption of DBT and TH onto the surface of the adsorbent. However, in fresh adsorbent all the functional groups were lost during the carbonization process. A huge reduction in BET surface area is confirming that the pores the spent adsorbent was occupied by the DBT/TH, which was also observed in the SEM images of spent adsorbent. After regeneration the regenerated adsorbent was again characterized using the similar characterization techniques used for spent

adsorbent. In regenerated adsorbent, BET area was regained up to the area of fresh adsorbent confirming the successful regeneration of spent adsorbent. Also, in FT-IR analysis no peaks were observed in regenerated adsorbent and the spectrum was similar to fresh adsorbent, confirming the desorption of DBT and TH from the spent adsorbent and successful regeneration of spent adsorbent without any change in physicochemical properties of the adsorbent. The regenerated adsorbent was used for fresh desulfurization test of DBT and TH. The results showing that approximately 95 – 97 % of desulfurization efficiency was regained up to three cycles in both type of adsorbent (Ni-ACB and Ni-CNF-ACB). The data indicating that regeneration by bacterial cells found efficient and also maintains the cost efficiency, therefore it could be used for industrial applications.

The novelty of this study includes the sequential integration of two different desulfurization techniques which are adsorption desulfurization and bacterial desulfurization for complete removal (~ 99%) of DBT and TH form liquid fuels. In addition, bacterial regeneration of spent adsorbent was found efficient in all the prospects and could be best alternative for spent adsorbent regeneration.

7.5 Conclusion

Integration of two different desulfurization techniques (i.e., adsorptive desulfurization and biodesulfurization) in a sequence was found efficient. The technique is capable in complete (~ 99%) removal of DBT and TH from the liquid fuels. In addition, bacterial regeneration was an efficient approach for regenerating

the spent adsorbent. Approximately 97% of adsorption capacity was regained up to three cycles of bacterial regeneration.

Chapter VIII

Summary

The purpose of this thesis was to study of desulfurization of DBT and TH using absorptive desulfurization as well as bacterial desulfurization. Additionally, a hybrid strategy was used for complete desulfurization of DBT and TH using both absorption and bacterial desulfurization.

For absorptive desulfurization, the beads were successfully synthesized through suspension polymerization reaction using phenol precursor and formaldehyde solvent. Further, the beads were carbonized, activated and metal nanoparticles present in the beads were then calcined and reduced to obtain nascent forms of the metal nanoparticles. In next, carbon nanofibers were grown onto the surface of the beads through chemical vapour deposition process. The adsorbent was characterized physicochemically using FE-SEM, BET, TPR, XRD, FT-IR, and TGA at different stages of its preparation. Resulting characterization data confirmed successful synthesis of the adsorbent. After synthesis of the adsorbent material, adsorptive desulfurization test was performed for DBT and TH using Ni-ACB and Ni-CNF-ACB adsorbent, respectively. Before the desulfurization test, calibration curves of DBT and TH was plotted using the gas-chromatography analysis. The value of regression coefficient was determined approximately 0.99 indicating the linear relationship between chromatographic area (signal) and concentration of DBT and TH.

Adsorptive desulfurization test was performed at 30 ^{O}C temperature for four hours in a specially designed reactor. The data showed that approximately 75 – 80 % DBT and TH were adsorbed onto the surface of adsorbent at four different initial concentrations, which were 300 ppm, 600 ppm, 900 ppm, and 1200 ppm. A separate desulfurization test was also performed in respect of time using the same concentrations to know the saturation time of adsorbent. After 2 to 2.5 hours, a

saturation was observed in the adsorbent's capacity for adsorption. This may be due to blockage of pores by adsorbed DBT or TH. The adsorbent Ni-ACB was found to be efficient for the adsorption of DBT, but Ni-CNF-ACB was more effective for the adsorption of TH due to TH's affinity toward the carbon material via π-π complexation.

To study the bacterial desulfurization of DBT and TH, *Bacillus zhangzhouensis* strain R-2 or *Enterococcus faecium* strain R5 was used. Desulfurization of DBT and TH was carried out using selected bacteria at 30 ^{O}C under shaking condition. At the initial concentration of 50-300 ppm, approximately 96-98 % of DBT and TH were removed using bacterial desulfurization.

The adsorptive desulfurization and bacterial desulfurization tests indicate that the adsorptive desulfurization test is effective for high concentrations of DBT and TH. For lower concentrations, bacterial desulfurization is an effective technique. The combination of these two techniques served as an effective method of removing thiol compounds (DBT/TH) from a very high concentration to a low level.

In addition, a complete sequential desulfurization was performed using the prepared adsorbent and the selected bacterial strain. The first time, 99% desulfurization of oils containing DBT and TH was achieved by sequentially applying adsorption at relatively high concentrations, followed by bacterial treatment at low concentrations. The metal nanoparticles-dispersed porous carbon-based beads (Ni-ACB and Ni-CNF-ACB) were used to reduce the sulfur concentration from a high level (300–1200 ppm) to a low level (50 – 300 ppm) via adsorption whereas *Bacillus zhangzhouensis* strain R-2 or *Enterococcus faecium* strain R5 was found to be effective in degrading the remaining S-compounds to ~ 3–15 ppm. Compared with

adsorption alone, the hybrid method demonstrated faster desulfurization or higher removal rates. Further, the selected bacteria survived and grew in numbers during the treatment, indicating that the prepared metal–carbon composite was non-toxic and conducive for the bacterial growth. The treated oils separated from the solid adsorbents, were found to be free from bacteria. Furthermore, both adsorptive and bacterial desulfurization were performed over the prepared Ni containing ACBs without necessity of removing the adsorbents from the liquid to be treated in the bacterial desulfurization step.

After the sequential adsorptive and bacterial desulfurization, the spent adsorbents were regenerated using *Enterococcus faecium* strain R5 and reused successfully up to three cycles of the hybrid method, with approximately 97% removal of DBT and 95% removal of TH in the last cycle. Therefore, bacterial regeneration showed an efficient removal of the S-containing compounds from the spent adsorbent surface at room temperature (~30 ^{O}C) without requiring any expensive chemicals.

The novelty of the present study includes integration of two different desulfurization techniques namely adsorptive desulfurization and bacterial desulfurization in sequence for complete (99%) desulfurization of liquid fuels. Additionally, the spent adsorbent was bacterially regenerated using *Enterococcus faecium* strain R5. The process was found efficient up to three regeneration cycles.

Chapter IX

Bibliography

- Abbad-Andaloussi S, Lagnel C, Warzywoda M, Monot F. Multi-criteria comparison of resting cell activities of bacterial strains selected for biodesulfurization of petroleum compounds. Enzyme Microb. Technol. 2003, 32:446-454.
- Abro R, Abdeltawab AA, Al-Deyab SS, Yu G, Qazi AB, Gao S, Chen X. A review of extractive desulfurization of fuel oils using ionic liquids. RSC Adv. 2014, 4:35302-35317.
- Ahmed I, Jhung SH. Adsorptive desulfurization and denitrogenation using metal-organic frameworks. J. Hazard. Mater. 2016, 301:259-276.
- Ai S, Sui H, Li H. Coordinative adsorption of thiophene with metallic silver/adsorbent cotton prepared via aqueous in situ reduction for desulfurization. Ind. Eng. Chem. Res. 2012, 51:12337-12343.
- Alhamed YA, Bamufleh HS. Sulfur removal from model diesel fuel using granular activated carbon from dates' stones activated by $ZnCl_2$. Fuel 2009, 88:87-94.
- Alves L, Marques S, Matos J, Tenreiro R, Gírio FM. Dibenzothiophene desulfurization by *Gordonia alkanivorans* strain 1B using recycled paper sludge hydrolyzate. Chemosphere 2008, 70:967-973.
- Alves L, Melo M, Mendonça D, Simoes F, Matos J, Tenreiro R, Girio FM. Sequencing, cloning and expression of the dsz genes required for dibenzothiophene sulfone desulfurization from *Gordonia alkanivorans* strain 1B. Enzyme Microb. Technol. 2007, 40:1598-1603.
- Alves L, Salgueiro R, Rodrigues C, Mesquita E, Matos J, Girio FM. Desulfurization of dibenzothiophene, benzothiophene, and other thiophene analogs by a newly isolated

bacterium, *Gordonia alkanivorans* strain 1B. Appl. Biochem. Biotechnol. 2005, 120:199-208.

- Andari MK, Bchbehani H, Stanislaus A. Sulfur compound type distribution in Naphtha and gas oil fractions of Kuwaiti crude. Fuel Sci. Technol. Int. 1996, 14:939-961.
- Anisimov AV, Fedorova EV, Lesnugin AZ, Senyavin VM, Aslanov LA, Rybakov VB, Tarakanova AV. Vanadium peroxocomplexes as oxidation catalysts of sulfur organic compounds by hydrogen peroxide in bi-phase systems. Catal. Today 2003, 78:319–325.
- Arora PK. Bacilli-mediated degradation of xenobiotic compounds and heavy metals. Front. Bioeng. Biotechnol. 2020:1100.
- Aslam S, Subhan F, Yan Z, Etim UJ, Zeng J. Dispersion of nickel nanoparticles in the cages of metal-organic framework: an efficient sorbent for adsorptive removal of thiophene. Chem. Eng. J. 2017, 315:469-480.
- Aslam S, Subhan F, Yan Z, Peng P, Qiao K, Xing W, Bai P, Ullah R, Etim UJ, Zeng J, Ikram M. Facile fabrication of Ni-based KIT-6 for adsorptive desulfurization. Chem. Eng. J. 2016, 302:239-248.
- Awadh M, Mahmoud H, Abed RM, El Nayal AM, Abotalib N, Ismail W. Diesel-born organosulfur compounds stimulate community re-structuring in a diesel-biodesulfurizing consortium. Biotechnol. Rep. 2020, 28:e00572.
- Babich IV, Moulijn JA. Science and technology of novel processes for deep desulfurization of oil refinery streams: a review. Fuel 2003, 82:607-631.

- Badoga S, Misra P, Kamath G, Zheng Y, Dalai AK. Hydrotreatment Followed by oxidative desulfurization and denitrogenation to attain low sulphur and nitrogen bitumen derived gas oils. Catalysts 2018, 8:645.
- Baeza P, Aguila G, Gracia F, Araya P. Desulfurization by adsorption with copper supported on zirconia. Catal. Commun. 2008, 9:751-755.
- Bahuguna A, Lily MK, Munjal A, Singh RN, Dangwal K. Desulfurization of dibenzothiophene (DBT) by a novel strain *Lysinibacillus sphaericus* DMT-7 isolated from diesel contaminated soil. J. Environ. Sci. 2011, 23:975-982.
- Bairagi PK, Verma N. Electrochemically deposited dendritic poly (methyl orange) nanofilm on metal-carbon-polymer nanocomposite: a novel non-enzymatic electrochemical biosensor for cholesterol. J. Electroanal. Chem. 2018, 814:134-143.
- Bairagi PK, Verma N. Electro-polymerized polyacrylamide nano film grown on a Ni-reduced graphene oxide-polymer composite: a highly selective non-enzymatic electrochemical recognition element for glucose. Sens. Actuators B Chem. 2019, 289:216-225.
- Bakhtiari G, Ghassabzadeh H, Royaee SJ, Abdouss M, Bazmi M. Process design for gas condensate desulfurization and synthesis of nano-13X zeolite adsorbent: equilibrium and dynamic studies. Pet. Sci. 2019, 16:417-427.
- Bandosz TJ. Activated carbon surfaces in environmental remediation. Amsterdam; London: Elsevier, 2006.
- Betiha MA, Rabie AM, Ahmed HS, Abdelrahman AA, El-Shahat MF. Oxidative desulfurization using graphene and its composites for fuel containing thiophene and its derivatives: An update review. Egypt. J. Pet. 2018, 27:715-730.

- Bhatia S, Sharma DK. Biodesulfurization of dibenzothiophene, its alkylated derivatives and crude oil by a newly isolated strain *Pantoea agglomerans* D23W3. Biochem. Eng. J. 2010, 50:104-109.
- Borole AP, Kaufman EN, Grossman MJ, Minak-Bernero V, Bare R, Lee MK. Comparison of the emulsion characteristics of *Rhodococcus erythropolis* and *Ecsherichia coli* SOXC-5 Cells expressing biodesulfurization genes. Biotechnol. Prog. 2002, 18:88-93.
- Boshagh F, Mokhtarani B, Mortaheb HR. Effect of electrokinetics on biodesulfurization of the model oil by *Rhodococcus erythropolis* PTCC1767 and *Bacillus subtilis* DSMZ 3256. J. Hazard. Mater. 2014, 280:781-787.
- Brosius J, Palmer ML, Kennedy PJ, Noller HF. Complete nucleotide sequence of a 16S ribosomal RNA gene from *Escherichia coli*. Proc. Natl. Acad. Sci. 1978,:4801-4805.
- Burakov AE, Galunin EV, Burakova IV, Kucherova AE, Agarwal S, Tkachev AG, Gupta VK. Adsorption of heavy metals on conventional and nanostructured materials for wastewater treatment purposes: A review. Ecotoxicol. Environ. Saf. 2018, 148:702-712.
- Buzanello EB, Rezende RP, Sousa FMO, Marques EDLS, Loguercio LL. A novel *Bacillus pumilus*-related strain from tropical landfarm soil is capable of rapid dibenzothiophene degradation and biodesulfurization. BMC Microbiol. 2014, 14:257.
- Calzada J, Heras S, Alcon A, Santos VE, Garcia-Ochoa F. Biodesulfurization of dibenzothiophene (DBT) using *Pseudomonas putida* CECT 5279: a biocatalyst formulation comparison. Energy Fuels 2009, 23:5491-5495.

- Caro A, Boltes K, Letón P, García-Calvo E. Dibenzothiophene biodesulfurization in resting cell conditions by aerobic bacteria. Biochem. Eng. J. 2007, 35:191-197.
- Caro A, Letón P, García-Calvo E, Setti L. Enhancement of dibenzothiophene biodesulfurization using β-cyclodextrins in oil-to-water media. Fuel 2007, 86:2632-2636.
- Castorena G, Suárez C, Valdez I, Amador G, Fernández L, Le Borgne S. Sulfur-selective desulfurization of dibenzothiophene and diesel oil by newly isolated *Rhodococcus* sp. strains. FEMS Microbiol. Lett. 2002, 215:157-161.
- Chao Y, Ju H, Luo J, Jin Y, Wang C, Xiong J, Wu P, Ji H, Zhu W. Synthesis of porous carbon via a waste tire leavening strategy for adsorptive desulfurization. RSC Adv. 2019, 9:30575-30580.
- Chauhan AK, Ahmad A, Singh SP, Kumar A. Biodesulfurization of benzonaphthothiophene by an isolated *Gordonia* sp. IITR100. Int. Biodeter. Biodegradation 2015, 104:105-111.
- Chen H, Cai YB, Zhang WJ, Li W. Methoxylation pathway in biodesulfurization of model organosulfur compounds with *Mycobacterium* sp. Bioresour. Technol. 2009, 100:2085-2097.
- Chen H, Zhang WJ, Chen JM, Cai YB, Li W. Desulfurization of various organic sulfur compounds and the mixture of DBT+ 4, 6-DMDBT by *Mycobacterium* sp. ZD-19. Bioresour. Technol. 2008, 99:3630-3634.
- Chen S, Zang M, Li L, Chen J, Liu Q, Feng X, Sun S, Zang C, Zhao C. Efficient biodesulfurization of diesel oil by *Gordonia* sp. SC-10 with highly hydrophobic cell surfaces. Biochem. Eng. J. 2021, 15:108094.

- Chen S, Zhao C, Liu Q, Zhang X, Sun S, Zang M. Biodesulfurization of diesel oil in oil–water two phase reaction system by Gordonia sp. SC-10. Biotechnol. lett. 2019, 41:547-554.
- Colvile RN, Hutchinson EJ, Mindell JS, Warren RF. The transport sector as a source of air pollution. Atmos. Environ. 2001, 35:1537-1565.
- Cowan ST, Steel KJ. Manual for the identification of medical bacteria.1965
- Crandall BS, Zhang J, Stavila V, Allendorf MD, Li Z. Desulfurization of liquid hydrocarbon fuels with microporous and mesoporous materials: metal-organic frameworks, zeolites, and mesoporous silicas. Ind. Eng. Chem. Res. 2019, 58:19322-19352.
- Crawford DL, Gupta RK. Oxidation of dibenzothiophene by *Cunninghamella elegans*. Curr. Microbiol. 1990, 21:229-231.
- Cychosz KA, Wong-Foy AG, Matzger AJ. Liquid phase adsorption by microporous coordination polymers: removal of organosulfur compounds. J. Am. Chem. Soc. 2008, 130:6938-6939.
- Dahlberg MD, Rohrer RL, Fauth DJ, Sprecher R, Olson GJ. Biodesulfurization of dibenzothiophene sulfone by *Arthrobacter* sp. and studies with oxidized Illinois No. 6 coal. Fuel 1993, 72:1645-1649.
- Danmaliki GI, Saleh TA,Shamsuddeen AA. Response surface methodology optimization of adsorptive desulfurization on nickel/activated carbon. Chem. Eng. J. 2017, 313:993-1003.
- Danmaliki GI, Saleh TA. Effects of bimetallic Ce/Fe nanoparticles on the desulfurization of thiophenes using activated carbon. Chem. Eng. J. 2017, 307:914-927.

- Dasgupta S, Divekar S, Arya A, Gupta P, Chauhan R, Bhadauria S, Hanif A, Garg MO Nanoti A. A vapor phase adsorptive desulfurization process for producing ultra lowsulphur diesel using NiY zeolite as a regenerable adsorbent. RSC Adv. 2015, 5:56060-56066.
- Dasgupta S, Gupta P, Nanoti A, Goswami AN, Garg MO, Tangstad E, Vistad ØB, Karlsson A, Stöcker M. Adsorptive desulfurization of diesel by regenerable nickel based adsorbents. Fuel 2013, 108:184-189.
- Davoodi-Dehaghani F, Vosoughi M, Ziaee AA. Biodesulfurization of dibenzothiophene by a newly isolated *Rhodococcus erythropolis* strain. Bioresour. Technol. 2010, 101:1102-1105.
- De lima FM, de Andrade Borges T, Braga RM, de AraújoMelo DM, Martinelli AE. Sulfur removal from model fuel by Zn impregnated retorted shale and with assistance of design of experiments. Environ. Sci. Pollut. Res. 2018, 25:13760-13774.
- Decoste JB, Peterson GW. Metal–organic frameworks for air purification of toxic chemicals. Chem. Rev. 2014, 114:5695-5727.
- Del olmo CH, Alcon A, Santos VE, Garcia-Ochoa F. Modeling the production of a *Rhodococcus erythropolis* IGTS8 biocatalyst for DBT biodesulfurization: influence of media composition. Enzyme. Microb. Technol. 2005, 37:157-166.
- Del olmo CH, Santos VE, Alcon A, Garcia-Ochoa F. Production of a *Rhodococcus erythropolis* IGTS8 biocatalyst for DBT biodesulfurization: influence of operational conditions. Biochem. Eng. J. 2005, 22:229-237.
- Demharter W, Hensel R. *Bacillus thermocloaceae* sp. nov., a new thermophilic species from sewage sludge. Syst. Appl. Microbiol. 1989, 11:272-276.

- Denis-Larose C, Labbe D, Bergeron H, Jones AM, Greer CW, Al-Hawari J, Grossman MJ, Sankey BM, Lau PC. Conservation of plasmid-encoded dibenzothiophene desulfurization genes in several *Rhodococci*. Appl. Environ. Microbiol. 1997, 63:2915-2919.
- Denome SA, Oldfield C, Nash LJ, Young KD. Characterization of the desulfurization genes from *Rhodococcus* sp. strain IGTS8. J. Bacteriol. 1994, 176:6707-6716.
- Dias da Silva P, Samaniego Andrade SK, Zygourakis K, Wong MS. Adsorptive desulfurization of liquid fuels at elevated temperatures using metal exchanged zeolite Y. Ind. Eng. Chem. Res. 2019, 58:19623-19632.
- Dizaji AK, Mortaheb HR, Mokhtarani B. Extractive-catalytic oxidative desulfurization with graphene oxide-based heteropolyacid catalysts: investigation of affective parameters and kinetic modelling. Catal. Lett. 2019, 149:259-271.
- Duan F, Chen C, Wang G, Yang Y, Liu X, Qin Y. Efficient adsorptive removal of dibenzothiophene by graphene oxide-based surface molecularly imprinted polymer. RSC Adv. 2014, 4:1469-1475.
- Estephane G, Lancelot C, Blanchard P, Toufaily J, Hamiye T, Lamonier C. Sulfur compounds reactivity in the ODS of model and real feeds on W–SBA based catalysts. RSC Adv. 2018, 8:13714–13721.
- Etemadi O, Yen TF. Surface characterization of adsorbents in ultrasound-assisted oxidative desulfurization process of fossil fuels. J. Colloid Interface Sci. 2007, 313:18-25.

- Fahim MA, Al-Sahhaf TA, Elkilani A. Fundamentals of petroleum refining. Elsevier 2009.
- Farshi A, Shiralizadeh P. Sulfur reduction of heavy fuel oil by oxidative desulfurization (ODS) method. Pet. Coal 2015, 57:295-302.
- Feng S, Yang H, Zhan X, Wang W. Enhancement of dibenzothiophene biodesulfurization by weakening the feedback inhibition effects based on a systematic understanding of the biodesulfurization mechanism by *Gordonia* sp. through the potential "4S" pathway. RSC Adv. 2016, 6:82872-82881.
- Fuel regulations: India: Diesel Fuel: Table 1: Diesel fuel quality in India (Last accessed in May 2022) https://dieselnet.com/standards/in/fuel.php
- Furuya T, Kirimura K, Kino K, Usami S. Thermophilic biodesulfurization of dibenzothiophene and its derivatives by *Mycobacterium phlei* WU-F1. FEMS Microbiol. Lett. 2001, 204:129-133.
- Ganiyu SA, Ajumobi OO, Lateef SA, Sulaiman KO, Bakare IA, Qamaruddin M, Alhooshani K. Boron-doped activated carbon as efficient and selective adsorbent for ultra-deep desulfurization of 4, 6-dimethyldibenzothiophene. Chem. Eng. J. 2017, 321:651-661.
- George JK, Yadav A, Verma N. Electrochemical hydrogen storage behaviour of Ni-Ceria impregnated carbon micro-nanofibers. Int. J. Hydrog. Energy 2021, 46:2491-2502.
- Gomez E, Alcon A, Escobar S, Santos VE, Garcia-Ochoa F. Effect of fluiddynamic conditions on growth rate and biodesulfurization capacity of *Rhodococcus erythropolis* IGTS8. Biochem. Eng. J. 2015, 99:138-146.

- González-Cortés JJ, Torres-Herrera S, Almenglo F, Ramírez M, Cantero D. Anoxic biogas biodesulfurization promoting elemental sulfur production in a Continuous Stirred Tank Bioreactor. J. Hazard. Mater. 2021, 401:123785.
- Gray KA, Mrachko GT, Squires CH. Biodesulfurization of fossil fuels. Curr. Opin. Microbiol. 2003, 6:229-235.
- Gray KA, Pogrebinsky OS, Mrachko GT, Xi L, Monticello DJ, Squires CH. Molecular mechanisms of biocatalytic desulfurization of fossil fuels. Nat. Biotechnol. 1996, 14:1705-1709.
- Grossman MJ, Siskin M, Ferrughelli DT, Lee MK, Senius JD, inventors; ExxonMobil Research, Engineering Co, assignee. Method for the removal of organic sulfur from carbonaceous materials. 1999, United States patent No 5,910:440.
- García-Solache M, Rice LB. The Enterococcus: a Model of Adaptability to Its Environment. Clin. Microbiol. Rev. 2019, 32:e00058-18.
- Guobin S, Huaiying Z, Jianmin X, Guo C, Wangliang L, Huizhou L. Biodesulfurization of hydrodesulfurized diesel oil with *Pseudomonas delafieldii* R-8 from high density culture. Biochem. Eng. J. 2006, 27:305-309.
- Gupta N, Roychoudhury PK, Deb JK. Biotechnology of desulfurization of diesel: prospects and challenges. Appl. Microbiol. Biotechnol. 2005, 66:356-366.
- Gupta P, Pandey K, Verma N. Augmented complete mineralization of glyphosate in wastewater via microbial degradation post CWAO over supported Fe-CNF. Chem. Eng. J. 2022, 428:132008.

- Gupta S, Plugge CM, Klok J, Muyzer G. Comparative analysis of microbial communities from different full-scale haloalkaline biodesulfurization systems. Applied Microbiology and Biotechnology. 2022, 106:1759-1776.
- Habimana F, Huo Y, Jiang S, Ji S. Synthesis of europium metal–organic framework (Eu-MOF) and its performance in adsorptive desulfurization. Adsorption 2016, 22:1147-1155.
- Han L, Zhang J, Mao Y, Zhou W, Xu W, Sun Y. Facile and green synthesis of MIL-53 (Cr) and its excellent adsorptive desulfurization performance. Ind. Eng. Chem. Res. 2019, 58:15489-15496.
- Hartdegen FE, Coburn JM, Roberts RL. Microbiol desulfurization of petroleum. Chem. Eng. Prog. 1984, 80:63-67.
- Hasan Z, Jhung SH. Facile method to disperse nonporous metal organic frameworks: composite formation with a porous metal organic framework and application in adsorptive desulfurization. ACS Appl. Mater. Interfaces 2015, 7:10429-10435.
- Hassan SI, Sif El-Din OI, Tawfik SM, Abd El-Aty DM. Solvent extraction of oxidized diesel fuel: Phase equilibrium. Fuel Process. Technol. 2013, 106:127–132.
- Holland HL, Khan SH, Richards D, Riemland E. Biotransformation of polycyclic aromatic compounds by fungi. Xenobiotica 1986, 16:733-741.
- Hou Y, Kong Y, Yang J, Zhang J, Shi D, Xin W. Biodesulfurization of dibenzothiophene by immobilized cells of *Pseudomonas stutzeri* UP-1. Fuel 2005, 84:1975-1979.

- Houda S, Lancelot C, Blanchard P, Poinel L, Lamonier C. Oxidative desulfurization of heavy oils with high sulfur content: a review. Catalysts 2018, 8:344.
- Hua R, Li Y, Liu W, Zheng J, Wei H, Wang J, Lu X, Kong H, Xu G. Determination of sulfur-containing compounds in diesel oils by comprehensive two-dimensional gas chromatography with a sulfur chemiluminescence detector. J. Chromatogr. A 2003, 1019:101-109.
- Huo Q, Li J, Liu G, QiX, Zhang X, Ning Y, Zhang B, Fu, Y, Liu S. Adsorption desulfurization performances of Zn/Co porous carbons derived from bimetal-organic frameworks. Chem. Eng. J. 2019, 362:287-297.
- Huo Q, Li J, Qi X, Liu G, Zhang X, Zhang B, Ning Y, Fu Y, Liu J, Liu S. Cu, Zn-embedded MOF-derived bimetallic porous carbon for adsorption desulfurization. Chem. Eng. J. 2019, 378:122106.
- Hyrslova I, Kana A, Kantorova V, Krausova G, Mrvikova I, Doskocil I. Selenium accumulation and biotransformation in *Streptococcus*, *Lactococcus*, and *Enterococcus* strains. J. Funct. Foods 2022, 92:105056.
- Ibrahim MH, Hayyan M, Hashim MA, Hayyan A. The role of ionic liquids in desulfurization of fuels: A review. Renew. Sust. Energ. Rev. 2017, 76:1534-1549.
- Isoda D. Challenges in the hydrodesulfurization of polyaromatic sulfur compounds. Adv. Catal. 1998, 42:60631-60638.
- Javadli R, De klerk A. Desulfurization of heavy oil. Appl. Petrochem. Res. 2012, 1:3-19.

- Jha D, Haider MB, Kumar R, Byamba-Ochir N, Shim WG, Marriyappan Sivagnanam B, Moon H. Enhanced adsorptive desulfurization using mongolian anthracite-based activated carbon. ACS Omega 2019, 4:20844-20853.
- Jha D, Haider MB, Kumar R, Shim WG, Marriyappan Sivagnanam B. Batch and continuous adsorptive desulfurization of model diesel fuels using graphene nanoplatelets. J. Chem. Eng. Data 2020, 65:2120-2132.
- Jha D, Mubarak NM, Haider MB, Kumar R, Balathanigaimani MS, Sahu JN. Adsorptive removal of dibenzothiophene from diesel fuel using microwave synthesized carbon nanomaterials. Fuel 2019, 244:132-139.
- Jia Y, Li G, Ning G. Efficient oxidative desulfurization (ODS) of model fuel with H_2O_2 catalyzed by $MoO_3/\gamma\text{-}Al_2O_3$ under mild and solvent free conditions. Fuel Process. Technol. 2011, 92:106-111.
- Jung BK, Jhung SH. Adsorptive removal of benzothiophene from model fuel, using modified activated carbons, in presence of diethylether. Fuel 2015, 145:249-255.
- Kayser KJ, Cleveland L, Park HS, Kwak JH, Kolhatkar A, Kilbane JJ. Isolation and characterization of a moderate thermophile, *Mycobacterium phlei* GTIS10, capable of dibenzothiophene desulfurization. Appl. Microbiol. Biotechnol. 2002, 59:737-746.
- Kazakov AA, Tarakanov GV, Ionov NG. Mechanisms of oxidative desulfurization of straight-run residual fuel oil using ozonized air. Chem. Technol. Fuels Oils 2016, 52:33–37.
- Kertesz MA. Riding the sulfur cycle–metabolism of sulfonates and sulfate esters in Gram-negative bacteria. FEMS Microbiol. Rev. 2000, 24:135-175.

- Khan NA, Jhung SH. Low-temperature loading of Cu+ species over porous metal-organic frameworks (MOFs) and adsorptive desulfurization with Cu+-loaded MOFs. J. Hazard. Mater. 2012, 237:180-185.
- Khan NA, Jun JW, Jeong JH, Jhung SH. Remarkable adsorptive performance of a metal–organic framework, vanadium-benzenedicarboxylate (MIL-47), for benzothiophene. Chem. Comm. 2011, 47:1306-1308.
- Khan NA, Kim CM, Jhung SH. Adsorptive desulfurization using Cu–Ce/metal–organic framework: Improved performance based on synergy between Cu and Ce. Chem. Eng. J. 2017, 311:20-27.
- Khan NA, Yoon JW, Chang JS, Jhung SH. Enhanced adsorptive desulfurization with flexible metal–organic frameworks in the presence of diethyl ether and water. Chem. Comm. 2016, 52:8667-8670.
- Kharisov BI, González MO, Quezada TS, de la Fuente IG, Longoria F. Materials and nanomaterials for the removal of heavy oil components. J. Pet. Sci. Eng. 2017, 156:971-982.
- Kilbane II JJ, Jackowski K. Biodesulfurization of water-soluble coalderived material by *Rhodococcus rhodochrous* IGTS8. Biotechnol. Bioeng. 1992, 40:1107–1114.
- Kilbane II JJ. Enzyme from *Rhodococcus rhodochrous* ATCC 53968, *Bacillus sphaericus* ATCC 53969 or a mutant thereof for cleavage of organic C–S bonds. 1996, US patent number 5,516,677.
- Kilbane II JJ. Mutant microorganisms useful for cleavage of organic C–S bonds. 1992, US patent number 5,104,801

- Kilbane JJ, Bielaga BA. Toward sulfur-free fuels. Chem. Tech. 1990, 20:747–751
- Kilbane JJ. Desulfurization of coal: the microbial solution. Trends. Biotechnol. 1989, 7:97-101.
- Kim JH, Ma X, Zhou A, Song C. Ultra-deep desulfurization and denitrogenation of diesel fuel by selective adsorption over three different adsorbents: a study on adsorptive selectivity and mechanism. Catal. Today 2006, 111:74-83.
- Kim TS, Kim HY, Kim BH. Petroleum desulfurization by *Desulfovibrio desulfuricans* M6 using electrochemically supplied reducing equivalent. Biotechnol. Lett. 1990, 12:757-760.
- Kirimura K, Furuya T, Nishii Y, Ishii Y, Kino K, Usami S. Biodesulfurization of dibenzothiophene and its derivatives through the selective cleavage of carbon-sulfur bonds by a moderately thermophilic bacterim *Bacillus subtilis* WU-S2B. J. Biosci. Bioeng. 2001, 91:262-266.
- Koch TA, Krause KR, Manzer LE, Mehdizadeh M, Odom JM, Sengupta SK. New J. Chem. 1996, 20:163–173.
- Kodama K, Nakatani S, Umehara K, Shimizu K, Minoda Y, Yamada K. Microbial conversion of petro-sulfur compounds: Part III. Isolation and identification of products from dibenzothiophene. Agric. Biol. Chem. 1970, 34:1320-1324.
- Kong L, Zhang T, Yao R, Zeng Y, Zhang L, Jian P. Adsorptive desulfurization of fuels with Cu (I)/SBA-15 via low-temperature reduction. Microporous Mesoporous Mater. 2017, 251:69-76.

- Konishi J, Ishii Y, Okumura K, Suzuki M, inventors; Petroleum Energy Center Foundation, assignee. High-temperature desulfurization by microorganisms. 1999, United States patent No 5,925,560.
- Krivtsov EB, Golovko AK. The kinetics of oxidative desulfurization of diesel fraction with a hydrogen peroxide-formic acid mixture. Pet. Chem. 2014, 54:51–57.
- Kropp KG, Andersson JT, Fedorak PM. Biotransformations of three dimethyldibenzothiophenes by pure and mixed bacterial cultures. Environ. Sci. Technol. 1997, 31:1547-1554.
- Kulkarni PS, Afonso CAM. Deep desulfurization of diesel fuel using ionic liquids: Current status and future challenges. Green Chem. 2010, 12:1139–1149.
- Kumar S, Srivastava VC, Badoni RP. Studies on adsorptive desulfurization by zirconia based adsorbents. Fuel 2011, 90:3209-3216.
- Kumar A, Verma N. Wet air oxidation of aqueous dichlorvos pesticide over catalytic copper-carbon nanofiberous beads. Chem. Eng. J. 2018, 351:428-440.
- Kumar A, Omar RA, Verma N. Efficient electro-oxidation of diclofenac persistent organic pollutant in wastewater using carbon film-supported Cu-rGO electrode. Chemosphere 2020, 248:126030.
- Laborde AL, Gibson DT. Metabolism of dibenzothiophene by a *Beijerinckia* species. Appl. Environ. Microbiol. 1977, 34:783-790.
- Larrubia MA, Gutièrrez-Alejandre A, Ramìrez J, Busca G. A FT-IR study of the adsorption of indole, carbazole, benzothiophene, dibenzothiophene and 4, 6-dibenzothiophene over solid adsorbents and catalysts. Appl. Catal. A: Gen. 2002, 224:167-178.

- Lee KX, Tsilomelekis G, Valla JA. Removal of benzothiophene and dibenzothiophene from hydrocarbon fuels using CuCe mesoporous Y zeolites in the presence of aromatics. Appl. Catal. B. 2018, 234:130-142.
- Lee KX, Valla JA. Adsorptive desulfurization of liquid hydrocarbons using zeolite-based sorbents: a comprehensive review. React. Chem. Eng. 2019, 4:1357-1386.
- Lee KX, Wang H, Karakalos S, Tsilomelekis G, Valla JA. Adsorptive desulfurization of 4, 6-dimethyldibenzothiophene on bimetallic mesoporous y zeolites: effects of cu and ce composition and configuration. Ind. Eng. Chem. Res. 2019, 58:18301-18312.
- Li F, Zhang Z, Feng J, Cai X, Xu P. Biodesulfurization of DBT in tetradecane and crude oil by a facultative thermophilic bacterium *Mycobacterium goodii* X7B. J. Biotechnol. 2007, 127:222-228.
- Li FL, Xu P, Ma CQ, Luo LL, Wang XS. Deep desulfurization of hydrodesulfurization-treated diesel oil by a facultative thermophilic bacterium *Mycobacterium* sp. X7B. FEMS Microbiol. Lett. 2003, 223:301-307.
- Li J, Yang Z, Li S, Jin Q, Zhao J. Review on oxidative desulfurization of fuel by supported heteropolyacid catalysts. J. Ind. Eng. Chem. 2020, 82:1-16.
- Li W, Tang H, Liu Q, Xing J, Li Q, Wang D, Yang M, Li X, Liu H. Deep desulfurization of diesel by integrating adsorption and microbial method. Biochem. Eng. J. 2009, 44:297-301.
- Li W, Wang MD, Chen H, Chen JM, Shi Y. Biodesulfurization of dibenzothiophene by growing cells of *Gordonia* sp. in batch cultures. Biotechnol. Lett. 2006, 28:1175-1179.

- Li W, Xing J, Xiong X, Shan G, Liu H. Bio-regeneration of π-complexation desulfurization adsorbents. Sci. China Ser. B. 2005, 48:538-544.
- Li W, Zhang Y, Wang MD, Shi Y. Biodesulfurization of dibenzothiophene and other organic sulfur compounds by a newly isolated *Microbacterium* strain ZD-M2. FEMS Microbiol. Lett. 2005, 247:45-50.
- Li X, Zhu H, Liu C, Yuan P, Lin Z, Yang J, Yue Y, Bai Z, Wang T, Bao X. Synthesis, modification, and application of hollow mesoporous carbon submicrospheres for adsorptive desulfurization. Ind. Eng. Chem. Res. 2018, 57:15020-15030.
- Li YH, Tan P, Liu XQ, Zu DD, Huang CL, Sun LB. Facile fabrication of AgCl nanoparticles and their application in adsorptive desulfurization. J. Nanosci. Nanotechnol. 2015, 15:4373-4379.
- Li YX, Jiang WJ, Tan P, Liu XQ, Zhang DY, Sun LB. What matters to the adsorptive desulfurization performance of metal-organic frameworks?. J. Phys. Chem. C. 2015, 119:21969-21977.
- Liang J, Liang Z, Zou R, Zhao Y. Heterogeneous catalysis in zeolites, mesoporous silica, and metal–organic frameworks. Adv. Mater. 2017, 29:1701139.
- Liao J, Wang Y, Chang L, Bao W. Preparation of M/γ-Al 2 O 3 sorbents and their desulfurization performance in hydrocarbons. RSC Adv. 2015, 5:62763-62771.
- Liu C, Yuan P, Duan A, Mei J, Zheng P, Meng Q, Cai A, Cheng T, Gong Y. Monodispersed dendritic mesoporous silica/carbon nanospheres with enhanced active site accessibility for selective adsorptive desulfurization. J. Mater. Sci. 2019, 54:8148-8162.

- Luo MF, Xing JM, Gou ZX, Li S, Liu HZ, Chen JY. Desulfurization of dibenzothiophene by lyophilized cells of *Pseudomonas delafieldii* R-8 in the presence of dodecane. Biochem. Eng. J. 2003, 13:1-6.
- Ma CQ, Feng JH, Zeng YY, Cai XF, Sun BP, Zhang ZB, Blankespoor HD, Xu P. Methods for the preparation of a biodesulfurization biocatalyst using *Rhodococcus* sp. Chemosphere 2006, 65:165-169.
- Ma T, Li G, Li J, Liang F, Liu R. Desulfurization of dibenzothiophene by *Bacillus subtilis* recombinants carrying dsz ABC and dsz D genes. Biotechnol. Lett. 2006, 28:1095-1100.
- Maghsoudi S, Kheirolomoom A, Vossoughi M, Tanaka E, Katoh S. Selective desulfurization of dibenzothiophene by newly isolated *Corynebacterium* sp. strain P32C1. Biochem. Eng. J. 2000, 5:11-16.
- Maghsoudi S, Vossoughi M, Kheirolomoom A, Tanaka E, Katoh S. Biodesulfurization of hydrocarbons and diesel fuels by *Rhodococcus* sp. strain P32C1. Biochem. Eng. J. 2001, 8:151-156.
- Mahmoudian M, Abdali A, Eskandarabadi SM, Nozad E, Enayati M. The performance of an efficient polymer and Cloisite 30B derivatives in the adsorption desulfurization process. Polym. Bull. 2020, 78:795-812.
- Malani RS, Batghare AH, Bhasarkar JB, Moholkar VS. Kinetic modelling and process engineering aspects of biodesulfurization of liquid fuels: Review and analysis. Bioresour. Technol. Rep. 2021, 14:100668.
- Malik KA, KA M. Microbial removal of organic sulphur from crude oil and the environment: some new perspectives. Process Biochem. 1978, 13:10-13

- Mansouri A, Khodadadi AA, Mortazavi Y. Ultra-deep adsorptive desulfurization of a model diesel fuel on regenerable Ni–Cu/γ-Al_2O_3 at low temperatures in absence of hydrogen. J. Hazard. Mater. 2014, 271:120-130.
- Martinez I, Santos VE, Gomez E, Garcia-Ochoa F. Biodesulfurization of dibenzothiophene by resting cells of *Pseudomonas putida* CECT5279: influence of the oxygen transfer rate in the scale-up from shaken flask to stirred tank reactor. J. Chem. Technol. Biotechnol. 2016, 91:184-189.
- Mate MS, Pathade G. Biodegradation of C.I. Reactive Red 195 by *Enterococcus faecalis* strain YZ66. World J. Microbiol. Biotechnol. 2012, 28:815-826.
- Mcfarland BL, Boron DJ, Deever W, Meyer JA, Johnson AR, Atlas RM. Biocatalytic sulfur removal from fuels: applicability for producing low sulfur gasoline. Crit. Rev. Microbiol. 1998, 24:99-147.
- Mcfarland BL. Biodesulf urization. Curr. Opin. Microbiol. 1999, 2:257-264.
- Mcnamara ND, Neumann GT, Masko ET, Urban JA, Hicks JC. Catalytic performance and stability of (V) MIL-47 and (Ti) MIL-125 in the oxidative desulfurization of heterocyclic aromatic sulfur compounds. J. Catal. 2013, 305:217-226.
- Mei H, Mei BW, Yen TF. A new method for obtaining ultra-low sulfur diesel fuel via ultrasound assisted oxidative desulfurization. Fuel 2003, 82:405–414.
- Mello PDA, Duarte FA, Nunes MAG, Alencar MS, Moreira EM, Korn M, Dressler VL, Flores ÉMM. Ultrasound-assisted oxidative process for sulfur removal from petroleum product feedstock. Ultrason. Sonochem. 2009, 16:732–736.
- Menzel R, Iruretagoyena D, Wang Y, Bawaked SM, Mokhtar M, Al-Thabaiti SA, Basahel SN, Shaffer MS. Graphene oxide/mixed metal oxide hybrid materials for

enhanced adsorption desulfurization of liquid hydrocarbon fuels. Fuel 2016, 181:531-536.

- Mohebali G, Ball AS, Rasekh B, Kaytash A. Biodesulfurization potential of a newly isolated bacterium, *Gordonia alkanivorans* RIPI90A. Enzyme. Microb. Technol. 2007, 40:578-584.
- Mohr SH, Wang J, Ellem G, Ward J, Giurco D. Projection of world fossil fuels by country. Fuel 2015, 141:120-135.
- Monticello DJ, Bakker D, Finnerty WR. Plasmid-mediated degradation of dibenzothiophene by *Pseudomonas* species. Appl. Environ. Microbiol. 1985, 49:756-760.
- Monticello DJ, Kilbane JJ. Microemulsion process for direct biocatalytic desulfurization of organosulfur molecules. 1994, US patent number 5,358,870.
- Monticello DJ. Biodesulfurization and the upgrading of petroleum distillates. Curr. Opin. Biotechnol. 2000, 11:540-546.
- Monticello DJ. Riding the fossil fuel biodesulfurization wave. Chemtech 1998, 28:38-45.
- Moradi M, Karimzadeh R, Moosavi ES. Modified and ion exchanged clinoptilolite for the adsorptive removal of sulfur compounds in a model fuel: New adsorbents for desulfurization. Fuel 2018, 217:467-477.
- Moreira AM, Brandão HL, Hackbarth FV, Maass D, de Souza, AU, de Souza SGU. Adsorptive desulfurization of heavy naphthenic oil: equilibrium and kinetic studies. Chem. Eng. Sci. 2017, 172:23-31.

- Nair S, Hussain AS, Tatarchuk BJ. The role of surface acidity in adsorption of aromatic sulfur heterocycles from fuels. Fuel 2013, 105:695-704.
- Nassar HN, Abu Amr SS, El-Gendy NS. Biodesulfurization of refractory sulfur compounds in petro-diesel by a novel hydrocarbon tolerable strain Paenibacillus glucanolyticus HN_4. Environ. Sci. Pollut. 2021, 28:8102-8116.
- Nehlsen JP. Developing clean fuels: Novel techniques for desulfurization. Princeton University, 2006.
- Nejad NF, Shams E, Amini MK, Bennett JC. Synthesis of magnetic mesoporous carbon and its application for adsorption of dibenzothiophene. Fuel Process. Technol. 2013, 106:376-384.
- Neubauer R, Kienzl N, Hochenauer C. Integration of an adsorptive desulfurization unit into an SOFC-based auxiliary power unit operated with diesel fuel. Chem. Eng. Res. Des. 2019, 141:47-55.
- Nkomzwayo T, Mguni L, Hildebrandt D, Yao Y. Adsorptive desulfurization using period 4 transition metals oxide: A study of Lewis acid strength derived from the adsorbent ionic-covalent parameter. Chem. Eng. J. 2022, 444:136484.
- Nojiri H, Habe H, Omori T. Bacterial degradation of aromatic compounds via angular dioxygenation. J. Gen. Appl. Microbiol. 2001, 47:279-305.
- Nuntang S, Prasassarakich P, Ngamcharussrivichai C. Comparative study on adsorptive removal of thiophenic sulfurs over Y and USY zeolites. Ind. Eng. Chem. Res. 2008, 47:7405-7513.

- Nunthaprechachan T, Pengpanich S, Hunsom M. Adsorptive desulfurization of dibenzothiophene by sewage sludge-derived activated carbon. Chem. Eng. J. 2013, 228:263-271.
- Ogunlaja AS, Alade OS, Tshentu ZR. Vanadium(IV) catalysed oxidation of organosulfur compounds in heavy fuel oil. C. R. Chim. 2017, 20:164–168.
- Ohshiro T, Hine Y, Izumi Y. Enzymatic desulfurization of dibenzothiophene by a cell-free system of *Rhodococcus erythropolis* D-1. FEMS Microbiol. Lett. 1994, 118:341-344.
- Ohshiro T, Izumi Y. Microbial desulfurization of organic sulfur compounds in petroleum. Biosci. Biotechnol. Biochem. 1999, 63:1-9.
- Olajire AA, Olanrewaju SA, Lawal WH. Silver nanoparticle-assisted adsorptive desulfurization by composted agro-waste activated carbons. Int. J. Environ. 2017, 11:263-279.
- Omar RA, Verma N, Arora PK. Sequential desulfurization of thiol compounds containing liquid fuels: Adsorption over Ni-doped carbon beads followed by biodegradation using environmentally isolated *Bacillus zhangzhouensis*. Fuel 2020, 277:118208.
- Omar RA, Verma N, Arora PK. Successive bacterial desulfurization and regeneration of liquid fuel over Ni-doped carbon beads using a single *Enterococcus faecium* strain isolated from an industrial wastewater. Fuel 2022, 309:122209.
- Onodera-Yamada K, Morimoto M, Tani Y. Degradation of dibenzothiophene by sulfate-reducing bacteria cultured in the presence of only nitrogen gas. J. Biosci. Bioeng. 2001, 91:91-93.

- Otsuki S, Nonaka T, Takashima N, Qian W, Ishihara A, Imai T, Kabe T. Oxidative desulfurization of light gas oil and vacuum gas oil by oxidation and solvent extraction. Energy Fuels 2000, 14:1232–1239.
- Pacheco M, Paixao SM, Silva TP, Alves L. On the road to cost-effective fossil fuel desulfurization by *Gordonia alkanivorans* strain 1B. RSC Adv. 2019, 9:25405-24513.
- Park JG, Ko CH, Yi KB, Park JH, Han SS, Cho SH, Kim JN. Reactive adsorption of sulfur compounds in diesel on nickel supported on mesoporous silica. Appl. Catal. B. 2008, 81:244-250.
- Park TH, Cychosz KA, Wong-Foy AG, Dailly A, Matzger AJ. Gas and liquid phase adsorption in isostructural Cu 3 [biaryltricarboxylate] 2 microporous coordination polymers. Chem. Comm. 2011, 47:1452-1454.
- Passe-Coutrin N, Altenor S, Cossement D, Jean-Marius C, Gaspard S. Comparison of parameters calculated from the BET and Freundlich isotherms obtained by nitrogen adsorption on activated carbons: A new method for calculating the specific surface area. Microporous Mesoporous Mater. 2008, 111:517-522.
- Pawelec B, Campos-Martin JM, Cano-Serrano E, Navarro RM, Thomas S, Fierro JLG. Removal of PAH compounds from liquid fuels by Pd catalysts. Environ. Sci. Technol. 2005, 39:3374-3381.
- Peh S, Mu T, Zhong W, Yang M, Chen Z, Yang G, Zhao X, Sharshar MM, Samak NA, Xing J. Enhanced Biodesulfurization with a Microbubble Strategy in an Airlift Bioreactor with Haloalkaliphilic Bacterium *Thioalkalivibrio versutus* D306. ACS Omega. 2022.

- Peighami R, Motamedian E, Rasekh B, Yazdian F. Investigating role of abiotic side and finding optimum abiotic condition for improving gas biodesulfurization using *Thioalkalivibrio versutus*. Sci. Rep. 2022, 12:1-4.
- Piddington CS, Kovacevich BR, Rambosek J. Sequence and molecular characterization of a DNA region encoding the dibenzothiophene desulfurization operon of *Rhodococcus* sp. strain IGTS8. Appl. Environ. Microbiol. 1995, 61:468-475.
- Prajapati YN, Verma N. Adsorptive desulfurization of diesel oil using nickel nanoparticle-doped activated carbon beads with/without carbon nanofibers:Effects of adsorbate size and adsorbent texture. Fuel 2017, 189:186-194.
- Prajapati YN, Verma N. Fixed bed adsorptive desulfurization of thiophene over Cu/Ni-dispersed carbon nanofiber. Fuel 2018, 216:381-389.
- Prajapati Y, Verma N. Hydrodesulfurization of thiophene on activated carbon fiber supported NiMo catalysts. Energy Fuel 2018, 32:2183-2196.
- Prasad VVDN, Jeong KE, Chae HJ, Kim, CU, Jeong SY. Oxidative desulfurization of 4,6-dimethyl dibenzothiophene and light cycle oil over supported molybdenum oxide catalysts. Catal. Commun. 2008, 9:1966–1969.
- Prasoulas G, Dimos K, Glekas P, Kalantzi S, Sarris S, Templis C, Vavitsas K, Hatzinikolaou DG, Papayannakos N, Kekos D, Mamma D. Biodesulfurization of Dibenzothiophene and Its Alkylated Derivatives in a Two-Phase Bubble Column Bioreactor by Resting Cells of *Rhodococcus erythropolis* IGTS8. Processes. 2021, 9:2064.
- Přech J. Catalytic performance of advanced titanosilicate selective oxidation catalysts–a review. Catal. Rev. 2018, 60:71-131.

- Qin L, Zhou Y, Li D, Zhang L, Zhao Z, Zuhra Z, Mu C. Highly dispersed HKUST-1 on milimeter-sized mesoporous γ-Al_2O_3 beads for highly effective adsorptive desulfurization. Ind. Eng. Chem. Res. 2016, 55:7249-7258.
- Rafiee E, Sahraei S, Moradi GR. Extractive oxidative desulfurization of model oil/crude oil using KSF montmorillonite-supported 12-tungstophosphoric acid. Pet. Sci. 2016, 13:760–769.
- Rakhmanov EV, Domashkin AA, Myltykbaeva ZK, Kairbekov Z, Shigapova AA, Akopyan AV, Anisimov AV. Peroxide oxidative desulfurization of a mixture of nonhydrotreated vacuum gas oil and diesel fraction. Pet. Chem. 2016, 56:742–744.
- Ren X, Miao G, Xiao Z, Ye F, Li Z, Wang H, Xiao J. Catalytic adsorptive desulfurization of model diesel fuel using TiO_2/SBA-15 under mild conditions. Fuel 2016, 174:118-125.
- Rouquerol F. Adsorption by clays, pillared layer structures and zeolites. Adsorption by powders and porous solids, 1999.
- Rüger HJ, Fritze D, Spröer C. New psychrophilic and psychrotolerant Bacillus marinus strains from tropical and polar deep-sea sediments and emended description of the species. Int. J. Syst. Evol. Microbiol. 2000, 50:1305-1313.
- Safari M, Ghiaci M, Rahimi F. Preparation of rGO/ZrP as a new adsorbent in dibenzothiophene removal from n-decane with high capacities and good regenerability. RSC Adv. 2016, 6:68445-68453.
- Saleh TA, Al-Hammadi SA, Tanimu A, Alhooshani K. Ultra-deep adsorptive desulfurization of fuels on cobalt and molybdenum nanoparticles loaded on activated carbon derived from waste rubber. J. Colloid Interface Sci. 2018, 513:779-787.

- Saleh TA, Sulaiman KO, AL-Hammadi SA, Dafalla H, Danmaliki GI. Adsorptive desulfurization of thiophene, benzothiophene and dibenzothiophene over activated carbon manganese oxide nanocomposite: with column system evaluation. J. Clean. Prod. 2017, 154:401-412.
- Saleh TA. Simultaneous adsorptive desulfurization of diesel fuel over bimetallic nanoparticles loaded on activated carbon. J. Clean. Prod. 2018, 172:2123-2132.
- Santos SC, Alviano DS, Alviano CS, Pádula M, Leitao AC, Martins OB, Ribeiro CM, Sassaki MY, Matta CP, Bevilaqua J, Sebastián GV. Characterization of *Gordonia* sp. strain F. 5.25. 8 capable of dibenzothiophene desulfurization and carbazole utilization. Appl. Microbiol. Biotechnol. 2006, 71:355-362.
- Schnobrich JK, Lebel O, Cychosz KA, Dailly A, Wong-Foy AG, Matzger AJ. Linker-directed vertex desymmetrization for the production of coordination polymers with high porosity. J. Am. Chem. Soc. 2010, 132:13941-13948.
- Selvavathi V, Chidambaram V, Meenakshisundaram A, Sairam B, Sivasankar B. Adsorptive desulfurization of diesel on activated carbon and nickel supported systems. Catal. Today 2009, 141:99-102.
- Sentorun-Shalaby C, Saha SK, Ma X, Song C. Mesoporous-molecular-sieve-supported nickel sorbents for adsorptive desulfurization of commercial ultra-low-sulfur diesel fuel. Appl. Catal. B. 2011, 101:718-726.
- Seredych M, Wu CT, Brender P, Ania CO, Vix-Guterl C, Bandosz TJ. Role of phosphorus in carbon matrix in desulfurization of diesel fuel using adsorption process. Fuel 2012, 92:318-326.

- Shah MS, TsapatsisM, Siepmann JI. Hydrogen sulfide capture: From absorption in polar liquids to oxide, zeolite, and metal–organic framework adsorbents and membranes. Chem. Rev. 2017, 117:9755-9803.
- Shang H, Zhang H, Du W, Liu Z. Development of microwave assisted oxidative desulfurization of petroleum oils: A review. J. Ind. Eng. Chem. 2013, 19:1426-1432.
- Shavandi M, Sadeghizadeh M, Zomorodipour A, Khajeh K. Biodesulfurization of dibenzothiophene by recombinant *Gordonia alkanivorans* RIPI90A. Bioresour. Technol. 2009, 100:475-479.
- Shen JX, Mao SX, Wan L, Wu WX, Jin MM, Li YX, Liu XQ, Sun LB. Stabilizing CuI in MIL-101 (Cr) by introducing long-chain alkane for adsorptive desulfurization. Sep. Purif. Technol. 2022, 290:120892.
- Shi Y, Zhang X, Liu G. Activated carbons derived from hydrothermally carbonized sucrose: remarkable adsorbents for adsorptive desulfurization. ACS Sustain. Chem. Eng. 2015, 3:2237-2346.
- Shi Y, Zhang X, Liu G. Adsorptive desulfurization performances of ordered mesoporous carbons with tailored textural and surface properties. Fuel 2015, 158:565-571.
- Shiraishi Y, Hirai T, Komasawa I. A deep desulfurization process for light oil by photochemical reaction in an organic two-phase liquid−liquid extraction system. Ind. Eng. Chem. Res. 1998, 37:203-211.
- Shiraishi Y, Hirai T. Desulfurization of Vacuum Gas Oil Based on Chemical Oxidation Followed by Liquid - Liquid Extraction. Energy Fuels 2004, 18:37–40.

- Smibert RM. Phenotypic characterization. Methods for general and molecular bacteriology. 1994
- Skennan VBD. A guide to the identification of the genera of bacteria, 2nd edn. Baltimore: Williams & Wilkins. 1967
- Soleimani M, Bassi A, Margaritis A. Biodesulfurization of refractory organic sulfur compounds in fossil fuels. Biotechnol. Adv. 2007, 25:570-596.
- Song H, Li X, Jiang B, Gong M, Hao T. Preparation of novel and highly stable Py/MOF and its adsorptive desulfurization performance. Ind. Eng. Chem. Res. 2019, 58: 19586-91958.
- Sotelo JL, Uguina MA, Águeda VI. Fixed bed adsorption of benzothiophene over zeolites with faujasite structure. Adsorption 2007, 13:331-339.
- Sousa JP, Neves RP, Sousa SF, Ramos MJ, Fernandes PA. Reaction mechanism and determinants for efficient catalysis by DszB, a key enzyme for crude oil bio-desulfurization. ACS Catal. 2020, 10:9545-9554.
- Srivastav A, Srivastava VC. Adsorptive desulfurization by activated alumina. J. Hazard. Mater. 2009, 170:1133-1140.
- Srivastava VC. An evaluation of desulfurization technologies for sulfur removal from liquid fuels. RSC Adv. 2012, 23:759-783.
- Stevens Jr SE, Burgess WD. Biological desulfurization of coal. 1987, US patent number 4,659,670.
- Stevens Jr SE, Burgess WD. Microbial desulfurization of coal. 1989, US patent number 4,851,350

- Stratas Advisors. A Global Overview and Outlook of On-Road Diesel Quality, Vehicle Emissions and Fuel Efficiency. https://stratasadvisors.com/insights/2020/0220 2020-top-100-diesel-sulfur-ranking (last accessed in May, 2022).
- Stylianou M, Vyrides I, Agapiou A. Oil biodesulfurization: A review of applied analytical techniques. J. Chromatograph. 2021, 1171:122602.
- Subhan F, Aslam S, Yan Z, Naeem M, Ullah R, Etim UJ. Size regulation and dispersion of ceria using confined spaces for adsorptive desulfurization. Chem. Eng. J. 2018, 348:319-326.
- Tanaka Y, Matsui T, Konishi J, Maruhashi K, Kurane R. Biodesulfurization of benzothiophene and dibenzothiophene by a newly isolated *Rhodococcus* strain. Appl. Microbiol. Biotechnol. 2002, 59:325-328.
- Tang Q, Lin S, Cheng Y, Liu S, Xiong J-R. Ultrasound-assisted oxidative desulfurization of bunker-C oil using tert-butyl hydroperoxide. Ultrason Sonochem. 2013, 20:1168–1175.
- Teymouri M, Samadi-Maybodi A, Vahid A, MiranbeigiA,. Adsorptive desulfurization of low sulfur diesel fuel using palladium containing mesoporous silica synthesized via a novel in-situ approach. Fuel Process Technol. 2013, 116:257-264.
- Thaligari SK, Srivastava VC, Prasad B. Adsorptive desulfurization by zinc-impregnated activated carbon: characterization, kinetics, isotherms, and thermodynamic modeling. Clean Technol. Environ. Policy. 2016, 18:1021-1030.
- Toteva V, Georgiev A, Topalova L. Oxidative desulphurization of light cycle oil: Monitoring by FTIR spectroscopy. Fuel Process Technol. 2009, 90:965–970.

- Trakarnpruk W, Rujiraworawut K. Oxidative desulfurization of Gas oil by polyoxometalates catalysts. Fuel Process. Technol. 2009, 90:411–414.
- Tran DT, Palomino JM, Oliver SR. Desulfurization of JP-8 jet fuel: challenges and adsorptive materials. RSC Adv. 2018, 8:7301-7314.
- Triantafyllidis KS, Deliyanni EA. Desulfurization of diesel fuels: adsorption of 4, 6-DMDBT on different origin and surface chemistry nanoporous activated carbons. Chem. Eng. J. 2014, 236:406-414.
- USDE (U.S. Department of energy) Industrial technologies program 2003 (Last accessed in May 2022): https://www.energy.gov/sites/prod/files/2014/05/f16/gasbiopet_final.pdf
- Van Afferden M, Schacht S, Klein J, Trüper HG. Degradation of dibenzothiophene by *Brevibacterium* sp. DO. Arch. Microbiol. 1990, 153:324-328.
- Van Hamme JD, Singh A, Ward OP. Recent advances in petroleum microbiology. Microbiol. Mol. Biol. Rev. 2003, 67:503-549.
- Wu H, Gong Q, Olson DH, Li J. Commensurate adsorption of hydrocarbons and alcohols in microporous metal organic frameworks. Chem. Rev. 2012, 112:836-868.
- Wu L Ye F Lei D, Miao G, Liu B, Li Z, Xiao J. Regeneration of Ag X O@ SBA-15 for reactive adsorptive desulfurization of fuel. Pet. Sci. 2018, 15:857-869.
- Xia Y, Li Y, Gu Y, Jin T, Yang Q, Hu J, Liu H,Wang H. Adsorption desulfurization by hierarchical porous organic polymer of poly-methylbenzene with metal impregnation. Fuel 2016, 170:100-106.

- Xiao J, Wang X, Chen Y, Fujii M, Song C. Ultra-deep adsorptive desulfurization of light-irradiated diesel fuel over supported TiO_2–CeO_2 adsorbents. Ind. Eng. Chem. Res. 2013, 52:15746-15755.
- Xiong J, Luo J, Di J, Li X, Chao Y, Zhang M, Zhu W,Li H. Macroscopic 3D boron nitride monolith for efficient adsorptive desulfurization. Fuel 2020, 261:116448.
- Xu Cz, Zheng Mq, Keng Chen, Hui Hu, Chen Xh. CeOx doping on a TiO_2-SiO_2 supporter enhances Ag based adsorptive desulfurization for diesel. J. Fuel Chem. Technol. 2016, 44:943-953.
- Xu J, Zhang B, Lu Y, Wang L, Tao W, Teng X, Ning W, Zhang Z. Adsorption desulfurization performance of PdO/SiO2@ graphene oxide hybrid aerogel: Influence of graphene oxide. J. Hazard. Mater. 2022, 421:126680.
- Yadav A, Faisal M, Subramaniam A, Verma N. Nickel nanoparticle-doped and steam-modified multiscale structure of carbon micro-nanofibers for hydrogen storage: effects of metal, surface texture and operating conditions. Int. J. Hydrog. Energy 2017, 42:6104-6117.
- Yamada K, Minoda Y, Kodama K, Nakatani S, Akasaki T. Microbial conversion of petro-sulfur compounds: Part I. Isolation and identification of dibenzothiophene-utilizing bacteria. Agric. Biol. Chem. 1968, 32:840-845.
- Yang J, Hu Y, Zhao D, Wang S, Lau PC, Marison IW. Two-layer continuous-process design for the biodesulfurization of diesel oils under bacterial growth conditions. Biochem. Eng. J. 2007, 37:212-218.

- Yang J, Marison IW. Two-stage process design for the biodesulphurisation of a model diesel by a newly isolated *Rhodococcus globerulus* DAQ3. Biochem. Eng. J. 2005, 27:77-82.
- Yang K, Yan Y, Chen W, Kang H, Han Y, Zhang W, Fan Y,Li Z. Nut-like MOF/hydroxylated graphene hybrid materials for adsorptive desulfurization of thiophene. RSC Adv. 2018, 8:23671-23678.
- Yang Q, Liu D, Zhong C, Li JR. Development of computational methodologies for metal–organic frameworks and their application in gas separations. Chem. Rev. 2013, 113:8261-8323.
- Yang RT. Adsorbents: fundamentals and applications. 2003, John Wiley & Sons.
- Yang X, Cao C, Klabunde KJ, Hohn KL, Erickson LE. Adsorptive desulfurization with xerogel-derived zinc-based nanocrystalline aluminum oxide. Ind. Eng. Chem. Res. 2007, 46:4819-4823.
- Yang Y, Chiang K, Burke N. Porous carbon-supported catalysts for energy and environmental applications: A short review. Catal. Today 2011, 178:197-205.
- Yeong H, Kim TS, Kim BH. Degradation of ogranic sulfur compounds and the reduction of dibenzothiophene to biphenyl and hydrogen sulfide by *Desulfovibrio desulfuricans* M6. Biotechnol. Lett. 1990, 12:761-764.
- Yi Z, Ma X, Song J, Yang X, Tang Q. Investigations in enhancement biodesulfurization of model compounds by ultrasound pre-oxidation. Ultrason. Sonochem. 2019, 54:110-120.

- Yu C, Qiu JS, Sun YF, Li XH, Chen G, Zhao ZB. Adsorption removal of thiophene and dibenzothiophene from oils with activated carbon as adsorbent: effect of surface chemistry. J. Porous Mater. 2008, 15:151-157.
- Zanin E. Scapinello J. de Oliveira M. Rambo CL, Franscescon F, Freitas L, de Mello JMM, Fiori MA, Oliveira JV, Dal Magro, J. Adsorption of heavy metals from wastewater graphic industry using clinoptilolite zeolite as adsorbent. Process Saf. Environ. 2017, 105:194-200.
- Zannikos F, Lois E, Stournas S. Desulfurization of petroleum fractions by oxidation and solvent extraction. Fuel Process. Technol. 1995, 42:35–45.
- Zhang JC, Song LF, Hu JY, Ong SL, Ng WJ, Lee LY, Wang YH, Zhao JG, Ma RY. Investigation on gasoline deep desulfurization for fuel cell applications. Energy Convers. Manag. 2005, 46:1-9.
- Zhang Q, Tong MY, Li YS, Gao HJ, Fang XC. Extensive desulfurization of diesel by *Rhodococcus erythropolis*. Biotechnol. Lett. 2007, 29:123-127.
- Zhang ZY, Shi TB, Jia CZ, Ji WJ, Chen Y, He MY. Adsorptive removal of aromatic organosulfur compounds over the modified Na-Y zeolites. Appl. Catal. B. 2008, 82:1-10.
- Zhao R, Jin Z, Wang J, Zhang G, Zhang D, Sun Y, Guan T, Zhao J, Li K. Adsorptive desulfurization of model fuel by S, N-codoped porous carbons based on polybenzoxazine. Fuel 2018, 218:258-265.
- Zhao S, Ge C, Yan Z, Zhang J, Ren S, Liang H, Chen F, Li X. One-pot microwave-assisted combustion synthesis of $NiFe_2O_4$-reduced graphene oxide composite for adsorptive desulfurization of diesel fuel. Mater. Chem. Phys. 2019, 229:294-302.

- Zhou A, Ma X, Song C. Effects of oxidative modification of carbon surface on the adsorption of sulfur compounds in diesel fuel. Appl. Catal. B. 2009, 87:190-199.
- Zhu L, Jia X, Bian H, Huo T, Duan Z, Xiang Y, Xia D. Structure and adsorptive desulfurization performance of the composite material MOF-5 AC. New J. Chem. 2018, 42:3840-3850.

List of publication

- **Omar, R.A.**, Verma, N. and Arora, P.K., 2022. Successive bacterial desulfurization and regeneration of liquid fuel over Ni-doped carbon beads using a single *Enterococcus faecium* strain isolated from an industrial wastewater. Fuel, 309, p.122209.
- **Omar, R.A.**, Verma, N. and Arora, P.K., 2020. Sequential desulfurization of thiol compounds containing liquid fuels: Adsorption over Ni-doped carbon beads followed by biodegradation using environmentally isolated *Bacillus zhangzhouensis*. Fuel, 277, p.118208.
- **Omar, R.A.**, Verma, N. and Arora, P.K., 2021. Development of ESAT-6 Based Immunosensor for the Detection of *Mycobacterium tuberculosis*. Frontiers in immunology, 12.
- Arora, P.K., Saroj, R.S., Mishra, R., **Omar, R.A.**, Kumari, P., Srivastava, A., Garg, S.K. and Singh, V.P., 2021. Draft genome sequence data of a 4-nitrophenol-degrading bacterium, *Pseudomonas alloputida* strain PNP. Data in Brief, 38, p.107390.
- Arora, P.K., Mishra, R., **Omar, R.A.**, Saroj, R.S., Srivastava, A., Garg, S.K. and Singh, V.P., 2021. Draft genome sequence data of a chromium reducing bacterium, *Bacillus licheniformis* strain KNP. Data in Brief, 34, p.106640.

Fuel 309 (2022) 122209

Contents lists available at ScienceDirect

Fuel

journal homepage: www.elsevier.com/locate/fuel

Full Length Article

Successive bacterial desulfurization and regeneration of liquid fuel over Ni-doped carbon beads using a single *Enterococcus faecium* strain isolated from an industrial wastewater

Rishabh Anand Omar [a], Nishith Verma [b,c,*], Pankaj Kumar Arora [a,*]

[a] Department of Environmental Microbiology, Babasaheb Bhimrao Ambedkar University, Lucknow 226025, India
[b] Centre for Environmental Science and Engineering, Indian Institute of Technology Kanpur, Kanpur 208016, India
[c] Department of Chemical Engineering, Indian Institute of Technology Kanpur, Kanpur 208016, India

ARTICLE INFO

Keywords:
Desulfurization
Liquid fuels
Bacterial regeneration
Activated carbon
Organosulfur compounds

ABSTRACT

Adsorptive desulfurization of liquid fuels over a wide sulfur (S) concentration range remains as challenging as the regeneration of spent materials. This study describes the efficient desulfurization of the dibenzothiophene (DBT) and thiophene (TH) containing liquid fuels over 300 – 1200 mg L^{-1} S-concentration range, using a hybrid approach combining adsorptive desulfurization (ADS) and bacterial desulfurization (BDS) sequentially at 30 °C and 1 atm-pressure, with the Ni-doped activated carbon beads and *Enterococcus faecium* bacterium serving as the ADS and BDS agent, respectively. The novelty is in the successful regeneration of spent adsorbents using the identical bacterium that was used in the BDS step. Notably, the bacterium was isolated from the waste effluent of a petroleum industry, and was characterized via the colony morphology, Gram staining, and identification by 16S rRNA sequencing. ADS step was used over 300 – 1200 mg L^{-1}, before switching over to BDS over the 50 – 300 mg L^{-1} S- concentration range, the sequential steps indicating an approximately 99% removal of the thiol compounds from the liquid. The spent adsorbents, post sequential test, were regenerated using the bacterial dose of 1% (v/v) of the liquid, and successfully reused up to five cycles of the hybrid method, with ~97% DBT and 95% TH removal measured in the last cycle. The spent and regenerated materials were physicochemically characterized by FE-SEM, FT-IR and BET analysis. As the regulations decrease the limits of sulfur content in on-road fuels globally, the proposed hybrid approach combining ADS with BDS, in conjunction with bacterial regeneration can be a potentially energy and cost effective solution to the desulfurization of liquid fuels.

1. Introduction

Significant amounts of sulfur containing gases including sulfur dioxide (SO_2) are emitted during combustion of liquid fuels, especially diesel. Thus, many countries have imposed the maximum sulfur concentration limits of 10 – 2000 ppm (w/w) (16 – 50 ppm in India) in diesel [1–3]. As per the new regulation of Environmental Protection Agency (EPA) imposed in 2020, the maximum allowable sulfur concentration in on-road diesel is 15 ppm [2,4].

Adsorptive desulfurization (ADS) is an efficient desulfurization and less energy-intensive technique [5–9]. Removal efficiency of ADS depends on the textural properties of the adsorbent material. The main characteristics of an efficient adsorbent are high surface area and pore volume, high mesoporosity, a relatively greater number of active sites, and good stability and structural strength [10,11]. A wide range of materials such as alumina, zeolite, metal oxides, metal organic framework (MOF) and carbon have been studied as an adsorbent for ADS [12–18]. These materials have also been doped with different transition metals such as Cu, Ag, Ni, and Zn with a view to enhancing their adsorption efficiencies under low to moderate temperature conditions [19–21]. The transition metals bind with sulfur compounds via direct metal-sulfur interaction and/or π-complexation [22]. Lio et al have used four different metals, namely, Ag, Cu, Ni, and Zn, and reported the comparative adsorption capacities in the following order: Zn < Cu < Ni < Ag [22]. Activated carbon beads (ACBs) supported Ni are potentially a good candidate for ADS. Such adsorbents are relatively inexpressive,

* Corresponding authors at: Centre for Environmental Science and Engineering, Indian Institute of Technology Kanpur, Kanpur 208016, India (Nishith Verma), and Department of Environmental Microbiology, Babasaheb Bhimrao Ambedkar University, Lucknow 226025, India (Pankaj Kumar Arora).
E-mail addresses: vermanishith@gmail.com (N. Verma), arora484@gmail.com (P.K. Arora).

https://doi.org/10.1016/j.fuel.2021.122209
Received 17 July 2021; Received in revised form 10 September 2021; Accepted 3 October 2021
Available online 15 October 2021

Fuel 277 (2020) 118208

Contents lists available at ScienceDirect

Fuel

journal homepage: www.elsevier.com/locate/fuel

Full Length Article

Sequential desulfurization of thiol compounds containing liquid fuels: Adsorption over Ni-doped carbon beads followed by biodegradation using environmentally isolated *Bacillus zhangzhouensis*

Rishabh Anand Omar[a], Nishith Verma[b,c,*], Pankaj Kumar Arora[a,*]

[a] Department of Microbiology, Babasaheb Bhimrao Ambedkar University, Lucknow 226025, India
[b] Centre for Environmental Science and Engineering, Indian Institute of Technology Kanpur, Kanpur 208016, India
[c] Department of Chemical Engineering, Indian Institute of Technology Kanpur, Kanpur 208016, India

GRAPHICAL ABSTRACT

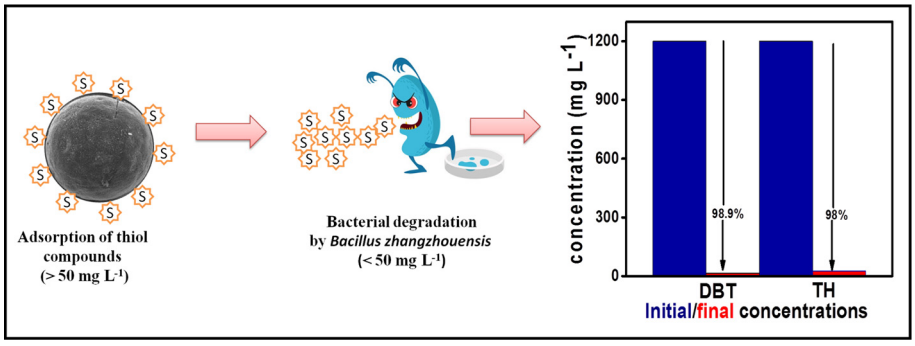

ARTICLE INFO

Keywords:
Desulfurization
Thiol compounds
Adsorptive desulfurization
Bacterial degradation
Ni nanoparticles
Carbon nanofibers

ABSTRACT

Desulfurization of liquid fuels over a wide concentration range continues to be challenging. This study recommends a novel hybrid route to efficiently desulfurizing the thiols or organosulfur compounds containing liquid fuels. The tests performed on the dibenzothiophene (DBT) and thiophene (TH) containing n-octane over sulfur concentration range 300–1200 mg/L showed adsorptive desulfurization followed by the bacterial treatment to be efficient in decreasing the concentration level to 3–15 mg/L at 30 °C and 1 atm pressure. Adsorption performed using the Ni nanoparticles-dispersed porous carbon beads of ~ 0.8 mm size was effective at relatively higher concentrations. Upon nearly saturation in the adsorption step, further removal of the thiol compounds to low concentrations was possible by bacterial degradation using *Bacillus zhangzhouensis* isolated from the wastewater effluent of a petroleum industry. Fresh and spent adsorbents were characterized using various analytical techniques. Bacterial characterization involved the Christian gram staining and 16S rRNA sequencing. The data demonstrate for the first time ~ 99% removal of the thiol compounds, at rates faster than adsorption alone. The proposed sequential approach in this study can be effective in meeting the globally ever increasing stringent regulations for low sulfur content in fuel oils.

* Corresponding authors at: Centre for Environmental Science and Engineering, Indian Institute of Technology Kanpur, Kanpur 208016, India; Department of Microbiology, Babasaheb Bhimrao Ambedkar University, Lucknow 226025, India.
E-mail addresses: vermanishith@gmail.com (N. Verma), arora484@gmail.com (P.K. Arora).

https://doi.org/10.1016/j.fuel.2020.118208
Received 1 February 2020; Received in revised form 18 April 2020; Accepted 24 May 2020
Available online 04 June 2020
0016-2361/

frontiers in Immunology

ORIGINAL RESEARCH
published: 19 May 2021
doi: 10.3389/fimmu.2021.653853

Development of ESAT-6 Based Immunosensor for the Detection of *Mycobacterium tuberculosis*

Rishabh Anand Omar[1], *Nishith Verma*[2,3]* *and Pankaj Kumar Arora*[1]*

[1] Department of Environmental Microbiology, Babasaheb Bhimrao Ambedkar University, Lucknow, India, [2] Centre for Environmental Science and Engineering, Indian Institute of Technology Kanpur, Kanpur, India, [3] Department of Chemical Engineering, Indian Institute of Technology Kanpur, Kanpur, India

Early secreted antigenic target of 6 kDa (ESAT-6) has recently been identified as a biomarker for the rapid diagnosis of tuberculosis. We propose a stable and reusable immunosensor for the early diagnosis of tuberculosis based on the detection and quantification of ESAT-6 *via* cyclic voltammetry (CV). The immunosensor was synthesized by polymerizing aniline dispersed with the reduced graphene oxide (rGO) and Ni nanoparticles, followed by surface modification of the electroconductive polyaniline (PANI) film with anti-ESAT-6 antibody. Physicochemical characterization of the prepared materials was performed by several analytical techniques, including FE-SEM, EDX, XRD, FT-IR, Raman, TGA, TPR, and BET surface area analysis. The antibody-modified Ni-rGO-PANI electrode exhibited an approximately linear response (R^2 = 0.988) towards ESAT-6 during CV measurements over the potential range of -1 to +1 V. The lower detection limit for ESAT-6 was approximately 1.0 ng mL^{-1}. The novelty of this study includes the development of the reusable Ni-rGO-PANI-based electrochemical immunosensor for the early diagnosis of tuberculosis. Furthermore, this study successfully demonstrates that electro-conductive PANI may be used as a polymeric substrate for Ni nanoparticles and rGO.

Keywords: ***Mycobacterium tuberculosis*, cyclic voltammetry, ESAT-6, immunosensor, reduced graphene oxide, polyaniline**

OPEN ACCESS

Edited by:
Christof Geldmacher, University of Munich, Germany

Reviewed by:
Antresh Kumar, Central University of South Bihar, India
Yogendra Kumar Mishra, University of Southern Denmark, Denmark
Kamlesh Shrivas, Pandit Ravishankar Shukla University, India

***Correspondence:**
Nishith Verma
vermanishith@gmail.com
Pankaj Kumar Arora
arora484@gmail.com

Specialty section:
This article was submitted to Microbial Immunology, a section of the journal Frontiers in Immunology

Received: *15 January 2021*
Accepted: *04 May 2021*
Published: *19 May 2021*

Citation:
Omar RA, Verma N and Arora PK (2021) Development of ESAT-6 Based Immunosensor for the Detection of Mycobacterium tuberculosis. Front. Immunol. 12:653853. doi: 10.3389/fimmu.2021.653853

INTRODUCTION

Tuberculosis (TB) is an airborne disease that can be transmitted through coughing, sneezing, laughing, and even talking (1). It is one of the leading causes of death in the world. The causative agent of tuberculosis is the *Mycobacterium tuberculosis* (*Mtb*) bacterium. Therefore, an early detection of *Mtb* is critical to preventing the spread of infection and to eradicating the disease.

Many traditional biochemical methods, including acid-fast staining, culturing, and colony counting have been used to detect tuberculosis. However, these methods are time-consuming, often inaccurate, and provide only qualitative data. In recent years, various transduction techniques have been developed using fiber optics, surface plasmon resonance, piezoelastics, and magnetoelastics. These techniques are rapid and accurate but too expensive to be used on a diagnostic level, especially in developing countries where the spread of *Mtb* is common (2–4).

Data in Brief 34 (2021) 106640

Contents lists available at ScienceDirect

Data in Brief

journal homepage: www.elsevier.com/locate/dib

Data Article

Draft genome sequence data of a chromium reducing bacterium, *Bacillus licheniformis* strain KNP

Pankaj Kumar Arora [a,*], Rupali Mishra [a], Rishabh Anand Omar [a], Raj Shekhar Saroj [a], Alok Srivastava [b], Sanjay Kumar Garg [b], Vijay Pal Singh [b]

[a] *Department of Microbiology, Babasaheb Bhimrao Ambedkar University, Lucknow 226025, India*
[b] *Department of Plant Science, Faculty of Applied Sciences, MJP Rohilkhand University, Bareilly, India*

ARTICLE INFO

Article history:
Received 3 October 2020
Revised 25 November 2020
Accepted 7 December 2020
Available online 15 December 2020

Keywords:
Chromium
Bacillus
Chromate transporter
Reduction

ABSTRACT

A chromium-reducing bacterium designated as strain KNP was isolated from a sample collected from a tannery effluent of Kanpur, India. Phylogenetic analysis based on the 16S rRNA gene sequences revealed that strain KNP belonged to the *Bacillus* genus and showed 100% similarity with *Bacillus licheniformis*. Furthermore, average nucleotide identity and digital DNA-DNA hybridization between strain KNP and its closely related strains confirmed its affiliation with *Bacillus licheniformis* species. Whole-genome sequencing of *Bacillus licheniformis* KNP was performed using the Illumina Hiseq platform. Here, we present the draft genome sequence of *Bacillus licheniformis* KNP. The total size of the draft assembly was 4,280,093 bp, distributed into 21 contigs with an N50 value of 4,186,229. The genome has 45.9% G + C content, 4255 coding sequences and 86 putative RNA genes. This Whole Genome Shotgun project has been deposited at DDBJ/ENA/GenBank under the accession

* Corresponding author.
E-mail address: arora484@gmail.com (P.K. Arora).
Social media: (P.K. Arora)

https://doi.org/10.1016/j.dib.2020.106640

Data in Brief 38 (2021) 107390

Contents lists available at ScienceDirect

Data in Brief

journal homepage: www.elsevier.com/locate/dib

Data Article

Draft genome sequence data of a 4-nitrophenol- degrading bacterium, *Pseudomonas alloputida* strain PNP ☆

Pankaj Kumar Arora [a,*], Raj Shekhar Saroj [a], Rupali Mishra [a], Rishabh Anand Omar [a], Puja Kumari [a], Alok Srivastava [b], Sanjay Kumar Garg [b], Vijay Pal Singh [b]

[a] *Department of Environmnetal Microbiology, Babasaheb Bhimrao Ambedkar University, Lucknow 226025, India*
[b] *Department of Plant Science, Faculty of Applied Sciences, MJP Rohilkhand University, Bareilly, India*

ARTICLE INFO

Article history:
Received 28 May 2021
Revised 6 September 2021
Accepted 9 September 2021
Available online 20 September 2021

Keywords:
4-Nitrophenol
Average nucleotide identity
Genome
Sequencing
Bacteria
Pseudomonas

ABSTRACT

A 4-nitrophenol-degrading bacterial strain PNP was isolated from pesticide-contaminated soil collected from Lucknow. Strain PNP utilized 0.5 mM 4-nitrophenol as its carbon source and degraded it completely within 24 h with stoichiometric release of nitrite ions. Strain PNP was associated with the genus *Pseudomonas* in a phylogentic tree and exhibited highest 16S rRNA gene sequence similarity to *Pseudomonas juntendi* BML3 (99.79%) and *Pseudomonas inefficax* JV551A3 (99.79%). Based on values of average nucleotide identity and digital DNA-DNA hybridization among strain PNP and its closely related type strains, it concluded that strain PNP belongs to *Pseudomonas alloputida.* The Illumina HiSeq platform was used to sequence the PNP genome. The draft genome sequence of *Pseudomonas alloputida* PNP was presented here. The total size of the draft assembly was 6,087,340 bp, distributed into 87 contigs with N50 value of 139502. The genome has an average GC content of 61.7% and contains 5461 coding sequences and 77 putative RNA genes. This Whole Genome Shotgun project has been submitted at DDBJ/ENA/GenBank under the accession JAGKJH000000000.

☆ Given his role as Editorial Board Member of this journal, Pankaj Kumar Arora had no involvement in the peer-review of this article and has no access to information regarding its peer-review.

* Corresponding author.
E-mail address: arora484@gmail.com (P.K. Arora).

https://doi.org/10.1016/j.dib.2021.107390

BABASAHEB BHIMRAO AMBEDKAR UNIVERSITY

प्रज्ञा शील करूणा

ESTABLISHED 1996

बाबासाहेब भीमराव अम्बेडकर विश्वविद्यालय

(केन्द्रीय विश्वविद्यालय) विद्या विहार रायबरेली रोड, लखनऊ -226025

BABASAHEB BHIMRAO AMBEDKAR UNIVERSITY

(A Central University), Vidya Vihar, Raebareli Road, Lucknow-226025

Research Excellence Award-2022

This is to certify that Mr. *Rishabh Anand Omar* Research Scholar in Department of Microbiology has contributed significantly in academic and research in his subject during the year 2021. The University recognizes his contribution and bestows upon him **"Research Excellence Award"** in the discipline of Life Sciences on 26th January 2022.

R.P.S. Ph

Prof. Rana Pratap Singh
Dean Academic Affair

Sanjay Singh

Prof. Sanjay Singh
Vice Chancellor

INSCR

Indian Network for Soil Contamination Research

6th Annual International E-Conference of Indian Network for Soil Contamination Research (INSCR)

Certificate of Appreciation

This is presented to

Rishabh Anand Omar, Babasaheb Bhimrao Ambedkar University

for the ORAL PRESENTATION (Student) during the 6th Annual International Conference of INSCR on "MICROBES IN SUSTAINABLE DEVELOPMENT" organized in association with the Department of Zoology (DU), Acharya Narendra Dev College (DU), Deen Dayal Upadhyaya College (DU), Gargi College (DU), Kirori Mal College (DU), PG Department of Zoology (MU), Maitreyi College (DU), Ramjas College (DU), Sri Venkateswara College (DU), C.M.P. College (AU), SGTB Khalsa College (DU), COCAS (PU) & PhiXgen Pvt. Ltd., Gurugram from November 15 to 18, 2021.

Rup Lal

PROF. RUP LAL
President, INSCR

Yogendra Singh

PROF. YOGENDRA SINGH
General Secretary, INSCR

Certificate Number: 20211028202

International Conference on Advancements in Interdisciplinary Research (ICAIR-2021)

Jointly Organised By

Shia P.G. College, Lucknow

(An Associated College of Lucknow University)

&

Science Tech Institute, Lucknow

(RUN by: Manraj Kuwar Singh Educational Society)

(Registered by : Govt. of UP & Ordinance No. 21 of 1860 Reg. No. LUC/03140/UP, India)

(Registered by : Govt. Of India, NITI Aayog, Reg. No.UP/2019/0248444)

Certificate for Appreciation

This is to Certify that Mr. Rishabh Anand Omar, Research Scholar, Environmental Microbiology, Babasaheb Bhimrao Ambedkar University Lucknow, has successfully delivered Oral Presentation on the Title "Biochemical Desulfurization and Bacterial Regeneration of Spent Adsorbent Using an Environmentally Isolated Single Bacterial Strain" **in the three days International Conference on Advancement in Interdisciplinary Research (ICAIR-2021), Jointly organised by Shia P.G. College, Lucknow, UP & Science Tech Institute, Lucknow, UP India during October 26th-28th, 2021.**

Prof. R. K. Shukla
Conference Chair
University of Lucknow
Lucknow, UP

Dr. Mohammad Miyan
Principal,
Shia PG College,
Lucknow, UP, India

Dr. Bhuvan Bhasker Srivastava
Convenor
Shia PG College,
Lucknow, UP, India

Mrs. Shweta Singh
Chairman
MKSES, Lucknow
UP, India

MICROBIOLOGIST SOCIETY, INDIA

(Reg No. MAH/4814/SAT)

Certificate Of Participation

Certified that Mr./~~Ms.~~/~~Dr.~~/~~Prof.~~ **Rishabh Anand Omar** Department of Environmental Microbiology, Babasaheb Bhimrao Ambedkar University, Lucknow (U.P.), India participated and presented ~~Oral~~/ Poster Paper entitled **Sequential Desulfurization of Thiol Compounds in Liquid Fuels Using Activated Cabon Beads and an Environmentally Isolated Bacterium** in the "International e-Conference on Microbes with Entrepreneurship" organized by Microbiologist Society, India on October 24, 2021.

Prof. Amritesh C. Shukla
Chairperson- IeCME &
State President (U.P.)
Microbiologists Society, India

Dr. Arvind Deshmukh
President
Microbiologists Society, India